PHYTOPLANKTON MORTALITY IN AN URBAN POND: UNDERSTANDING THE ROLES OF ABIOTIC FACTORS, GRAZING PRESSURE AND ALLELOPATHY

by

Lauren J Simmons

A Dissertation Submitted in

Partial Fulfillment of the

Requirements for the Degree of

Doctor of Philosophy

in Biological Sciences

at

The University of Wisconsin-Milwaukee

May 2022

ABSTRACT

PHYTOPLANKTON MORTALITY IN AN URBAN POND: UNDERSTANDING THE ROLES OF ABIOTIC FACTORS, GRAZING PRESSURE AND ALLELOPATHY

by

Lauren J Simmons

The University of Wisconsin-Milwaukee, 2022
Under the Supervision of Professor John A Berges

Phytoplankton are found in dynamic aquatic environments, subjected to variations in abiotic (i.e., light, temperature, nutrients) and biotic (i.e., grazing, species interactions) conditions. Phytoplankton responses to these environmental variations are typically observed as changes in chlorophyll *a* (a surrogate for biomass), but such measurements do not provide information about individual taxa and cannot provide information about cell condition, for example, whether phytoplankton are living or dead. Furthermore, in examining the dynamics of phytoplankton, emphasis is placed on growth, but consideration of loss processes is usually limited to grazing and sedimentation, and not cell death The present study examined cell death in phytoplankton at a taxon-specific level in response to abiotic and biotic factors.

A combination of intensive field sampling in a local urban park pond and complementary laboratory experiments were used to correlate taxon-specific abundances of phytoplankton (living and dead cells, using a combination of flow cytometry and mortal staining) with temperature, light and nutrient concentrations. In addition, the effects of grazing by zooplankton and allelopathic interactions among species were explored in field manipulations and laboratory co-culture experiments, respectively. There were few strong, consistent

correlations among abiotic parameters and abundances of living or dead phytoplankton cells. Changes in temperature and light were found to have some effect on phytoplankton cell death, with higher proportions of dead cells observed for some phytoplankton groups during periods of low temperatures or light. Other abiotic conditions, specifically nutrient concentrations, did not correlate with changes in phytoplankton abundance or cell death, consistent with previous studies. Thus, abiotic factors do not appear to be major drivers of cell death within the phytoplankton community of the local urban pond. In contrast, correlations were observed among taxa, especially among abundances of particular taxa and dead cells of another, suggesting that biotic interactions among phytoplankton may be influencing changes in the community. The effect of grazing on phytoplankton cell death was examined by using natural assemblages from the pond and varying concentrations across a 2-fold gradient. Little effect of grazing was found on any taxa in late summer/early autumn over two years, and grazing did not lead to the production of dead cells. Possible allelopathic relationships were studied using laboratory co-culturing experiments for the cyanobacterium *Microcystis aeruginosa*, the chlorophyte *Chlamydomonas reinhardtii* and the diatom *Synedra*, each belong to groups implicated in field studies. These experiments did not show evidence of allelopathic interactions.

While a specific driver was not identified in promoting cell death or changing phytoplankton abundances, these studies did provide further evidence that abiotic factors seem to be less important to cell death than biotic ones. Grazing by zooplankton does not directly cause phytoplankton cell death, though there is indirect evidence of allelopathic interactions, but we have not been able to demonstrate this in the species tested so far.

Dedicated to my husband, daughter, and son,
for all your love, support and understanding
throughout this journey in our lives.

Thank you for believing in me.

TABLE OF CONTENTS

LIST OF FIGURES

LIST OF TABLES

ACKNOWLEDGEMENTS

I want to begin by thanking my advisor, John Berges. Your patience, persistence, and belief in me helped keep our work moving along, even at the times where we thought it may never end. It was a mad dash to the finish, but I appreciate you working with me to help make the dream come true. Teamwork makes the dream work.

To my doctoral committee members – Erica Young, Doug Steeber, Harvey Bootsma and Christopher Klausmeier (Michigan State University) – thank you for sticking around for the long haul. The grace, patience and understanding that you all extended to me throughout this process was phenomenal. I am indebted to you all for that you have done and what you have invested in me and my work.

To my funding and organizational sources – UWM Graduate School, UWM Biological Sciences and NSF (IOS 1121513; DUE 0827217, 1120956) – thank you for providing the means for this work to even take place. Through your support we have collected a lot of data to provide hours of interpretation and understanding of some complex relationships in aquatic systems. Thank you to the UWM Biological Sciences department for their support as well, by way of teaching support, troubleshooting technology or a friendly face to say hello to.

I would also like to acknowledge those who assisted in a variety of ways with my investigations of the Estabrook Park Pond phytoplankton communities. First, thank you to Brian Russert and the Milwaukee County Park System for permitting access to Estabrook Park Pond for sampling and study purposes. Without your blessing, this work could not have been completed. I also want to thank Chrissy Kozik whose MS work helped propel the work presented here. Your observations and insights to Estabrook Park Pond are invaluable. Thank

you to the numerous undergraduates that helped with collecting field samples and assisted with experiments, including Erin Cox and Tim Trinklein for your contributions to the grazing studies, as well as Sierra Aguirre for your assistance with allelopathic studies. To the Alberto Lab – thank you for your hospitality and access to microscopes which were crucial to the identification of plankton observed in my studies. I also want to thank Michael Laiosa of the UWM School of Public Health for assistance on numerous occasions with sorting flow cytometry. Because of you, we were able to put a face to the name of some of our phytoplankton groups.

Thank you to my lab mates (past and present) for all your contributions to my time here on the 5th floor of Lapham. Whether it be critical bits of information relevant to my studies here (Chang Jae Choi, Alicia Hanson, Chrissy Kozik) or assistance in collecting samples (Deb Fobbe, Allison Driskill, Lindsay Reed), your contributions are much appreciated. Conversations amongst friends kept me mostly sane, so I am also thankful for those chats, especially those with Jake Grothjan and Sierra Wachala.

And last, but certainly not least, I would like to acknowledge and thank my family for sticking by me all this time. It hasn't been easy, and I know that we had our moments, but we made it. We did it. I could not have done this without you. Thank you from the bottom of my heart.

Chapter 1: General Introduction

Phytoplankton communities are dynamic assemblages of organisms that aid in regulating biogeochemical cycles, while functioning as a food source for primary consumers. These organisms encounter a variety of abiotic (e.g., light, temperature, nutrients) and biotic (e.g., grazing, species interactions) conditions, as aquatic environments are not homogenous, resulting in changes in phytoplankton biomass. Much is known about the physiology of phytoplankton and what regulates growth, but not about mortality or loss processes. It has been thought that losses in biomass can be attributed to grazing and sedimentation processes (Kirchman 1999), with little consideration to other potential causes of mortality (e.g., environmental regulation, allelopathy; Franklin et al. 2006). Developing a better understanding of mortality processes and their importance in regulating phytoplankton populations will allow for a better understanding of bloom dynamics, population regulation and cell signaling (Franklin et al. 2006).

Previous studies of phytoplankton cell death have typically focused on marine species (e.g., Llabrés and Agustí 2006, Llabrés et al. 2011), with freshwater species receiving less attention though this is becoming less the case (e.g., Rychtecký et al. 2014, Kozik et al. 2019). Flow cytometry provides a rapid method to assess the phytoplankton community based on cell characteristics such as chlorophyll fluorescence and cell size (Gasol and del Giorgio 2000) and quantify cell death with fluorescent staining techniques (e.g., Vaharanta et al. 2020), allowing for the collection of an extensive data series to assess relationships in representative groups. The methods can then be used in the assessment of phytoplankton responses to changes in

abiotic conditions through careful monitoring of the environment, as well as to monitor responses to interactions among phytoplankton and zooplankton.

The overall objective of this dissertation was to understand how abiotic and biotic factors affect phytoplankton community composition and cell mortality in an urban pond. It has been thought that abiotic factors, specifically light, temperature and nutrients affect phytoplankton growth, but the influence of these factors on cell mortality is not well understood (e.g., Franklin et al. 2006). Alternatively, biotic factors (e.g., grazing pressure, allelopathy, viral interactions) may influence changes in phytoplankton community composition and cell mortality as well (e.g., Wang et al. 2020). This dissertation focuses on how abiotic and biotic factors affect community composition and cell mortality in a small urban pond.

Much of what is known regarding cell mortality is based on multicellular animal models, although more recent work is beginning to focus on phytoplankton (Choi and Berges 2013, Bidle 2015, Liu et al. 2017). This dissertation will provide a more detailed analysis of how abiotic and biotic factors influence phytoplankton community structure and cell mortality in an urban pond. Based on my exploration of preliminary data (Kozik et al. 2019), showing few correlations among dead and dying phytoplankton and changes in abiotic parameters, I tested my central hypothesis that biotic factors, specifically grazing by herbivores and allelopathic interactions among taxa, have greater influences on phytoplankton than abiotic factors and are responsible for changes in phytoplankton community composition and cell mortality. To test my central hypothesis, I developed three specific aims: 1) Use regular flow cytometric counts of specific phytoplankton taxa in field samples to determine whether declines in specific taxa or the appearance of dead cells are associated with changes in abiotic parameters, e.g., light,

temperature, nutrients; 2) Use experimental manipulations to determine whether grazing by macrozooplankton is responsible for declines in specific phytoplankton taxa, specifically resulting in the appearance of dead cells; and 3) Use laboratory experiments to determine whether correlations among taxonomic groups of phytoplankton, specifically living cells of one species and dead cells of another, could be due to allelopathic interactions.

Thesis organization. Chapters 2 – 4 address both abiotic and biotic factors and their influences on cell death in the field and laboratory experiments. Chapter 2 addresses aim 1, focusing on using flow cytometric and mortal staining methods to observe phytoplankton community changes over three years in Estabrook Park Pond. This chapter and related appendices help provide a better understanding of abiotic influences on the phytoplankton community and cell death, along with the development and application of flow cytometric techniques for a freshwater system. This manuscript is being prepared for submission to *Hydrobiologia* (Simmons et al.).

Chapter 3 addresses aim 2, focusing on how grazing by herbivores affects natural phytoplankton assemblages and cell death. Observations from grazer gradient experiments are presented, demonstrating the minimal influences of grazing at Estabrook Park Pond and provide a novel way to investigate community responses to grazing pressure using flow cytometry. This manuscript will be submitted as a short communication to the *Journal of Plankton Research* (Simmons and Berges).

Chapter 4 addresses aim 3. The chapter presents the outcomes of co-culturing experiments conducted to better understand inter-taxon relationships of phytoplankton known

to have allelopathic tendencies. The work provided here compares the cell death and population responses of select phytoplankton (*Chlamydomonas reinhardtii*, *Synedra*) when exposed to a known producer of allelochemical, the cyanobacterium *Microcystis aeruginosa*. This manuscript was originally prepared in response to an invitation to contribute to a special issue of *Microorganisms* on cyanobacteria, but due to delay we instead will submit it to the *European Journal of Phycology* (Simmons and Berges).

Appendix A: This appendix documents the flow cytometric gating strategy used to group phytoplankton groups based upon red and orange fluorescence characteristics. Additional methods are described for the estimation of cell death for gated phytoplankton groups based upon an increase in green fluorescence due to the application of Sytox Green® mortal stain. This would be included as supplementary material to the publication of Chapter 2.

Appendix B: This appendix provides a list of species identified through microscopic enumeration of preserved samples collected to identify phytoplankton that comprise the flow cytometric gated phytoplankton groups. This list expands upon the generalizations of taxonomic group identification in Table 1. This would be included as supplementary material to the publication of Chapter 2.

Appendix C: This appendix provides an overview of applying agent-based modeling techniques to better understand how individuals within phytoplankton groups respond to varying abiotic conditions. Included here is a literature review and an attempt at modeling phytoplankton responses based upon environmental conditions observed in our timeseries study completed for aim 1. Originally envisioned as a distinct chapter in this thesis, but due to

incomplete modeling work written as an appendix. I hope that this will serve as the basis for future proposals.

REFERENCES

Bidle, K.D. 2015. The molecular ecophysiology of programmed cell death in marine phytoplankton. *Ann Rev Mar Sci* 7: 341-375.

Choi, C.J. and Berges, J.A. 2013. New types of metacaspases in phytoplankton reveal diverse origins of cell death proteases. *Cell Death Dis* 4: E490.

Franklin, D.J., Brussaard, C.P.D. and Berges, J.A. 2006. What is the role and nature of programmed cell death in phytoplankton ecology? *Eur J Phycol* 41: 1-14.

Kirchman, D.L. 1999. Phytoplankton death in the sea. *Nature* 398: 293-294.

Kozik, C.R., Young, E.B., Sandgren, C.D., and Berges, J.A. 2019. Cell death in individual freshwater phytoplankton species: relationshsips with population dynamics and environmental factors. *Eur J Phycol* 54: 369-379.

Llabrés, M. and Agustí, S. 2006. Picophytoplankton cell death induced by UV radiation: Evidence for oceanic Atlantic communities. *Limnol Oceanogr* 51: 21-29.

Llabrés, M., Agustí, S. and Herndl, G.J. 2011. Diel in situ picophytoplankton cell death cycles coupled with cell division. *J Phycol* 47: 1247-1257.

Liu, J., Cai, W., Fang, X., Wang, X. and Li, G. 2017. Virus-induced apoptosis and phosphorylation form of metacaspase in the marine coccolithophorid *Emiliania huxleyi*. *Arch Microbiol* 200: 413-422.

Rychtecký, P., Znachor, P., and Nedoma, J. 2014. Spatio-temporal study of phytoplankton cell viability in a eutrophic reservoir using SYTOX Green nucleic acid stain. *Hydrobiologia* 740: 177-189.

Simmons, L.J., Fobbe, D.J., Berges. J.A. and Young, E.B. Environmental influences on phytoplankton community structure and cell mortality in an urban pond. *Hydrobiologia* in prep.

Vanharanta, M., Elovaara, S., Franklin, D.J., Spilling, K. and Tamelander, T. 2020. Viability of pico- and nanophytoplankton in the Baltic Sea during spring. *Aquat Ecol* 54: 119 135.

Wang, H., Chen, F., Mi, T., Liu, Q., Yu, Z., and Zhen, Y. 2020. Responses of Marine diatom *Skeletonema marinoi* to nutrient deficiency: programmed cell death. *Appl Environ Microbiol* 86: e02460-19.

Chapter 2: Environmental influences on phytoplankton community structure and cell mortality in an urban pond

INTRODUCTION

Phytoplankton are continuously dividing and producing new clonal cells, making them seem immortal (Kirchman 1999). Previously, sedimentation and grazing had been considered the main loss processes removing cells from the environment, although there had been issues in accounting for cell losses (Franklin et al. 2006). Difficulties in accounting for cell losses can be due in part to sinking and grazing affecting different species differently. For example, diatoms frequently sink down into the sediment, while motile species may be removed by grazing or other means (reviewed in Franklin et al. 2006). If attempting to observe how both processes affect a community, there may be an over/under estimation of the impact of grazing and sedimentation processes. In Lake Michigan, Scavia and Fahnenstiel (1987) found that while sedimentation and grazing were important contributors to cell loss during the spring and summer respectively, over 30% of loss in annual production was unaccounted for by these processes, suggesting that other processes are important. Indeed, lysis (cell death) of phytoplankton has been observed in the laboratory, as well as in the field (Franklin et al. 2006) and is often associated with changes in abiotic conditions, including exhaustion of nutrients, and changes in irradiance or temperature (reviewed by Bidle and Falkowski 2004, Franklin et al. 2006).

To develop a better understanding of how cell death is influenced by abiotic and biotic factors, studies to examine cell mortality need to be conducted. Mortality studies have typically focused on marine species (e.g., Hayakawa et al. 2008, Llabrés and Agustí 2006, Llabrés et al. 2011) while freshwater species have received less attention, though there have been

exceptions in recent years (e.g., Agustí et al. 2006, Vardi et al. 1999, Rychtecký et al. 2014). Since phytoplankton are subjected to a variety of abiotic changes due to seasonality and weather events, to which they respond in a variety of ways (Berquist and Carpenter 1986, Carpenter and Kitchell 1993), it can be hypothesized that instances of mass mortality occur periodically in the natural environment in response to the changing abiotic conditions.

Responses to abiotic factors. Variations in light, nutrients and temperature are primary drivers of change to phytoplankton community structure (Hutchinson 1961). Environmental conditions are not static, therefore natural phytoplankton populations are exposed to conditions that change daily, though not all taxa will respond similarly (Berquist and Carpenter 1986, Carpenter and Kitchell 1993). Varying combinations of these conditions may work to promote cell death rather than cell growth and division (Berges and Falkowski 1998).

Irradiance influences phytoplankton productivity because photosynthesis varies with irradiance (Falkowski et al. 1985). Under certain light conditions, cells may not grow or divide (Litchman 2000, Veldhuis et al. 2001, Llabrés et al. 2011). For example, cells exposed to high light and increased ultraviolet radiation may be unable to photosynthesize effectively due to photoinhibition, resulting in cell death or no net cellular production (Llabrés and Agustí 2006). Further, phytoplankton compete for light, and those that can respond to changing light conditions by either moving or acclimating their photosynthetic apparatus will be able to survive better and shape the phytoplankton community (Litchman and Klausmeier 2001). Motile cells can minimize this potential photoinhibition, as they can change their position in the water column (Hansson 1995, Beckmann and Hense 2004). Cells that can photo acclimate efficiently, particularly through the xanthophyll cycle, limiting oxidative stress by way of

regulating the amount of photoprotective pigment in the cells, are more likely to be survive exposure to higher irradiances (Dimier et al. 2007).

Variation in irradiance may coincide with temperature fluctuations in the environment (i.e., higher irradiance periods fall within summer months when higher surface temperatures occur). As with irradiance, temperature can also affect phytoplankton productivity and community structure, influencing seasonally dominant taxa. Different species have different temperature optima for growth (Eppley 1972). Coupled with variations in nutrient uptake and assimilation (Goldman 1977), growth of different species can exhibit greater variation. For example, cyanobacteria can dominate the community during periods of high temperatures, whereas diatoms may dominate under cold water conditions (Zhang and Prepas 1996). Temperature may also influence toxin production of some cyanobacteria, especially when associated with increased nutrient availability as has been observed in toxin producing *Microcystis* sp. where biomass and toxin production increased with higher temperatures and eutrophic conditions (Davis et al. 2009).

Responses to biotic factors. Despite the effects of irradiance and temperature on phytoplankton dynamics, resource supply may often be a more important factor regulating phytoplankton growth (Reynolds 2006, Marañón et al. 2014). Seasonal changes in essential macronutrients (nitrogen, phosphorus, and silica) can bring about limiting conditions where cellular growth and/or division can be inhibited for some taxa, as their cellular nutrient requirements are not being met (Sterner and Elser 2002, Reynolds 2006), which could result in cell death (Wang et al. 2020). Under nutrient limited conditions, nutrient competition among phytoplankton can occur, where phytoplankton will use available nutrients to the best of their

abilities, potentially achieving a stable coexistence, assuming each is limited by a different resource (Tilman 1977). If there are multiple limiting resources, there may be an increase in community diversity (Interlandi and Kilham 2001), as taxa present may be better suited to take up one of the nutrients more efficiently than another; each will fulfill a different nutrient availability niche.

Despite what is known about the importance of abiotic factors in phytoplankton growth and production, biotic factors can still influence phytoplankton community structure. Kozik et al. (2019) established that there a variety of both abiotic and biotic factors that could be influencing the phytoplankton community, as their findings suggested that individual abiotic factors could not be strongly or uniquely linked to cell death. Phytoplankton cell mortality could be influenced by viral infection which could lead to cell death pathway activation (Bidle et al. 2007, Evans and Brussaard 2012), grazing by zooplankton leading to damaged and/or dead cells, viral infection (Biggs et al. 2021) or allelopathy (e.g., Maestrini and Bonin 1981, Sukenik et al. 2002, Llabrés et al. 2011, Wang et al. 2017). To identify patterns of cell mortality for phytoplankton taxa, Kozik et al. (2019) recommended more frequent sampling of aquatic communities, providing a more robust dataset to fully assess the abiotic and community interaction influences on cell death of phytoplankton in the community.

Use of flow cytometry in the field. To tease apart relationships among phytoplankton groups, an extensive time-series with frequent sampling can provide insight to interactions within the environment. Flow cytometry provides a way for phytoplankton communities to be counted and assessed for cellular characteristics (fluorescence, cell size and shape), in a rapid and efficient manner (Gasol and del Giorgio 2000), facilitating the collection of a long-term data

series to assess the relationships. In the past, flow cytometry was mostly used when studying marine systems (Olson et al. 1989, Veldhuis and Kraay 2000, Llabrés and Agustí 2008), but is becoming more widely used in freshwater studies (Agustí et al. 2006, Reavie et al. 2010, Read et al. 2014, Yang et al. 2019). Phytoplankton populations can be estimated quantitatively using this method, as phytoplankton can be separated from other organisms/particles in the environment using their fluorescent properties, creating groups. These data, paired with microscopic observations, allow for the identification of phytoplankton taxa within a given group of particles detected with the flow cytometer. Microscopy can also allow for the identification of large, rare individuals within a sample and can help to account for changes in fluorescence of phytoplankton due to cellular stress. An alternative to this would be to process reference cultures in advance of processing field samples, establishing groups by phytoplankton class to aid in the identification of phytoplankton present (by taxonomic group) within the community (Dennis et al. 2011).

***Assessing cell mortality*.** To assess cell viability in the field, clear methods are necessary to reliably measure dead cells, which can be done in a variety of ways, including cell staining (Veldhuis and Kraay 2000, Reavie et al. 2010) or cell digestion (Agustí et al. 2006, Hayakawa et al. 2008, Llabrés and Agustí 2008). Cell staining can be done using a variety of fluorescent stains that allow for the detection of cell viability or apoptotic processes occurring. Using a mortal stain such as Sytox Green®, cell mortality can be assessed as it will stain only the DNA of compromised cells. Dead cells can then be quantified using epifluorescent microscopy (e.g., Rychtecký et al. 2014, Znachor et al. 2015, Kozik et al. 2019) with dead cells appearing green due to Sytox Green infiltrating the cells through compromised membranes, or with flow

cytometry where dead cells will have a higher green fluorescence signal. Samples that stain positive for Sytox are then compared to unstained control samples to determine proportions of dead cells which can be used to obtain mortality estimates. In using Sytox Green with flow cytometric analyses, there can be fluorescence "carryover": fluorescence emitted from Sytox Green-stained cells (i.e., 'green' or FL-1 channel fluorescence) 'bleeds' into channels used to detect the inherent fluorescence of living cells ('orange' or FL-2 channel fluorescence and to a lesser extent, 'red' or FL-3 channel fluorescence), making it difficult to either identify the original phytoplankton group that was stained, or to unambiguously distinguish the proportions of living and dead cells in environmental samples. An additional complication may be that different phytoplankton species do not stain to the same extent (Veldhuis et al. 1997, Peperzak and Brussaard 2011), limiting the ability to accurately detect taxon-specific cell mortality, particularly in mixed assemblages. In the Baltic Sea, Vaharanta et al. (2020) assessed mortality of phytoplankton by groups which were established from flow cytometric output based on red fluorescence and size estimates providing generalized summaries of similar phytoplankton responses. By monitoring group responses, differences in mortality estimates for groups were observed that would have been otherwise overlooked in a viability analysis of the entire community which found that viability was relatively stable. Vaharanta et al. (2020) also showed that concentrations of Sytox Green® stain may need to be scaled relative to chlorophyll *a* biomass estimates, as staining of cells at high densities was variable leading to potential overrepresentation of group viability.

Cell digestion is an alternative method for assessing cell viability that has been shown to be an effective way to determine cell viability for environmental samples (Agustí et al. 2006).

The cell digestion method removes dead cells from the sample by digestion, leaving living cells behind (Agustí et al. 2006, Llabrés and Agustí 2008, Rychtecký et al. 2014). The difference in flow cytometric counts of control and digested samples provides an estimate of the viable cells within the sample. This method eliminates background staining and other concerns that may be encountered using cell staining techniques but is more time-consuming compared to cell staining practices.

Objectives and hypotheses. The objective of this study was to determine whether declines in specific taxa or the detection of dead cells were associated with changes in abiotic parameters, e.g., light, temperature, nutrients. To address this objective, I worked to identify correlations of each abiotic parameter with flow cytometric counts of phytoplankton and dead cells, to better understand their influences on cell mortality in a natural phytoplankton community over a three-year period. To address this objective, I used flow cytometric counts of natural phytoplankton assemblages coupled with mortal staining methods, and hypothesized that: 1) If cell mortality is an important process involved in regulating phytoplankton populations in Estabrook Park Pond, then declines in the abundance of at least some phytoplankton groups will be accompanied by the appearance of large numbers of dead cells.; 2) Where dead cells appear during declines in phytoplankton groups, they will be correlated with thresholds or rapid change of at least one macronutrient; 3) Where dead cells appear during declines in phytoplankton groups, they will be correlated with thresholds or rapid change in temperature and/or irradiance; and 4) If species interactions are important in phytoplankton dynamics, abundances of phytoplankton groups will be correlated with the total abundances of other phytoplankton groups and/or dead cells.

MATERIALS AND METHODS

Study site and water sampling. Sampling was done at Estabrook Park Pond (43°01'N, 87°54'W), a small (0.45 ha) urban pond located in Shorewood, Wisconsin, USA with a maximum depth of 2.5 meters as described by Kozik et al. (2019). Sampling was carried out January 2014 – November 2016, weekly during open water periods (April-October) and monthly during periods of ice cover (November-March). Measurements of conductivity, dissolved oxygen concentration, pH, and temperature were made using a multiparameter sonde (YSI 6920 Yellow Springs Instruments, Yellow Springs, Ohio) which was calibrated monthly. Irradiance and temperature data were collected *in situ* using submersible sensors (Odyssey Irradiance Logger, Dataflow Systems, Ltd, New Zealand; HOBO Water Temperature Pro Model H20-001, Onset Computer Corporation, Massachusetts, USA) that were recovered quarterly to data.

During open-water periods, water was sampled using a 1 L swing sampler (as in Kozik et al. 2019; Nasco, Fort Atkinson, WI, USA) to collect surface (<0.5 m) water samples from six locations around the pond (Fig. 1). Samples were pooled in a 2 L clear polypropylene bottle to create a single representative sample, stored in the dark and transported to the laboratory for processing. During periods of ice cover, a hand auger (Strikemaster Ice Auger, 15.24 cm blade) was used to cut holes in the ice, and water was sampled approximately 0.5 m below the surface from a single site (Fig. 1) using a custom-built sampling bottle device (1 L Winter Estabrook Sampling Bottle Device, WESBD) which could be lowered and inverted through the hole cut in the ice.

Water collected was used for chlorophyll and nutrient analyses, in addition to flow cytometric counts of phytoplankton and viruses. Samples for total particulate phosphorus

analyses were taken as unfiltered collected pond water in replicate and frozen (-20°C) prior to analysis. All other nutrient analyses were done in replicate using water that was filtered through a glass fiber filter (25 mm, 1.0 µm nominal pore size, Pall A/E, New York) and frozen (-20°C) prior to analysis. Filters were stored in microcentrifuge tubes at -20°C and analyzed for chlorophyll *a* (chl *a*). 100 mL subsamples of water were passed through a 153 µm screen to remove large detrital particles and macro zooplankton. The filtrate was preserved with Lugol's iodine for later phytoplankton cell counts via microscopy. Flow cytometric counts were done as described below, with phytoplankton samples processed within 1 hour of collection.

Flow cytometry: phytoplankton. Flow cytometric counts were completed to quantify stained (dead) and unstained (living) particles, providing estimates of the cell mortality in a sample, which could then be correlated with environmental conditions. To complete these counts, water collected from the pond was passed through a 153 µm screen to remove large particles and prevent clogging of the flow cytometer. The filtrate was allocated into triplicate 1 mL samples that were counted (3-5 min., depending upon density of particles, 66 µL min^{-1}, 22 µm core size) to obtain particle counts of the natural phytoplankton community. Flow cytometric counts were made using a BD Accuri C6 flow cytometer (BD Biosciences, Michigan), outfitted with blue (488 nm) and red (640 nm) excitation lasers and four emission detectors (FL-1 533/30 nm, 'green'; FL-2 585/40 nm, 'orange'; FL-3 > 670 nm, 'red'; FL-4 675/25 nm, 'far red'). 90% attenuation filters were used on FL-1, FL-2 and FL-3. Counts were set to trigger on red fluorescence, with a threshold of 500 (relative units) on FL-3 so that only putative algal cells are counted. FL-3 versus FL-2 axes were used to distinguish and monitor eleven phytoplankton "groups" throughout the sampling period (Fig. 2). These axes were used as they each measure

fluorescence commonly associated with phytoplankton (FL-3: red fluorescence, FL-2: orange/phycobilin fluorescence), and provided good resolution among the groups. Additional replicate 1 mL samples were treated with 10 µL of diluted Sytox Green® (S7020, Invitrogen; Stock (50 µM), 1 µL:99 µL dilution, Sytox Green:DDW) and incubated in the dark for 15 min. at 18°C. Sytox Green® stains the DNA of cells with compromised membranes because the dye can permeate, and will fluoresce green under blue excitation (FL-1) as the cells are counted with the flow cytometer. Cells that have higher green fluorescence (typically an order of magnitude) relative to an unstained control sample were deemed dead. Groups previously identified using FL-3 and FL-2 parameters were separately assessed for their FL-1 signal relative to that of the unstained paired sample. Briefly, data for each gated group was extracted, re-plotted on FL-4 versus forward scatter axes and a FL-1 criterion applied to determine stained and unstained (i.e., dead and living) cells (see Appendix A).

Flow cytometry: viruses. Samples for viral counts were collected and prepared according to the method of Ma et al. (2013). Briefly, replicate 4.5 mL water samples collected from the pond were filtered through 0.22 µm membrane filters into cryotubes, fixed with 0.25% glutaraldehyde for 15 min., capped, flash frozen in liquid nitrogen, and stored at -70^{o}C until processing.

For counting, samples were thawed and transferred to flow cytometry. EDTA (5 mM) was added to each tube, followed by 5 µl mL^{-1} SYBR Green I stain (100X in DMSO). Samples were stained in the dark at 80^{o}C in a water bath for 10 min., then diluted with 0.02 µm filtered Milli-Q water to allow viruses to be counted at rates of <1,000 events s^{-1}.

Viruses were counted with an Accuri C6 flow cytometer, set to trigger on the green fluorescence (FL-1; 533/30 nm) of SYBR Green I. Each sample was processed in triplicate with a slow flow rate (14 µL min^{-1}) and core size of 10 µm. A minimum of 50,000 events were collected for each sample. An unstained set of samples using the same dilutions were used to correct for background FL-1 signal.

Chlorophyll and nutrient analyses. Chlorophyll pigments were extracted from frozen filters in 3 mL of 90 % acetone for 24 h at -20°C (Parsons et al. 1984). Samples were centrifuged to remove filter fragments and supernatant absorbance was read using a Beckman DU64 spectrophotometer using an acidification correction for phaeopigments.

Ammonium, nitrate, silicate, and soluble reactive phosphorus were analyzed using filtered water. Total phosphorus was analyzed using whole water. Ammonium was measured using the phenol hypochlorite method (Solórzano 1969; read at 640 nm). Nitrate was analyzed using the cadmium reduction method (*in* Parsons et al. 1984; read at 543 nm). Total particulate phosphorus samples were analyzed using the persulfate oxidation method (Menzel and Corwin 1965), while soluble reactive phosphorus (SRP) samples were analyzed using the colorimetric method (Parsons et al. 1984). Absorption measurements for soluble reactive phosphorus samples were made using an LKB BioChrom Ultrospec II (885 nm, 10 cm cell), while all other samples (250 µl) were placed in 96-well plates and read using a Molecular Devices VersaMax plate reader.

Phytoplankton analyses. Attempts were made to identify gated flow cytometric groups using a mixed approach of microscopy and sorting flow cytometry (Appendix B). To identify taxonomic groups present in the pond, preserved phytoplankton samples were selected for dates where

different gated groups were dominant in order to correlate flow cytometric counts with taxa identified from microscope counts. Samples were settled for 10 min. using an Utermöhl chamber and counted using random fields, transects or full chamber scans with an Olympus IX70 inverted microscope (200 – 400 x magnification). Phytoplankton were identified using the appropriate taxonomic keys (Prescott 1951, Whitford and Schumacher 1973, Nygaard 1976, Dillard 2007). In order to identify the particular taxa that comprised the gated groups identified using flow cytometry, two approaches were taken. First, sorting flow cytometry was done for unpreserved samples using a FACS-ARIA III (BD Sciences, New Jersey, USA). Cells were sorted directly into Lugol's preservative so that they were not affected by the saline sheath fluid and kept for later enumeration. Preserved sorted cells were enumerated via microscopy, using the method described above. Secondly, flow cytometric counts were correlated with microscopic observations to identify the phytoplankton within a particular gated group. We looked for samples in the time series that were dominated by a single gated group. The corresponding sample was settled and counted to identify the dominant group. Using this information, we then selected another sample where two groups dominated including the previously identified group, settling and counting for identification purposes. This was repeated until identifications were made for all eleven gated flow cytometry groups.

Statistical analyses. Pearson's correlational analyses (Zar 2009) were done to determine if declines in phytoplankton populations were associated with increasing dead cell counts using SigmaPlot 12.5. The influence of environmental parameters on phytoplankton community changes were investigated using multiple correlations between the cell abundance and dead cell counts of the different gated groups, and with different parameters across time in

individual years of (annual) and across the entire three-year time series (interannual). To account for the fact that the phytoplankton might have taken some time to respond to changing parameters, we also correlated the abundances and dead cell numbers with environmental parameters one or two weeks previously ("lagged" correlations of +1 or +2 weeks). To assess patterns in community abundances (total and dead cells) as they relate to changing environmental conditions throughout the study period, non-metric multidimensional scaling (NMDS) analyses were done using the PAST (PAleontological STatistics) package (Hammer et al. 2001) to synthesize a complex series of data and assess the strength of stressors (changing abiotic conditions) on the community. Additional correlational analyses were completed to identify potential relationships among abiotic conditions and dead cells throughout the dataset (annual and complete series).

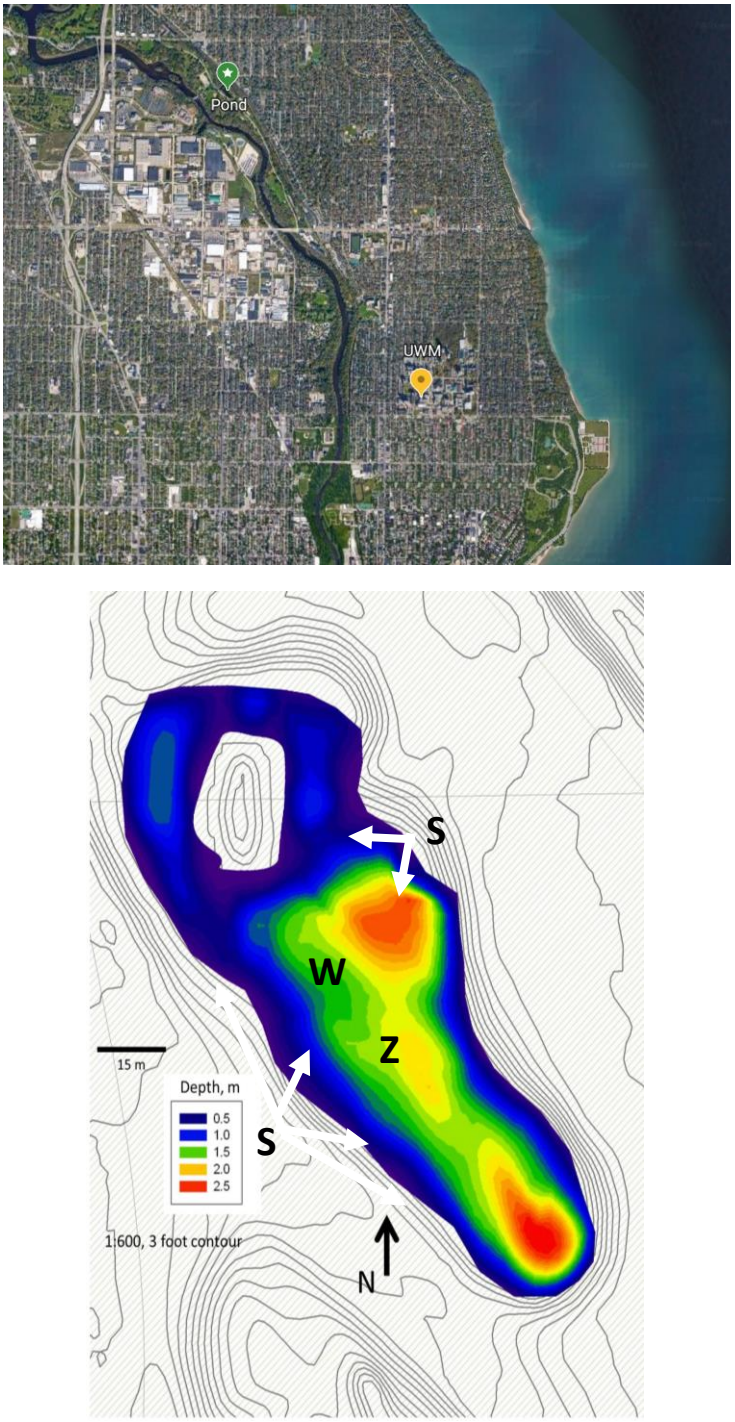

Figure 1. Field sampling location at Estabrook Park Pond, Milwaukee, WI. Upper panel: Map of the Milwaukee area, noting location of Estabrook Park Pond (green star) and UWM campus (yellow dot). Lower panel: Estabrook Park Pond bathymetric map. Approximate sampling locations are denoted by an "S" (summer) and with a "W" (winter). "Z" is the location where zooplankton were collected from for grazing experiments (*see* "Chapter 2: Biologically mediated mortality in phytoplankton: understanding grazing effects").

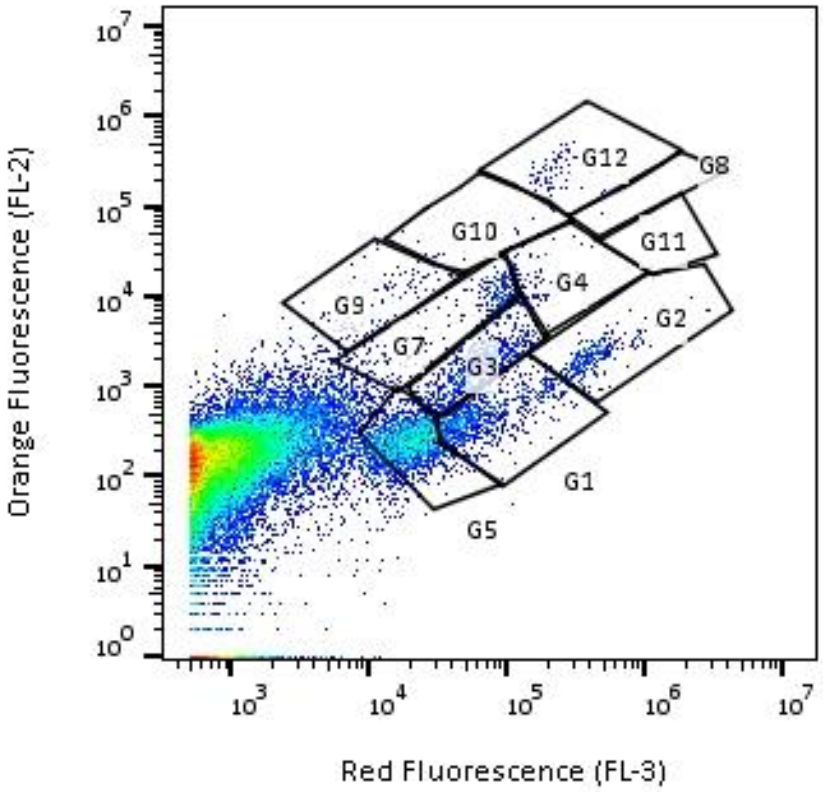

Figure 2. Example of flow cytometry analysis of eleven gated phytoplankton populations determined by fluorescence of FL-3/FL-2 (see Appendix A). Gates were created through manual assessment of all sampling dates. Each box was drawn utilizing FlowJo software, with each indicating a group of phytoplankton based upon their detected red and orange fluorescence.

RESULTS

Environmental conditions. Environmental data (irradiance, temperature, nutrients) were sampled and analyzed throughout the study period (Figs. 3-5 A-B). Regular, sinusoidal seasonal changes in irradiance were observed, though there were variations. For example, irradiance was low during both under ice periods and during the summer months, most notably in 2014, due to the in-pond sensor being covered by Eurasian milfoil (personal observation). Temperatures also followed seasonal patterns, increasing as the summer months approached, declining as the year progressed and were low during ice cover periods (Figs. 3-5A). Nitrate remained relatively low (< 1 µM) throughout the study period, though periodic pulses did occur commonly in the spring and summer (Figs. 3-5B). SRP and silicate (Figs. 3-5B) showed greater variations, with concentrations changing weekly, with occasional large pulses detected (autumn 2014, spring/autumn 2016).

Chlorophyll and flow cytometric cell count data. Fluctuations in chlorophyll *a* (Figs. 3-5C) and phytoplankton groups (Figs. 3-5D) occurred throughout the study period. In 2014, chlorophyll *a* biomass reached as summer maximum of 40 µg L^{-1} by day 200 (July 19) before declining. Phytoplankton biomass increased into the autumn, reaching an annual maximum of over 70 µg L^{-1} by day 290 (October 19) before rapidly declining as winter approached (Fig. 3C). In 2015, chlorophyll *a* biomass fluctuated between 10 and 20 µg L^{-1} throughout the winter and spring before increasing as summer approached (Fig. 4C). Summer biomass remained elevated compared to the other seasons in 2015, with biomass observed to be between 30 - 60 µg L^{-1} before decreasing to 5 - 10 µg L^{-1} in the autumn (Fig. 4C). Chlorophyll *a* biomass in 2016 reached

a maximum of 60 µg L^{-1} in the mid-Spring (day 140, May 20) before dropping to and stabilizing around 10 - 20 µg L^{-1} for the remainder of the year (Fig. 5C).

Like chlorophyll *a* biomass, flow cytometric cell counts of phytoplankton groups (with most probable identities given in Table 1) were dynamic, with groups increasing and decreasing in abundance throughout the study period (Fig. 3-5D). Increases in some of these group counts coincide with increases in chlorophyll *a* biomass suggesting that a particular group made up a large amount of the biomass.

In 2014, cell counts for phytoplankton groups remained relatively low (< 2000 cells mL^{-1}) throughout much of the year, although counts for four of the eleven groups were more dynamic during the summer months (Fig. 3D). In the summer, green algae (groups 1 and 5), *Cryptomonas* (group 3) and euglenoids (group 4) had periods where populations would increase and decrease, with euglenoids becoming the dominant (> 4000 cells mL^{-1}) population early in the summer (day 190, July 9), coinciding with the summer chlorophyll biomass maximum on day 200 (July 19). Green algae (group 5) increased shortly after to become dominant for a couple of weeks until *Cryptomonas* (group 3) became dominant late summer and throughout the autumn, reaching a maximum of 14000 cells mL^{-1} around day 280 (October 7), which coincides with the autumnal chlorophyll *a* biomass maximum of 70 µg L^{-1} (Fig. 3C).

In 2015 cell counts were dynamic as in 2014, although only groups 1, 3 and 5 (Table 1) were dominant at various times of the year (Fig. 4D). Green algae (group 1) were dominant at the beginning of 2015, reaching maxima of 6000 cells mL^{-1} in January (day 24) before declining as spring approached. In spring, *Cryptomonas* became dominant, reaching maxima of 6000 cells mL^{-1} as well. In the early summer (~ day 170, June 19) green algae (group 5) dominated

reaching 10000 cells mL^{-1} for the week coinciding with an increase in chlorophyll *a* biomass to 50 µg L^{-1} (Fig. 4C-D) before rapidly falling to 2000 cells mL^{-1} the following week, although chlorophyll *a* biomass remains elevated until late summer. Despite this decline, green algae remained the dominant group going into autumn with cell counts of ≤ 5000 cells mL^{-1}. In Autumn, *Cryptomonas* became the dominant group again at counts of ≤ 5000 cells mL^{-1} coinciding with lower chlorophyll *a* biomass (5 - 10 µg L^{-1}) (Figs. 4C-D).

In 2016, green algae and *Cryptomonas* (groups 1, 3 and 5; Table 1) dominated the phytoplankton population at various times throughout the year (Fig. 5D) as was observed in 2015 (Fig. 4D). *Cryptomonas* was dominant in early spring, reaching maxima of 6000 cells mL^{-1}. Green algae (group 1) dominated for a week in the spring (day 240, May 20) at 8000 cells mL^{-1}, with group 5 green algae becoming dominant (increasing to 10000 cells mL^{-1}) as the season changed to summer. The increases in abundance for all three groups of algae coincide with the spring chlorophyll *a* biomass maximum of 60 µg mL^{-1} on day 140 as well (Figs. 5C-D). Group 5 green algae remained dominant until late summer, though at lower densities (<4000 cells mL^{-1}), when *Cryptomonas* became dominant (≤ 2000 cells mL^{-1}) for the remainder of the year.

Statistical comparisons of environmental conditions and total abundance flow cytometric data. Throughout the study period cell abundances of six of eleven groups (groups 5, 8-12; *see* Table 1 for taxonomic identification) correlated with environmental conditions, albeit weakly ($r < 0.6$ in most cases; Table 2). Correlations among environmental conditions and cell counts were overall weaker when assessed interannually (across all three years) compared to annually (Table 2). Temperature positively correlated weakly ($r = 0.4 - 0.56$) with three of eleven groups (green algae/desmids - groups 5, 9, 10; Table 2) when assessed globally, compared to the

annual analyses where in 2015 only group 5 green algae correlated negatively (r = -0.57) with temperature. In 2016 temperature positively correlated (r = 0.59-0.71) with group 5 green algae and group 10 desmids (Table 2). Irradiance followed a similar relationship with flow cytometric count data, weakly correlating (r = 0.5) with group 5 green algae when assessed globally compared to annual analyses that revealed a negative correlation with pennate diatoms (group 2) in 2014 (Table 2). Irradiance did not correlate with any groups in 2015, although in 2016 the delayed responses (irradiance+1 and +2) correlated positively with three groups (green algae and pennate diatoms - groups 1, 2, 5; Table 2). Nutrients correlated poorly with flow cytometric counts overall, though SRP correlated (r = 0.6) with two of eleven groups (groups 8 & 12 – desmids and cyanobacteria, respectively) when assessed globally (Table 2) compared to the annual analyses where group 12 (cyanobacteria) in 2015 (r = 0.62) and group 1 (green algae) in 2016 (r = 0.58) correlated with SRP. Ammonium concentrations did not correlate at the global level but did reveal correlate (r = 0.65) in 2014, while nitrate negatively correlated with cell abundances of groups 1 and 5 (green algae) in 2016.

Flow cytometric cell death estimates. In 2014 the proportion of cell counts that were identified as dead following cell staining was dynamic throughout the year, with group 12 (cyanobacteria) measuring as 100 % dead for most of sampling points over the year (Fig. 3E). Dead cell count proportions for groups 1, 3, 4, 7, 10 and 11 (*see* Table 1 for general taxonomic classification) were dynamic throughout the year, ranging from 20 to 80 % dead. Remaining groups were estimated to have less than 20 % of cells dead.

In 2015, dead cell proportions were negligible (near zero) for most of the year, although dead cell proportions were dynamic in the winter, as well as late spring and throughout the

summer months (Fig. 4E). Groups 8-12 (green algae, diatoms and cyanobacteria, Table 1) were detected as dead most frequently, with cyanobacteria (group 12) reaching 100 % dead late in the winter, spring, and summer. Desmids in group 8 also measured 100% dead in mid-January (day 24, January 24) and in early autumn. Dead cells for groups 9-11 ranged from 0 to 60 % of the count, though dead proportions were most commonly < 20 % of the cells.

The proportion of dead cells counted in 2016 was negligible with most groups having less than 5% of cells stain as dead (Fig. 5E). Exceptions to this include groups 1, 10, 11 and 12 (green algae, diatoms and cyanobacteria; Table 1) which ranged from 5 to 10 0% dead cells at various times of the year. Large diatoms in group 11 reached 100 % dead three times during the spring, while group 8 desmids reached 100 % dead in the summer twice (days 200 and 225, July 18 and August 12). Group 12 cyanobacteria measured as 100% dead in late autumn. Group 1 green algae reached 50% dead in mid-spring, while Group 10 desmids reached 60% dead in mid-summer (day 200, July 18).

Statistical comparisons of environmental conditions and dead cell flow cytometric data.

Proportions of dead cells were dynamic throughout the study period, but few environmental conditions correlated with dead cells observations (Tables 3). Environmental conditions correlated with total abundances on some occasions with temperature, irradiance and some nutrients though the correlations were weaker in the global analysis compared to the annual analyses. Globally, correlations among temperature and irradiance were found to be negative (r= -0.35 to -0.45) as they related to proportions of dead cells (Table 3). Five of eleven groups (groups 3, 4, 7, 8 and 12; *see* Table 1 for taxonomic identification) were negatively correlated with temperature at the time of observation, but only three of these groups (7, 8 and 12 –

Peridinium, desmids and cyanobacteria) negatively correlated a week later (temperature +1). Irradiance was negatively correlated with group 9 green algae alone (Table 3), although when looking at the subsequent weeks, two groups (9 and 10, both green algae) were negatively correlated with irradiance (r= -0.33 to -0.38). Total phosphorus +1 correlated positively (Table 4) with dead cells for two of the groups (11, 12 - large diatoms and cyanobacteria), while silicate +2 correlated with group 2 (pennate diatoms).

In comparison, annual analyses revealed few correlations between environmental conditions and proportions of dead cells, although most correlations that were identified were negative (Table 3). In 2014, SRP had strong positive correlations with two groups (7, 12 – *Peridinium* and cyanobacteria) both at the time of observation and a week after (Table 3). Nitrate had a positive correlation as well with only green algae (r = 0.68). Comparatively in 2015, most correlations were negative. Temperature negatively correlated most strongly with proportions of dead cells (6 groups) with fewer groups correlating at time points one (+1) or two (+2) weeks in the future (Table 3). Silicate concentrations two weeks after observation positively correlated with one group (Table 3).

Flow cytometric counts and viruses. Chlorophyll *a* biomass and viral counts were variable (Figs. 3-4C). Lower chlorophyll *a* biomass in 2014 appeared to coincide with higher viral counts (and vice versa; Fig. 3C), though there was not statistically significant relationship ($p > 0.05$). This was a similar observation to that of Hanson et al. (2017) in Estabrook Park Pond. In contrast, chlorophyll *a* biomass and viral counts positively correlated in 2015 (Fig. 4C, $p < 0.05$).

Correlations between taxa. Phytoplankton groups were dynamic throughout the study period, with observations of group correlations among total abundances of phytoplankton groups (Table 4). Global analyses of total phytoplankton group abundance suggested that one weak (r = 0.38) positive correlation existed between pennate diatoms and desmid species (groups 2 and 5, Fig. 6A) over the three-year study period, suggesting that as pennate diatoms became more abundant, so did desmid species. In assessing relationships annually, only 2014 and 2016 communities had positive correlations between total abundances of phytoplankton groups. In 2014, green algae and pennate diatom (groups 1 and 2) abundances frequently correlated with desmids, chain-forming diatoms, and cyanobacteria (r = 0.67 to 0.85, groups 8, 11 and 12), while in 2016 only dinoflagellates positively correlated with cyanobacteria (r = 0.76).

In assessing the relationship between total abundance of phytoplankton groups and dead cell abundance, global analyses revealed five of eleven groups having weak positive correlations (r = 0.3 to 0.59) with dead cells abundance (Table 5). Correlations were stronger in the annual analyses (Table 5). In both 2014 and 2015, four groups (groups 1, 8, 11 and 12 and groups 1, 4, 8 and 11, respectively; *see* Table 1 for identification) were positively correlated (r = 0.6 to 0.9) with dead cell counts of uncommon/low abundance phytoplankton groups. In 2014, all significant correlations of abundance were with the dead cells of dinoflagellates (group 7; ex. Fig. 6C). In 2016, three groups had positive correlations with dead cells abundances. Green algae and cyanobacterial (groups 1 and 12, respectively; r = 0.58 to 0.94) abundances positively correlated with dead cell counts of low abundance groups, while pennate diatom (group 2) abundance correlated with dead cell abundances of *Cryptomonas* (group 3, r = 0.70).

Multivariate analyses. As an alternative to correlation analyses, non-metric multidimensional scaling (NMDS) analyses were done to try and find relationships among taxa that could be related to environmental variables. NMDS plots were done using the Manhattan method for both interannually and annually for both total abundances (Fig. 7A-D) and dead cell (Fig. 8A-D) relationships (7 environmental variables). Analyses were done using the gated phytoplankton groups determined by flow cytometry and extracting cell counts (total abundance and dead cells) to test relationships with the environmental variables including temperature, irradiance, and nutrient (phosphorus, silicate, nitrate, ammonia) concentrations. Though clear patterns did not appear in NMDS analyses, relationships between total abundance and environmental conditions were more similar (stress levels of 0.07 – 0.08) compared to those of dead cells with the same parameters (stress levels > 0.15).

Despite the lack of clear patterns in most parameters' effects on total abundances, temperature, and irradiance both commonly correlated with changes in phytoplankton communities, having the largest differences among the data, but those differences were inconsistent across the years (Fig. 7A-D). For example, in 2014 (Fig. 7B) light accounted for variation in abundances during the summer compared to temperature accounting for variations in the spring, compared to 2015 and 2016 (Figs. 7C-D) where light and temperature accounted for variations along similar vectors. This could be due to decreased light in the pond during the summer of 2014 from observed aquatic macrophyte growth. Dissolved phosphorus (SRP) stressors were similar in spring 2015-2016 when observed interannually (Fig. 7A) but annual analyses reveled SRP to correlate with autumn abundances in 2015 (Fig. 7C) compared to spring in 2016 (Fig. 7D). The influence of total phosphorus was similar throughout the study years

(2014-2016, Fig. 7A) for summer and autumn. These observations mirror what was observed in correlation analyses (Table 2) which indicated that total abundances of phytoplankton groups were weakly correlated with these parameters.

Observations of NMDS analyses relating to dead cells did not show much similarity interannually (Fig. 8A) or among years (Fig. 8B-D). Interannual analyses revealed that 2015-2016 data were most similar in their relationship with environmental conditions compared to 2014 (Fig. 8A). Annual analyses revealed that there was some seasonal variation in stressors leading to dead cells, but specific environmental conditions do not stand out as main stressors (Figs. 8B-D). The major axis that distinguished taxa with dead cells in summer was correlated with ammonium concentration in 2014, while total phosphorus correlated with dead cells most in autumn (Fig. 8B). Temperature had a variable influence, though most strongly related with the spring. These stressors contradict what was observed in correlation analyses which found dissolved phosphorus and nitrate to correlate with dead cells for groups of phytoplankton that year (Table 3). Dead cells in 2015 exhibited relationships with environmental parameters by seasons (Fig. 8C), with temperature and light having the strongest relationships in autumn. In 2016, there was high variability in seasonal distribution of dead cells, with no specific environmental condition standing out as a main stressor (Fig. 8D).

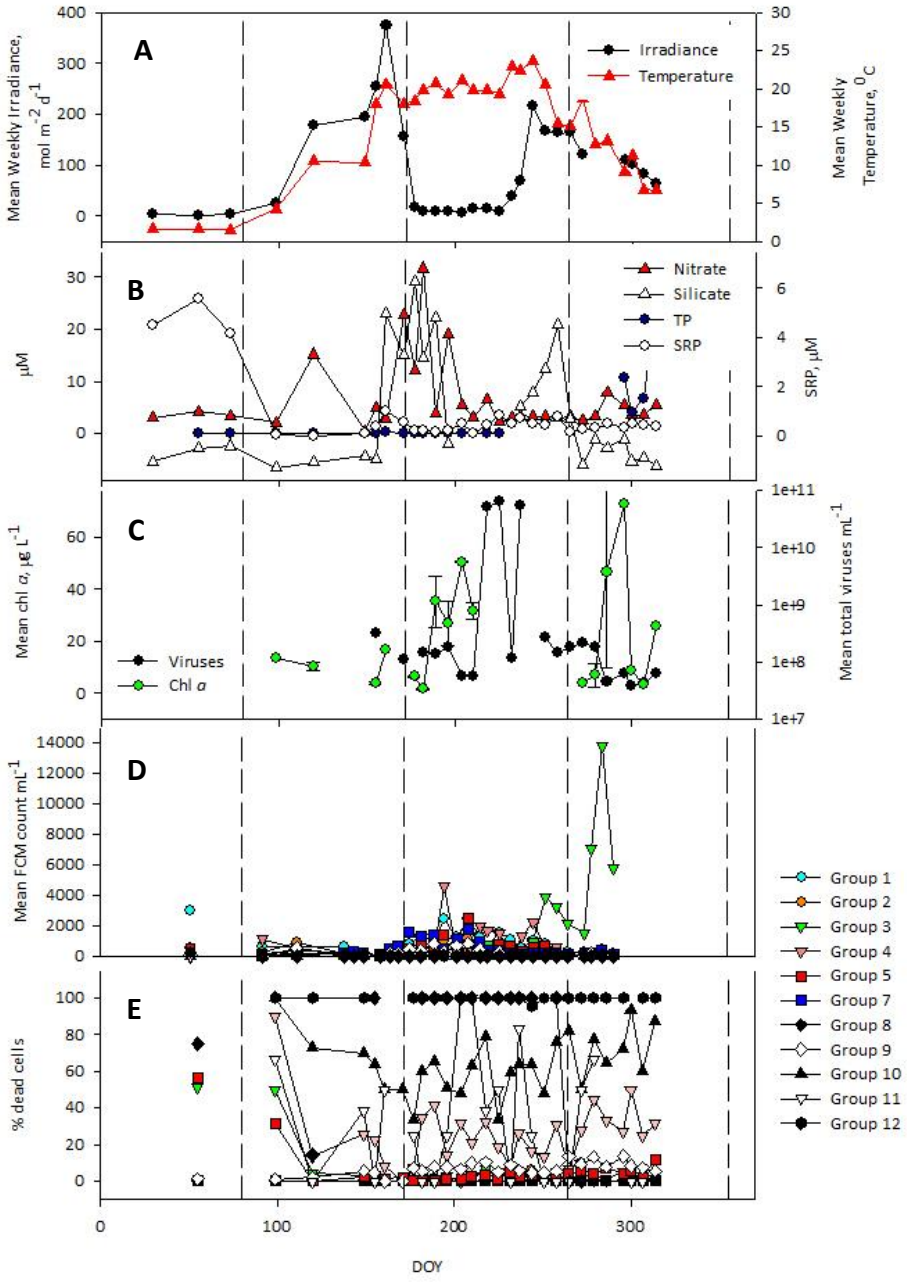

Figure 3. Field observations of abiotic conditions and phytoplankton community in Estabrook Park Pond, 2014. A. Mean weekly irradiance and temperature *in situ*. B. Pond nutrient (nitrate, silicate, TP, SRP) concentrations. C. Mean chlorophyll *a* biomass and viral abundance. D. Mean flow cytometric counts of phytoplankton group abundance. E. Cell mortality estimates by group as a percentage of dead cells relative to group cell abundance. Dotted vertical lines indicate meteorological seasons (Spring, Summer, Autumn, Winter). "DOY" means day of year.

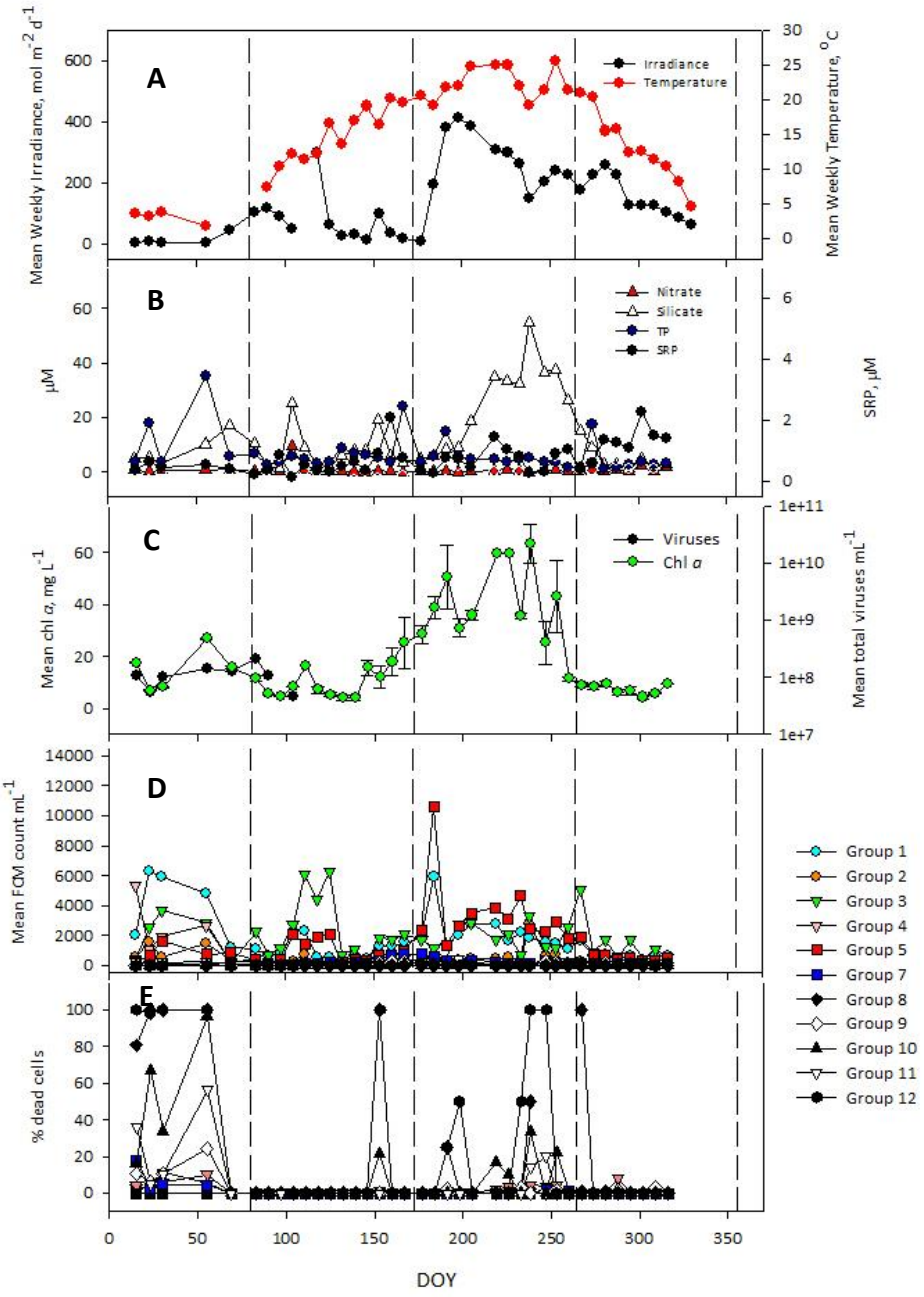

Figure 4. Field observations of abiotic conditions and phytoplankton community in Estabrook Park Pond, 2015. A. Mean weekly irradiance and temperature *in situ*. B. Pond nutrient (nitrate, silicate, TP, SRP) concentrations. C. Mean chlorophyll *a* biomass and viral abundance. D. Mean flow cytometric counts of phytoplankton group abundance. E. Cell mortality estimates by group as a percentage of dead cells relative to group cell abundance. Dotted vertical lines indicate meteorological seasons (Spring, Summer, Autumn, Winter). "DOY" means day of year.

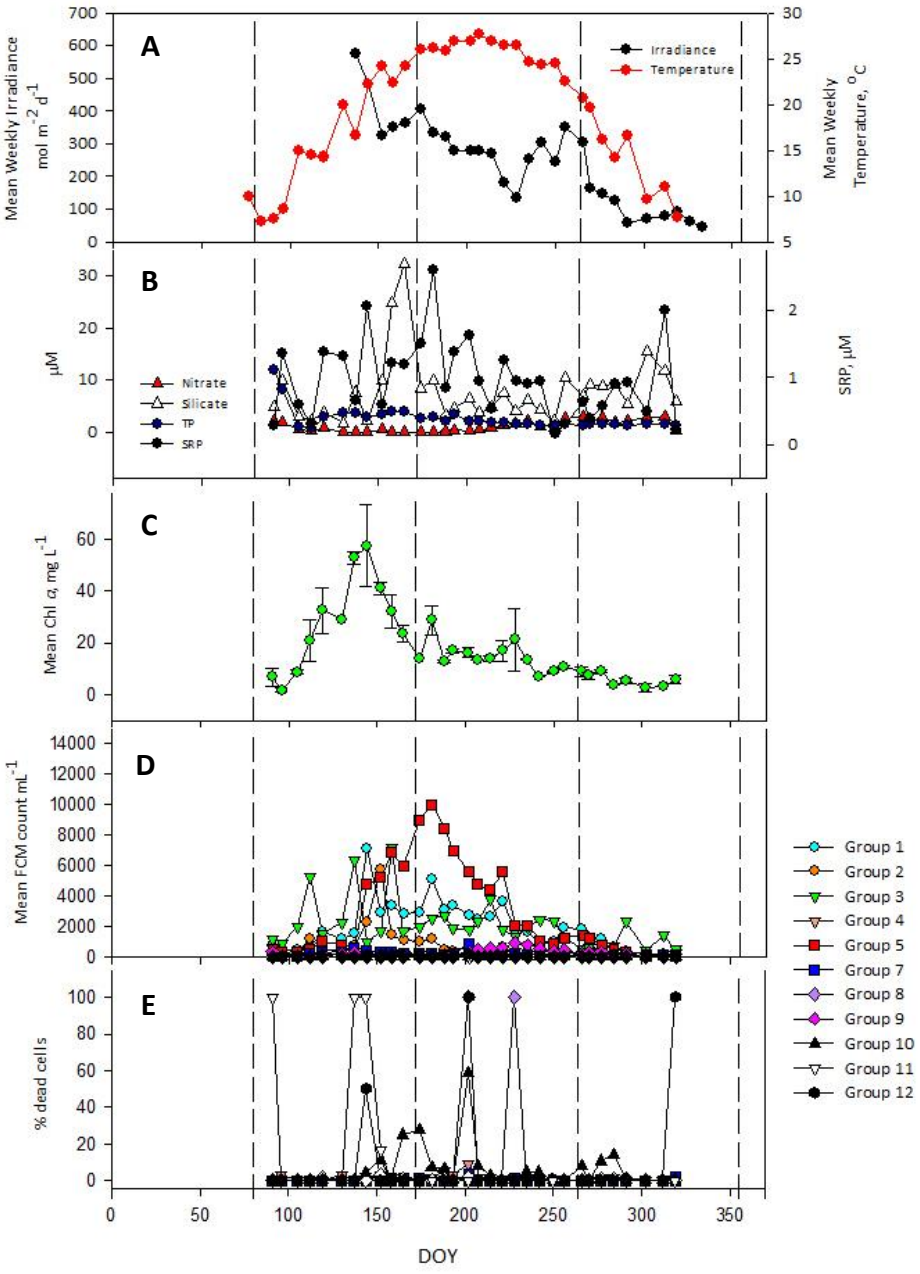

Figure 5. Field observations of abiotic conditions and phytoplankton community in Estabrook Park Pond, 2016. A. Mean weekly irradiance and temperature *in situ*. B. Pond nutrient (nitrate, silicate, TP, SRP) concentrations. C. Mean chlorophyll *a* biomass. D. Mean flow cytometric counts of phytoplankton group abundance. E. Cell mortality estimates by group as a percentage of dead cells relative to group cell abundance. Dotted vertical lines indicate meteorological seasons (Spring, Summer, Autumn, Winter). "DOY" means day of year.

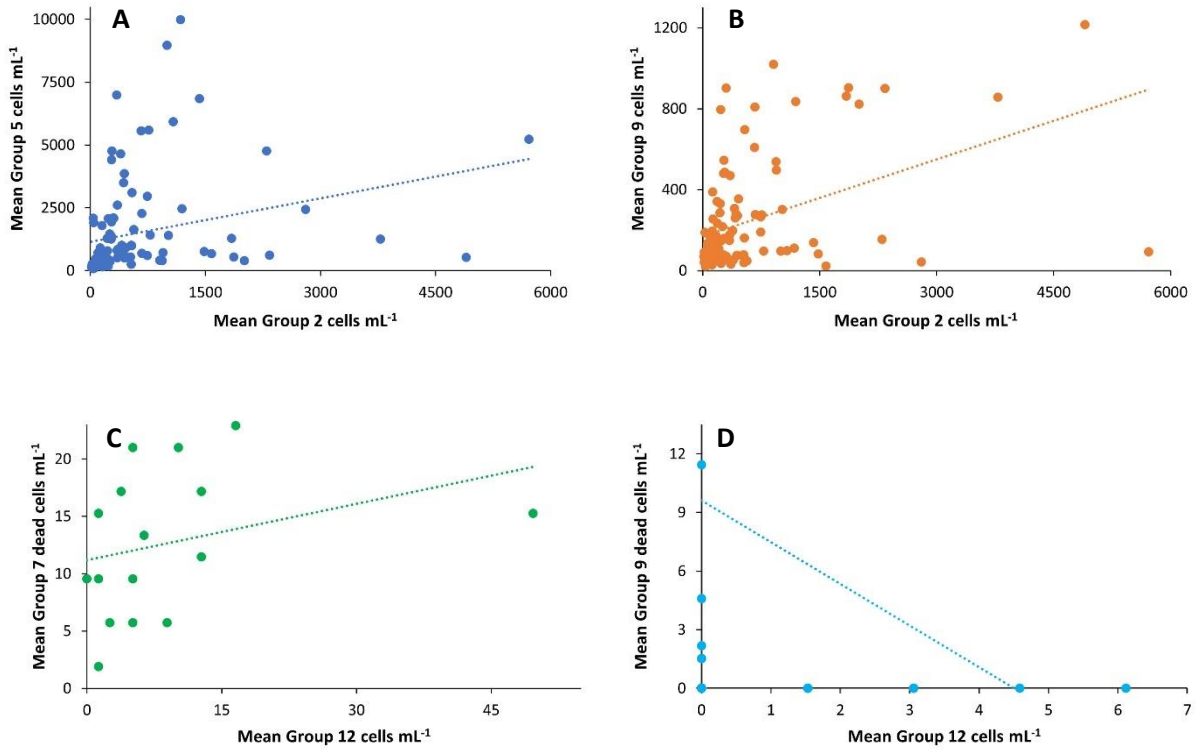

Figure 6. Examples of observed correlations as measured with flow cytometric measurements of the phytoplankton community at Estabrook Park Pond. A. Positive correlation of total abundance of *Synedra* (group 2) and green desmids (group 5) as determined by global analysis of flow cytometric data. B. Positive correlation of total abundance relationships of *Synedra* (group 2) and *Chlamydomonas* (group 9) as determined by global analysis of flow cytometric data. C. Positive correlation of total abundance of cyanobacteria (group 12) and dead cells of dinoflagellates (group 7) from 2014 as determined by analysis of flow cytometric data. D. Negative correlation of total abundance of cyanobacteria (group 12) and dead cells of *Chlamydomonas* (group 9) from 2016 as determined by analysis of flow cytometric data.

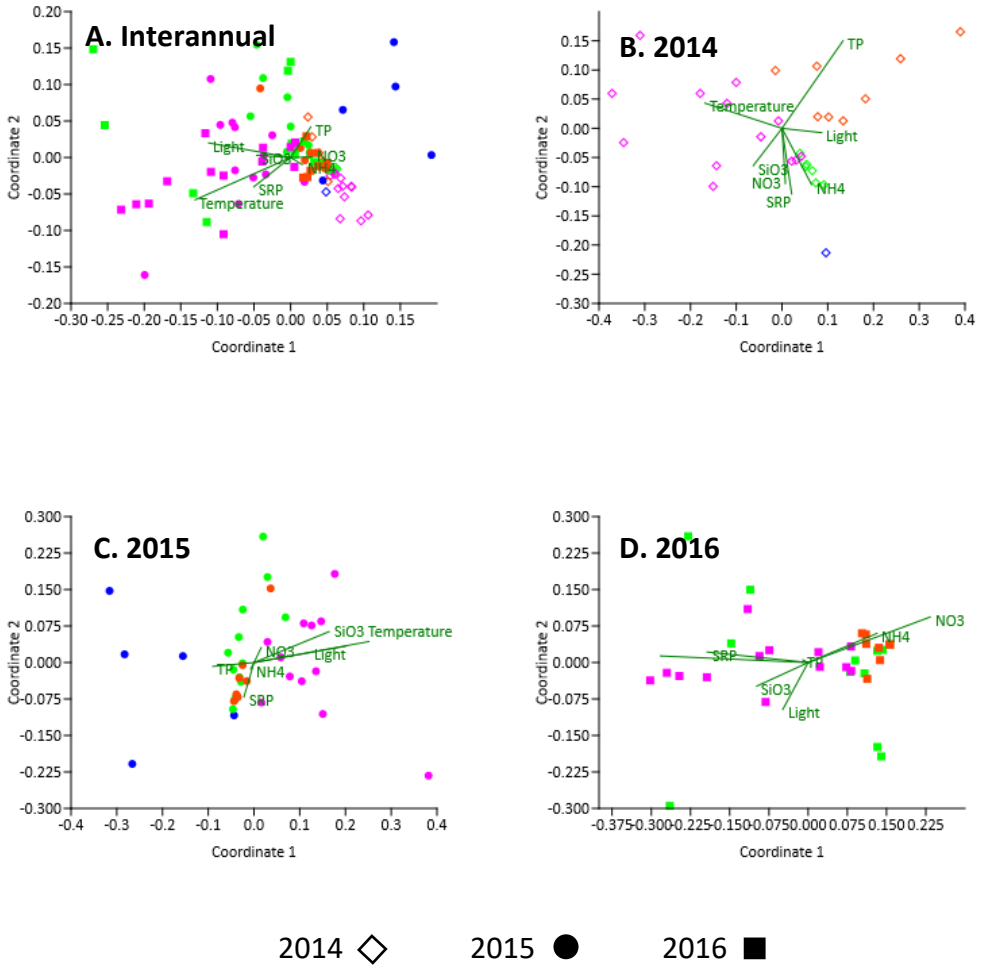

Figure 7. Non-metric multidimensional scaling analysis for three-year time series for total abundances and seven environmental conditions. A. Interannual analysis of total abundance of groups identified by flow cytometry (stress = 0.07). B. 2014 annual analysis (stress = 0.07). C. 2015 annual analysis (stress = 0.08). D. 2016 annual analysis (stress 0.07). Symbol coloration indicates season that data points were collected in: Pink – Spring, Green – Summer, Red – Autumn and Blue – Winter.

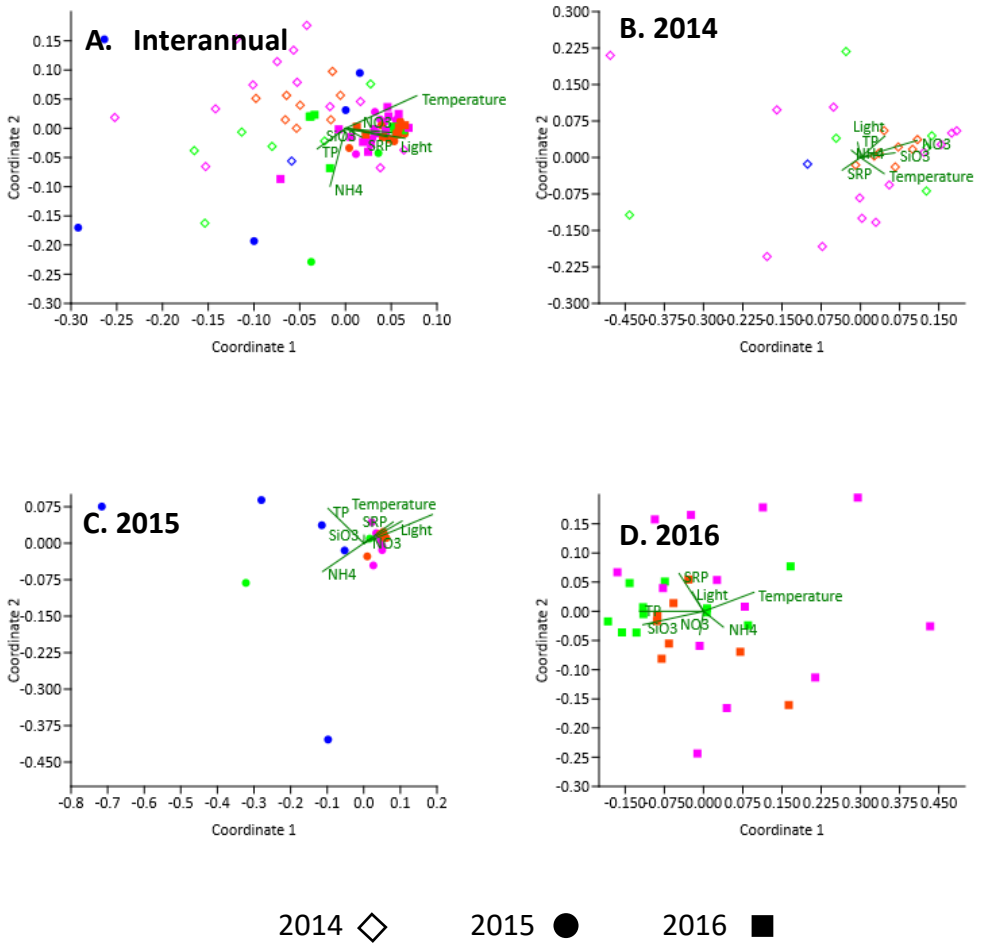

Figure 8. Non-metric multidimensional scaling analysis plot for analysis of the relationship between environmental conditions and dead cells of phytoplankton groups. A. Interannual analysis of total abundance of groups identified by flow cytometry (stress = 0.24). B. 2014 annual analysis (stress = 0.19). C. 2015 annual analysis (stress = 0.21). D. 2016 annual analysis (stress = 0.31). "TP" represents total phosphorus. Symbols indicate seasons that data points were collected in: Pink – Spring, Green – Summer, Red – Autumn and Blue – Winter.

Table 1. Summary of identified phytoplankton by flow cytometric (FCM) gated group. Taxonomic identification completed via microscopy. See Appendix B for full species list.

FCM Group Number	Taxonomic Identification
1	Miscellaneous Green Algae
2	Pennate diatoms (i.e., *Synedra*)
3	*Cryptomonas* sp.
4	*Euglena*
5	Green Algae (i.e., *Ankistrodesmus, Scenedesmus*)
7	Dinoflagellates (i.e., *Peridinium, Ceratium*)
8	Green Algae – Desmids (i.e., *Cosmarium*)
9	Green Algae (i.e., *Chlamydomonas, Dictyosphaerium*)
10	Green Algae – Desmids (i.e., *Closterium, Staurastrum*)
11	Large diatoms (i.e., *Tabellaria, Fragilaria*)
12	Chain-forming, colonial Cyanobacteria (i.e., *Anabaena, Microcystis*)

Table 2. Summary of statistically significant relationships (as r-values) between environmental parameters and total abundance of different phytoplankton groups (identified by flow cytometry, FCM). “Environmental Parameter +1 or “+2” indicates lagged data where total abundances were compared to environmental data from one (+1) or two (+2) weeks before abundances were observed. “TP” indicates total phosphorus. “SRP” indicates soluble reactive phosphorus. Interannual analyses contain between 98 and 108 time points for the time between 2014-2016 ($p<0.005$, using a Bonferroni correction based on 96 individual correlations). Annual analyses include between 25 and 40 time points, dependent upon the year ($p<0.001$, using a Bonferroni correction based on 35 individual correlations).

		FCM Group Number – *Total abundance*										
	Environmental Parameter	1	2	3	4	5	7	8	9	10	11	12
Interannual analysis	Temperature					0.56			0.41	0.45		
	Temperature +1					0.52			0.39	0.44		
	Temperature +2					0.47			0.40	0.43		
	Irradiance					0.51						
	Irradiance +1					0.53						
	Irradiance +2					0.52						
	TP +1										0.43	
	SRP							0.64				0.62
	SRP +1							0.48				0.46
Annual analysis												
2014	Irradiance +1		-0.63									
	TP +2			1.0								
	SRP							0.93				0.94
	SRP +1							0.68				0.67
	Ammonium							0.65				
2015	Temperature				-0.57							
	TP							0.65				
	SRP +2											0.62
	Silicate		0.54									
2016	Temperature	0.65				0.71				0.59		
	Temperature +1					0.64				0.61		
	Temperature +2					0.56				0.65		
	Irradiance +1	0.84	0.66			0.66						
	Irradiance +2	0.75	0.71			0.69						
	SRP	0.58										
	Nitrate					-0.58						
	Nitrate +1	-0.69				-0.70						
	Nitrate +2	-0.75				-0.76						

Table 3. Summary of statistically significant relationships (as r-values) between environmental parameters and dead cell abundance of different phytoplankton groups (identified by flow cytometry, FCM) for study period 2014-2016. Interannual analyses contain between 98 and 108 time points for the time between 2014-2016 ($p<0.005$, using a Bonferroni correction based on 96 individual correlations). The data set contains between 98 and 108 time points for the time between 2014-2016. Annual analyses include between 25 and 40 time points, dependent upon the year ($p<0.001$, using a Bonferroni correction based on 35 individual correlations). "TP" indicates total phosphorus while "SRP" indicates soluble reactive phosphorus. "Environmental Parameter +1 or "+2" indicates lagged data where dead cells were compared to environmental data from one (+1) or two (+2) weeks before dead cells were observed.

		FCM Group Number – *Dead cells*										
	Environmental Parameter	1	2	3	4	5	7	8	9	10	11	12
Interannual analysis	Temperature			-0.35	-0.38		-0.38	-0.40				-0.45
	Temperature +1						-0.37	-0.36				-0.40
	Irradiance								-0.38			
	Irradiance +1								-0.38	-0.36		
	Irradiance +2								-0.38	-0.33		
	TP +1										0.37	0.41
	Silicate +2		0.41									
Annual analysis												
2014	SRP						0.85					0.93
	SRP +1						0.77					0.77
	Nitrate +1	0.68										
2015	Temperature				-0.63		-0.55	-0.54	-0.66	-0.54		-0.56
	Temperature +1				-0.53		-0.52		-0.59	-0.52		
	Temperature +2								-0.54			
	Silicate +2		0.55									

Table 4. Summary of statistically significant relationships (as r-values) between total abundances of different phytoplankton groups (identified by flow cytometry, FCM). Data shown are significant at the equivalent of $p<0.05$ ($p<0.001$, using a Bonferroni correction based on 98 individual correlations for the interannual analysis, 25-40 for annual analysis).

		FCM Group Number – *Total abundance*										
	FCM Group Number – *Total abundance*	1	2	3	4	5	7	8	9	10	11	12
Interannual analysis	2					0.38						
Annual analysis												
2014	1							0.67			0.85	0.67
	2					0.78			0.79	0.68		
	11											0.71
2016	7											0.76

Table 5. Summary of statistically significant relationships (as r-values) between total abundance and dead cell abundance of different phytoplankton groups (identified by flow cytometry, FCM). Data shown are significant at the equivalent of $p<0.05$ ($p<0.001$, using a Bonferroni correction based on 98 individual correlations for the interannual analysis, 25-40 for annual analysis).

		FCM Group Number – *Dead Cells*										
	FCM Group Number – *Total abundance*	1	2	3	4	5	7	8	9	10	11	12
Interannual analysis	1						0.36			0.38		
	4								0.38			0.61
	8		0.31				0.59					
	11	0.36		0.40								0.52
Annual analysis												
2014	1						0.67					
	8						0.89					
	11						0.61					0.71
	12						0.89					
2015	1						0.67		0.66	0.72		
	4							0.82				
	8								0.73			
	11								0.59			0.55
2016	1											0.58
	2			0.70								
	12								0.99			

DISCUSSION

The phytoplankton community in Estabrook Park Pond was variable and dynamic, with eleven representative groups identified and monitored for their abundance and cell mortality responses over changing abiotic conditions for three years. The study provided an opportunity to further resolve observations made by Kozik et al. (2019), whose seasonal study provided a snapshot of community dynamics, focusing on a subset of species found in the pond. With flow cytometric techniques, the present study afforded the opportunity to observe dynamics of the entire community and relate them to an extensive abiotic dataset to identify patterns of responses in representative groups. The study reinforced the idea that changing abiotic factors do not necessarily tend to correlate with changes in community dynamics or cell mortality, suggesting that biotic influences such as grazing or inter-taxon relationships, rather than abiotic factors may be important in shaping the phytoplankton community.

Phytoplankton community dynamics and abiotic factors. Seasonal variability in chlorophyll *a* biomass was observed throughout the study period, which is to be expected given seasonal variability in temperature and irradiance, though annual maxima of chlorophyll *a* biomass were reached at different time points in each study year. The driver of the interannual variation of chlorophyll biomass observed was unclear as abiotic parameters did not correlate with the biomass measured. Using flow cytometric data to quantify phytoplankton groups provided an opportunity to tease apart the biomass observations a bit more, providing an opportunity to identify whether dynamics of specific phytoplankton groups were related to changing abiotic conditions.

Seasonal variation in abiotic conditions occurred as expected most years, i.e., increasing light and temperature moving from winter towards summer, nutrient levels remained relatively stable throughout, with no distinctive thresholds or rapid changes in conditions observed. The lack of variation in abiotic conditions throughout the study period made it difficult to assess the effect of these factors on the abundance of phytoplankton groups and appearance of dead cells within the community. Temperature and irradiance negatively correlated with total dead cell abundances of some phytoplankton groups (Table 3), indicating that thresholds for species may be reached as the year progresses, something that Kozik et al. (2019) considered when observing the increased abundance of dead cells after day 270. While the present study exhibits a similar pattern of cell death, with dead cell counts for some groups negatively correlating with changes in temperature and irradiance, higher proportions of dead cells were observed in the winter and spring. Temperature negatively correlated with total abundances of phytoplankton, the opposite of what would be expected if considering overall biomass as warmer temperatures tend to correlate with increased phytoplankton biomass, however this study focuses on how individual groups of phytoplankton are responding to temperature which can vary given taxon-specific temperature thresholds. For example, Tan (2011) found that green algae and diatoms were able to grow at cooler temperatures compared to that of cyanobacteria, but once above 19.5^{o}C cyanobacteria became dominant. In my study, cyanobacteria, as well as cryptomonads and green algal (euglenoids, desmids) abundances declined with an increase in temperature. The maximum pond temperature did not exceed 25^{o}C, which would not be considered limiting for phytoplankton growth (Butterwick et al. 2005). Furthermore, cyanobacteria were found to have some of the highest percentages of dead cells at the warmest temperatures, though the

maximum pond temperature was not far off from an optimal growth temperature of 29.2^{o}C (Lürling et al. 2013).

In evaluating the effect of irradiance on the community, it is important to note that light is a factor that can affect phytoplankton taxa differently as they may have different light requirements. For example, cryptomonads are often found lower in the water as their photosynthetic pigments are capable of absorbing light that penetrates deeper into the water, although they are capable of acclimating to higher irradiances when exposed to them (Litchman and Neale 2005) compared to green algae (among others) that have differing light requirements (Richardson et al. 1983). Irradiance in the study presented here was weakly and negatively correlated with the amount of dead algal species, including *Chlamydomonas* and large desmids suggesting that irradiance does not influence phytoplankton mortality in our system. This was reinforced with annual analyses which irradiance was not correlated with cell death in any year. This observation is similar to what Kozik et al. (2019) found in their seasonal study of the pond where irradiance did not have a significant effect on the phytoplankton populations studied.

In contrast, nutrients (i.e., TP, SRP, nitrate) tended to positively correlate with observed population dynamics. As summarized in Table 3, nutrients positively correlated with dead cell abundances, particularly for dinoflagellates (group 7), chain-forming diatoms (group 11) and cyanobacteria (group 12), indicating that with an increase in nutrients more dead cells were observed. This could be due in part to dead cells releasing nutrients back into the environment as they undergo lysis, which could alleviate nutrient limitation of other phytoplankton in the system, as observed by Gobler et al. (1997). If remaining phytoplankton were nutrient-limited,

we would expect to see an increase in abundances of other phytoplankton groups as more nutrients became available, though except for 2014, our data do not suggest that an increase in phytoplankton abundance occurred with increased nutrient availability, meaning that the phytoplankton were not nutrient-limited throughout the study.

Correlations between taxa. Phytoplankton dynamics observed could be due in part to interactions among phytoplankton taxa within Estabrook Park Pond. Previously, Kozik et al. (2019) observed what were considered potential correlations among species but could not fully explore these relationships given the time-limited data set (single year, only summer/autumn). In the study presented here, correlations among taxa were observed (Tables 4-5) which would suggest that phytoplankton may be releasing chemicals into the environment for allelopathic and/or communicative purposes. Interestingly, the phytoplankton groups that were frequently found to be affected by other groups tended to be those we would associate with toxin/allelochemical production that would result in cell death of others (e.g., Sukenik et al. 2002, Vardi et al. 2002). For example, when looking at relationships throughout the study, the total abundance of pennate diatoms (group 2, i.e., *Synedra*) related positively with abundances of desmid and *Chlamydomonas*-like green algae, as did the total abundance of dinoflagellates and cyanobacteria. The later interaction is interesting to note as previous studies (Sukenik et al. 2002, Vardi et al. 2002) have identified potential allelopathic interactions among dinoflagellates and cyanobacteria. Sukenik et al. (2002) observed positive correlations between *Microcystis* and *Peridinium* in Lake Kinneret which upon further study, revealed that *Peridinium* exhibited decreased fluorescence when exposed to spent *Microcystis* medium, indicating inhibition of photosynthesis. Vardi et al. (2002) found that *Peridinium* had an increase in reactive oxygen

species (stress indicator) when exposed to spent *Microcystis* medium, but also observed a response with *Microcystis* when exposed to spent *Peridinium* medium. *Microcystis* underwent cell death and increased production of microcystin, an allelochemical that can induce the generation of reactive oxygen species, an indicator of cellular stress in target species (i.e., *Peridinium*) in this instance. They concluded that this interaction may indicate that dinoflagellates and cyanobacteria communicate via allelochemicals. Interestingly, our study showed a positive correlation between the abundance of both species, rather than the negative effects that both studies observed. A closer look at the relationship between the two groups did reveal a correlation between the abundance of cyanobacteria and the generation of dead dinoflagellates (groups 12 and 7, respectively; Table 5), which would suggest that while abundances may correlate with one another, dinoflagellates may be undergoing cell death from being in the presence of cyanobacteria. Relationships such as this will be explored and discussed in more detail in chapter 4, focusing on allelopathic relationships of phytoplankton.

Assessing cell mortality & limitations. Flow cytometric methods coupled with mortal staining were used to assess cell death throughout the study. Proportions of dead cells in representative populations were like that observed by others (Agustí et al. 2006, Rychtecký et al. 2014), with cells being counted as dead 5-100% of the time. Groups with the fewest dead cells observed tended to be those that were most abundant as was observed by Agustí et al. (2006), with variability among phytoplankton groups as would be expected. Inherent physiological differences in phytoplankton can limit staining of a dead cell and the possibility of cells staining differently due to the point at which they are in the process of dying (Zetsche and Meysman 2012), adding to the variability among groups. To address this, we used a gating technique to

assess individual groups of phytoplankton (Appendix A) that gave us the ability to follow each group based upon their differences in fluorescence and cell size. This method is like that of Huang et al. (2017), who grouped cells based upon red and orange fluorescence. Our studies differ in two ways however in our identification of groups and approach to measuring cell death. Our study took the approach of identifying representative taxa in each of the groups utilizing sorting flow cytometry paired with microscopy methods to confirm species identification and used flow cytometry to detect cell death using the mortal stain Sytox Green®, whereas Huang et al. assessed cell viability with a cell digestion assay, discussed later as an alternative to fluorescent staining techniques.

In using mortal stains there arises complication with determining cut-offs of fluorescence dictating what is considered dead versus alive. Both our study and Rychtecký et al. (2014) encountered this and used different methods to assess viability. Rychtecký used the membrane integrity index, which uses the fluorescence of a kill positive control to obtain better estimates of cell viability. They found that while the integrity index helped to account for differences in taxa staining and such, Sytox Green® is still a good early indicator of cell death in natural phytoplankton, despite concerns raised by Agustí and Sanchez (2002, Agustí et al. 2006) cautioning the use of mortal stains in assessing natural assemblages. In comparison, we utilized a method of applying secondary gating to "follow" to assess mortality (Appendix A) which allowed us to obtain estimates of cell death by observing net positive staining with Sytox Green® for each group identified with flow cytometry. Use of other mortal stains like Sytox Blue® could improve resolution in studies such as ours, as the stain has minimal 'carryover' with the fluorescence channels used for phytoplankton groupings (Dashkova et al. 2016), though our

study was limited by the lasers outfitted on the flow cytometer (i.e., did not have the UV laser, 405 nm).

An alternative method to cell staining, the cell digestion assay (CDA; Agustí and Sanchez 2002), which leaves behind only living cells for quantification following a lengthy enzymatic digestion process, was also tested in preliminary studies to compare with mortal staining results and revealed that the CDA method and our mortality estimates were comparable (data not shown). CDA methods eliminate concerns of fluorescent carryover that we may observe when using fluorescent staining techniques, as cell counts will only reflect those intact, living cells that remain, with the difference between controls and what remains providing the viability estimate of the cells. While this method is effective, additional sample preparation and incubation times for samples hinder the ability to complete assessments in a relatively timely manner. In using fluorescent stains and flow cytometry as we have done here, we can assess the community and cell death in a matter of minutes. This is due to the gating technique used in our study, which have provided a way to use fluorescent staining methods while eliminating concerns of fluorescence carryover by following individual populations, identified first by red and orange fluorescence, and further grouped for size, providing fluorescence thresholds for living controls to estimate the dead populations.

Cell mortality and viability of phytoplankton taxa are important processes to understand, relating cell death with variable abiotic factors to help make up for accounting errors in cell loss assessments (Franklin et al. 2006). Mortal staining processes such as those used in this study allow for a rapid assessment of dead or dying cells when incorporated with flow cytometric processes but do lend to their own complications when assessing mortality in

environmental samples or mixed assemblage of phytoplankton. Phytoplankton may not all stain in the same manner due to physiological differences or even the point at which cells are in the cell death process (i.e., dead vs dying;). To address this complication, it is important to fully assess available methods to test for viability within samples to ensure appropriate estimates are realized.

SUMMARY

This study aimed to understand the influence of abiotic conditions on phytoplankton community composition and cell death in Estabrook Park Pond. Using flow cytometry and mortal staining techniques, we monitored the phytoplankton community for three consecutive annual years, while collecting a comprehensive set of environmental data. While some correlations were found between decreased irradiance and temperature with dead cell abundances in some taxa, more compelling inter-taxon relationships were found, especially among cyanobacteria, dinoflagellates and some green algae.

REFERENCES

Agusti, S., Alou, E., Hoyer, M.V., Frazer, T.K., and Canfield, D.E. 2006. Cell death in lake phytoplankton communities. *Freshw Biol* 51: 1496-1506.

Beckmann, A. and Hense, I. 2004. Beneath the surface: Characteristics of oceanic ecosystems under weak mixing conditions – A theoretical investigation. *Prog Oceanogr* 75: 771-796.

Berges, J.A. and Falkowski, P.G. 1998. Physiological stress and cell death in marine phytoplankton: induction of proteases in response to nitrogen or light limitation. *Limnol Oceanogr* 43: 129-135.

Berquist, A.M. and Carpenter, S.R. 1986. Limnetic herbivory: effects on phytoplankton populations and primary production. *Ecology* 67: 1351-1360.

Bidle, K. and Falkowski, P. 2004. Cell death in planktonic, photosynthetic microorganisms. *Nat Rev Microbiol* 2: 643–655.

Bidle, K., Haramaty, L., Barcelos e Ramos, J. and Falkowski, P. 2007. Viral activation and recruitment of metacaspases in the unicellular coccolithophore, *Emiliana huxleyi*. *PNAS* 104: 6049-6054.

Butterwick, C., Heaney, S.I. and Talling, J.F. 2004. Diversity in the influence of temperature on the growth rates of freshwater algae, and its ecological relevance. *Freshw Biol* 50: 291 300.

Carpenter, S.R. and Kitchell, J.F. 1993. The trophic cascade in lakes. Cambridge University Press, London, England.

Choi, C.J. 2011. *Cell death in response to reactive oxygen and nitrogen species in marine and freshwater Chlorophyte algae*. Theses and Dissertations. UMI Number: 3492465

Choi, C.J. and Berges, J.A. 2013. New types of metacaspases in phytoplankton reveal diverse origins of cell death proteases. *Cell Death and Disease* 4: E490.

Dashkova, V., Segev, E., Malashenkov, D., Kolter, R., Vorobjev, I. & Barteneva, N.S. 2016. Microalgal cytometric analysis in the presence of endogenous autofluorescent pigments. *Algal Res* 19: 370-380.

Davis, T.W., Berry, D.L., Boyer, G.L. and Gobler, C.J. 2009. The effects of temperature and nutrients on the growth and dynamics of toxic and non-toxic strains of *Microcystis* during cyanobacteria blooms. *Harmful Algae* 8: 715-725.

Dillard, G.E. 2007. *Freshwater Algae of the Southeastern United States. Part 8: Chrysophyceae, Xanthophyceae, Raphidophyceae, and Dinophyceae.* Bibliotheca Phycologia Band 112. J. Cramer, Berlin.

Dimier, C., Corato, F., Tramontano, F. and Brunet, C. 2007. Photoprotection and xanthophyll cycle activity in three marine diatoms. *J Phycol* 43: 937-947.

Eppley, R.W. 1972. Temperature and phytoplankton growth in the sea. *Fish Bull* 70: 1063-1085.

Evans, C., and Brussaard, C. P. 2012. Regional variation in lytic and lysogenic viral infection in the Southern Ocean and its contribution to biogeochemical cycling. *Appl Environ Microbiol* 78: 6741-6748.

Falkowski, P.G., Dubinsky, Z. and Wyman, K. 1985. Growth-irradiance relationships in phytoplankton. *Limnol Oceanogr* 30: 311-321.

Franklin, D.J., Brussaard, C.P.D. and Berges, J.A. 2006. What is the role and nature of programmed cell death in phytoplankton ecology? *Eur J Phycol* 41: 1-14.

Gobler, C.J., Hutchins, D.A., Fisher, N.S. and Cosper, E.M. 1997. Release and bioavailability of C, N, P, Se, and Fe following viral lysis of a marine chrysophyte. *Limnol Oceangr* 42: 1492-1504.

Goldman, J.C. 1977. Temperature effects on phytoplankton growth in continuous culture. *Limnol Oceanogr* 22: 932-936.

Hammer, Ø., Harper, D.A.T., and Ryan, P.D. 2001. Past: Paleontological Statistics Software Package for Education and Data Analysis. Palaeontologia Electronica, vol. 4, issue 1, art. 4: 9pp., 178kb. http://palaeo-electronica.org/2001_1/past/issue1_01.htm

Hansson, L. 1995. Diurnal recruitment patterns in algae: effects of light cycles and stratified conditions. *J Phycol* 31: 540-546.

Hayakawa, M., Suzuki, K., Saito, H., Takahashi, K. and Ito, S. 2008. Differences in cell viabilities of phytoplankton between spring a late summer in the northwest Pacific Ocean. *J Exp Mar Biol Ecol* 360: 63-70.

Huang, X., Liu, X., Chen, J., Wupeng, X., Cao, Z. and Huang, B. 2017. Seasonal variations of group-specific phytoplankton cell death in Xiamen Bay, China. *Chin. J. Ocean. Limnol.* 35: 324–335.

Hutchinson, G.E. 1961. The paradox of the plankton. *Am Nat* 95: 137-145.

Interlandi, S.J. and Kilham, S.S. 2001. Limiting resources and the regulation of diversity in phytoplankton communities. *Ecology* 82: 1270-1282.

Kirchman, D.L. 1999. Phytoplankton death in the sea. *Nature* 398: 293-294.

Kozik, C.R., Young, E.B., Sandgren, C.D., and Berges, J.A. 2019. Cell death in individual freshwater phytoplankton species: relationshsips with population dynamics and environmental factors. *Eur J Phycol* 54: 369-379.

Litchman, E. 2000. Growth rates of phytoplankton under fluctuating light. *Freshw Biol* 44: 223-225.

Litchman, E. and Klausmeier, C.A. 2001. Competition of phytoplankton under fluctuating light. *Am Nat* 157: 170-187.

Liu, J., Cai, W., Fang, X., Wang, X. and Li, G. 2017. Virus-induced apoptosis and phosphorylation form of metacaspase in the marine coccolithophorid *Emiliania huxleyi*. *Arch Microbiol* https://doi.org/10.1007/s00203-017-1460-4

Llabrés, M. and Agustí, S. 2006. Picophytoplankton cell death induced by UV radiation: Evidence for oceanic Atlantic communities. *Limnol Oceanogr* 51: 21-29.

Llabrés, M. and Agustí, S. 2008. Extending the cell digestion assay to quantify dead phytoplankton cells in cold and polar waters. *Limnol Oceanogr Methods* 6: 659-666.

Llabrés, M., Agustí, S. and Herndl, G.J. 2011. Diel in situ picophytoplankton cell death cycles coupled with cell division. *J Phycol* 47: 1247-1257.

Lürling, M., Eshetu, F., Faassen, E.J., Kosten, S. and Huszar, V.L. 2013. Comparison of cyanobacterial and green algal growth rates at different temperatures. *Freshw Biol* 58: 552-559.

Ma, L., Sun, R., Mao, G., Yu, H. and Wang, Y. 2013. Seasonal and spatial variability of virioplanktonic abundance in Haihe River, China. *BioMed Research International* 1-10.

Maestrini, S.Y. and Bonin, D.J. 1981. Allelopathic relationships between phytoplankton species. *Can Bull Fish Aquat Sci* 210: 323-338.

Marañón, E., Cermeño, P., Huete-Ortega, M., López-Sandoval, D.C., Mouriño-Carballido, B. and Rodríguez-Ramos, T. 2014. Resource supply overrides temperature as a controlling factor of marine phytoplankton growth. PLoS ONE 9(6): e99312. doi: 10.1371/journal.pone.0099312.

Menzel, D.W. and Corwin, N. 1965. The measurement of total phosphorus in sea water based on the liberation of organically bound fractions by persulfate oxidation. *Limnol Oceangr* 10: 280-282.

Nygaard, G. 1976. *Tavlerne fra "Dansk Planteplankton"*. Gylendal, Denmark.

Olson, R.J., Zettler, E.R. and Anderson, O.K. 1989. Discrimination of eukaryotic phytoplankton cell types from light scatter and autofluorescence properties measured by flow cytometry. *Cytometry* 10: 636-643.

Parsons, T.R., Miata, Y. and Lalli, C.M. 1984. *A manual of chemical and biological methods for seawater analysis*. Pergamon Press.

Peperzak, L. and Brussaard, C.P.D. 2011. Flow cytometric applicability of fluorescent vitality probes on phytoplankton. *J Phycol* 47: 692-702.

Prescott, G.W. 1951. *Algae of the western Great Lakes area.* Otto Koeltz Science Publishers, West Germany.

Read, D.S., Bowes, M.J., Newbold, L.K. and Whiteley, A.S. 2014. Weekly flow cytometric analysis of riverine phytoplankton to determine seasonal bloom dynamics. *Environ Sci: Processes Impacts* 16: 594-603.

Reavie, E.D., Cangelosi, A.A. and Allinger, L.E. 2010. Assessing ballast water treatments: evaluation of viability methods for freshwater microplankton assemblages. *J Great Lakes Res* 36: 540-547.

Reynolds, C. 2006. *The ecology of phytoplankton*. Cambridge University Press, New York.

Richardson, K., Beardall, J. and Raven, J.A. 1983. Adaptation of unicellular algae to irradiance: an analysis of strategies. *New Phytol* 83: 157-191.

Rychtecký, P., Znachor, P., and Nedoma, J. 2014. Spatio-temporal study of phytoplankton cell viability in a eutrophic reservoir using SYTOX Green nucleic acid stain. *Hydrobiologia* 740: 177-189.

Scavia, D. and Fahnenstiel, G.L. 1987. Dynamics of Lake Michigan phytoplankton: mechanisms controlling epilimnetic communities. *J Great Lakes Res* 13: 103-120.

Solórzano, L. 1969 Determination of ammonia in natural waters by the phenolhypochlorite method. *Limnol Oceanogr* 14: 799-801.

Sterner, R.W. and Elser, J.J. 2002. *Ecological stoichiometry: The biology of elements from molecules to the biosphere*. Princeton University Press, New Jersey.

Sukenik, A., Eshkol, R., Livne, A. and Hadas, O. 2002. Inhibition of growth and photosynthesis of the dinoflagellate *Peridinium gatunense* by *Microcystis* sp. (cyanobacteria): a novel allelopathic mechanism. *Limnol Oceangr* 47: 1656-1663.

Tan, X. 2011. Effects of temperature on recruitment and phytoplankton community composition. *Afr J Microbiol Res* 5: 5896-5901.

Tilman, D. 1977. Resource competition between planktonic algae: an experimental and theoretical approach. *Ecology* 58: 338-348.

Vanharanta, M., Elovaara, S., Franklin, D.J., Spilling, K. and Tamelander, T. 2020. Viability of pico- and nanophytoplankton in the Baltic Sea during spring. *Aquat Ecol* 54: 119-135.

Vardi, A., Berman-Frank, I, Rozenberg, T., Hadas, O., Kaplan, A. and Levine, A. 1999. Programmed cell death of the dinoflagellate *Peridinium gatunense* is mediated by CO_2 limitation and oxidative stress. *Curr Bio* 9: 1061-1064.

Vardi, A., Schatz, D., Beeri, K., Motro, U., Sukenik, A., Levine, A. and Kaplan, A. 2002. Dinoflagellate-cyanobacterium communication may determine the composition of phytoplankton assemblage in a mesotrophic lake. *Curr Biol* 12: 1767-1772.

Veldhuis, M.J.W., Cucci, T.L. and Sieracki, M.E. 1997. Cellular DNA content of marine phytoplankton using two new fluorochromes: taxonomic and ecological implications. *J Phycol* 33: 527-541.

Veldhuis, M.J.W. and Kraay, G.W. 2000. Application of flow cytometry in marine phytoplankton research: current applications and future perspectives. *Sci Mar* 64: 121-134.

Veldhuis, M.J.W., Kraay, G.W. and Timmermans, K.R. 2001. Cell death in phytoplankton: correlation between changes in membrane permeability, photosynthetic activity, pigmentation and growth. *Eur J Phycol* 36: 167-177.

Wang, H., Chen, F., Mi, T., Liu, Q., Yu, Z., and Zhen, Y. 2020. Responses of Marine diatom *Skeletonema marinoi* to nutrient deficiency: programmed cell death. *Appl Environ Microbiol* 86: e02460-19.

Whitford, L.A. and Schumacher, G.J. 1973. *A manual of fresh-water algae*. Sparks Press.

Yang, Y., Gu, X., Te, S. H., Goh, S. G., Mani, K., He, Y., and Gin, K. Y. H. 2019. Occurrence and distribution of viruses and picoplankton in tropical freshwater bodies determined by flow cytometry. *Water Research*, *149*, 342-350.

Zar, J.H. 2009. *Biostatistical analysis, 5th ed.* Prentice Hall.

Zetsche, E. and Meysman, F.J.R. 2012. Dead or alive? Viability assessment of micro- and mesoplankton. *J Plankton Res* 34: 493-509.

Znachor, P., Rychtecký, P., Nedoma, J., and Visocká, V. 2015. Factors affecting growth and viability of natural diatom populations in the meso-eutrophic Římov Reservoir (Czech Republic). *Hydrobiologia* 762: 253-265.

Zhang, Y. and Prepas, E.E. 1996. Regulation of the dominance of planktonic diatoms and cyanobacteria in four eutrophic hardwater lakes by nutrients, water column stability, and temperature. *Can J Fish Aquat Sci* 53: 621-633.

Chapter 3: Biologically mediated mortality in phytoplankton: understanding grazing effects

INTRODUCTION

Herbivore grazing can affect phytoplankton community composition, abundance and subsequently, mortality (e.g., Berquist et al. 1985, Lehman and Sandgren 1985). Changes in phytoplankton community composition are typically caused by selective grazing, where zooplankton preferentially feed on one phytoplankton species versus another due to differences in size, shape (Brooks and Dodson 1965) or nutritional status (Cowles et al. 1988), leading to altered phytoplankton succession, changes in community composition and decreases in total phytoplankton abundance (Vanni 1987, Vanni 1990, Ger et al. 2019). Grazing can also indirectly impact phytoplankton populations through nutrient regeneration (Sterner 1986, Vanni 2002, Vrede and Vrede 2005), which can improve the growth of nutrient-limited phytoplankton species through enhancement of nutrients, such as phosphorus and nitrogen. Further, grazing can facilitate shifts between limiting nutrients, e.g., shifting from nitrogen to phosphorus limitation, through zooplankton feeding behaviors and food preferences (higher-N or -P content food) in the environment (Elser et al. 1988).

A variety of zooplankton can selectively affect the phytoplankton community as described above, as well as the bacterial community within a system due to their feeding habits. Cladocerans (daphnids) can filter food into their mouths but can also handle prey items using their mandibles. Calanoid copepods and rotifers filter prey items, while cyclopoid copepods handle their food with appendages, allowing for rejection of inedible items. There is variation in filtration rates within taxonomic groups of zooplankton as well. For example, the copepod *Diaptomus oregonensis*, has previously been found to have a maximum filtration

(clearance) rate of 12.9 mL animal^{-1} d^{1} (McQueen 1970), while a review by Peters and Downing (1984) found that for marine calanoid copepods, the filtration rates are 7.6 mL animal^{-1} d^{-1}. The latter review also found that freshwater cladocerans can filter an average of 20 mL animal^{-1} d^{-1}. More recent laboratory studies pairing copepods with preferred (*Cryptomonas obovata*) and less preferred (*Raphidiopsis raciborskii*) prey items have estimated clearance rates for the calanoid copepod *Notodiaptomus iheringi* to be 1.5 mL animal^{-1} d^{-1} compared to the cyclopoid *Thermocyclops decipiens*' clearance rate of 0.3 mL animal^{-1} d^{-1} (Leitão et al. 2020). While both copepod species grazed upon *Cryptomonas*, it was found that both species limited the ability for *Raphidiopsis*, a cyanobacterium, to become dominant, instead decreasing the size of filaments. Interestingly, *Notodiaptomus* switched from its preferred prey item of *Cryptomonas* to *Raphidiopsis* when the availability of *Cryptomonas* declined (Leitão et al. 2020), further demonstrating the ability for zooplankton to selectively graze upon available prey items.

While selective grazing occurs, zooplankton may damage cells through "sloppy feeding", which can lead to an increase in dead and/or damaged cells within the environment. Cells that are damaged may release dissolved nutrients into the surrounding environment, to the benefit of nearby cells. For example, cladocerans and copepods have both been found to have direct effects on bacterial populations due to their feeding habits (Kamjunke and Zehrer 1999, Šimek et al. 2014, Titelman 2008). Observations of *Daphnia galeata* found that handling of prey items resulted in an increase in available dissolved organic carbon due to damage to prey items, resulting in an increase of bacterial biomass (Kamjunke and Zehrer 1999). When organic carbon declined due to a decrease in phytoplankton biomass, so did bacterial biomass indicative of bacterial dependence on the released carbon for growth. Titelman et al. (2008) observed that

not only bacterial growth increased due to sloppy feeding of prey by copepods but also bacterial alkaline phosphatase activity, suggestive of bacterial uptake and storage of available phosphorus for later use. Grazing damage may also lead to the production and release of allelochemicals by phytoplankton, which can be used as a means of communication to nearby cells (e.g., Ribalet et al. 2007, Venuleo et al. 2017), or as a grazing deterrent. In diatoms, polyunsaturated aldehydes (PUAs) are produced by the cells when damaged and can be released when cells lyse. Pohnert (2002) found that when *Thalassiosira* were damaged, oxylipins, a form of PUAs, were released into the environment by damaged cells and were found in highest concentrations in the vicinity of herbivores. This would suggest that the PUAs were produced within *Thalassiosira* and released post-grazing damage to function as a deterrent. A study by Ianora et al. (2004) found that rather than function as a grazing deterrent, PUAs produced by diatoms had a post-ingestion effect on copepods, resulting in declines in recruitment of the zooplankton. The same was not found with recruitment of *Daphnia* however, as PUAs produced and released were not found to negatively affect recruitment of daphnids in freshwater (Carotenuto et al. 2005). Dinoflagellates can produce β-dimethylsulfoniopropionate (DMSP), an important component of the sulfur cycle, which can function as a grazer deterrent when released (Frederickson and Strom 2009). Brevetoxins, toxins produced by the red tide species *Karenia brevis*, have also been found to limit rotifer grazing rates (Kubanek et al. 2007).

Chemical cues released by zooplankton can also alter phytoplankton populations, through the act of grazing resulting in cellular damage or the release of an infochemical of sorts. For example, *Scenedesmus* has been documented to exhibit changes in morphology (i.e.,

increased cells/colony) when in the presence of *Daphnia,* thought to be due to a chemical released by the grazer rather than *Scenedesmus* itself (Lürling 1998), as the response did not occur when cells were exposed to a homogenate of itself. A later study by Zhu et al. (2016) found that when exposed to *Daphnia*-free filtrate, *Scenedesmus* exhibited changes in morphology including cells/colony and spine length, suggesting an induced defense response to minimize grazing by *Daphnia*. Another green alga, *Chlorella vulgaris*, has been found to increase cell size when exposed to grazing pressure from the rotifer *Brachionus calyciflorus* (Yoshida et al. 2004), which could make it more difficult for the rotifer to graze upon them.

While herbivore grazing effects on phytoplankton communities have been studied extensively, most commonly using mixed phytoplankton assemblages (cultured or natural) and known zooplankton species to create dilution experiments, measuring total chlorophyll *a* to estimate algal biomass (Kamjunke and Zehrer 1999, Landry et al. 1995, Lehman and Sandgren 1985), few studies have used flow cytometry to assess overall phytoplankton mortality. Cucci et al. (1989) reviewed selective grazing by marine organisms, applying flow cytometry to detect changes in fluorescent properties of the cells, quantitatively tracking changes in phytoplankton abundance. One study included was done by Cowles et al. (1988), where the feeding preferences of the marine copepod, *Acartia tonsa*, were studied using laboratory grown *Thalassiosira weissflogii* of different nutritional values. Results indicated that *A. tonsa* was capable of selectively feeding upon the higher quality food source when provided *T. weissflogii* of differing nutritive states. Selectivity in this instance suggests that in a natural assemblage, zooplankton may selectively graze on phytoplankton due to their physiological state. More recently, Jungbluth et al. (2017) studied the grazing effects of the nauplii of two marine

copepods to determine species-specific effects on natural phytoplankton assemblages, finding that nauplii, the juvenile life stage of a copepod, selects for the lesser abundant size classes of phytoplankton.

My objective in this chapter was to determine whether grazing by macrozooplankton was responsible for declines in specific phytoplankton taxa, with detection of dead cells. I approached the question by enhancing natural zooplankton abundance in laboratory experiments and assessing phytoplankton mortality using flow cytometry. I hypothesized that: 1) Declines in the abundance of specific phytoplankton groups would be correlated with increasing zooplankton abundance, indicating that zooplankton are selectively consuming specific phytoplankton; and 2) With increasing zooplankton concentrations in experiments, the number of dead phytoplankton cells would increase as a result of the zooplankton grazing process, either because grazers damaged phytoplankton cells leading to death, or because grazers stimulated release of compounds that lead to cell death.

MATERIALS AND METHODS

Experimental set-up. In 2016, experiments were conducted in July and November, using surface (< 0.5 m) water collected from six locations around Estabrook Pond (Fig. 1). Experiments were also completed in September and October of 2019, again using surface water from Estabrook Park Pond. Pond water was pooled in a large pre-rinsed 120 L polypropylene pail to create a single representative sample, with large particulate matter (aquatic macrophytes, leaves) removed manually. A grazer control treatment was established in triplicate, with 2-L narrow-mouthed clear polycarbonate bottles filled with 300 µm screened pond water. Remaining bottles were filled with grazer removed (100 µm mesh) water (Fig. 9). Triplicate bottles were filled with the grazer removed water to establish a "no grazer" (0X) treatment to test phytoplankton responses with grazer removal.

Zooplankton concentrate. To create a zooplankton concentrate, zooplankton were collected from the pond and concentrated using a plankton net. In 2016, the concentrate was made by passing multiple buckets (ten 10-L buckets) of surface water (Fig. 1) through a large plankton net (1.0 m diameter, 153 µm mesh), collecting the concentrate in a 1000 mL cod-end (i.e., 100 L concentrated to 1 L = a hypothetical 100 x concentrate). The zooplankton concentrate for 2019 was passed through a smaller plankton net (0.5 m diameter, 63 µm mesh), to collect a wider size range of organisms. Large debris was then removed from the concentrate, and the contents of the cod-end was reconstituted in 1 L of 100 µm mesh grazer removed water (Fig. 9) which was then used to inoculate experimental treatments. Triplicate treatments were established to create an herbivore gradient (Fig. 9), including no herbivores (0X), and various concentrations of herbivores (Table 6) above ambient concentrations (grazing control), e.g.,

1.4X, 1.9X, representing 1.4 and 1.9 times the ambient concentration of zooplankton in the pond. Triplicate treatment bottles were then inoculated with appropriate amounts of the zooplankton concentrate (Fig. 9). Once all treatments were established, a small square of food-grade plastic was placed over the bottle mouth to prevent bubbles from being trapped, and bottles were capped and transported to the laboratory. Bottles were incubated on a small plankton wheel in the laboratory under ambient light and temperature conditions (16:8 light/dark, 18°C) for 2-4 days. Flow cytometric counts of the phytoplankton community were done at the beginning and end of the experimental period, following the methods described previously (See *Chapter 2 Materials and Methods: Flow cytometry*).

At both the beginning and end of the experiment, zooplankton and phytoplankton samples were preserved. For zooplankton, 100 mL of a treatment bottle was passed through a 53 µm screen, with material collected on the screen preserved in 70% ethyl alcohol. Phytoplankton samples were collected by screening water with a 153 µm screen and preserving the filtrate (phytoplankton < 153 µm) with Lugol's Iodine solution. Replicate chlorophyll samples were also collected, done by filtering 80 mL of treatment water with Pall A/E (25 mm, 1.0 µm nominal pore size) filters. In 2019, water was also collected for nutrient analyses (total phosphorus, soluble reactive phosphorus). Samples were stored and analyzed as previously described (See *Chapter 2 Materials and Methods: Chlorophyll and nutrient analyses*).

Statistical Analyses. Changes in total chlorophyll *a* (< 153 µm) and cell counts (taxon-specific counts) were calculated from the difference between initial (Day 0) and those collected at termination of the experiment values. These data were then plotted against zooplankton abundance/volume for the determination of both phytoplankton growth and zooplankton

grazing rates using graphical methods. Correlational analyses were conducted using SigmaPlot (version 12.3) to identify potential correlations among changes in cell abundance and percentage of dead cells and nutrient concentrations as well.

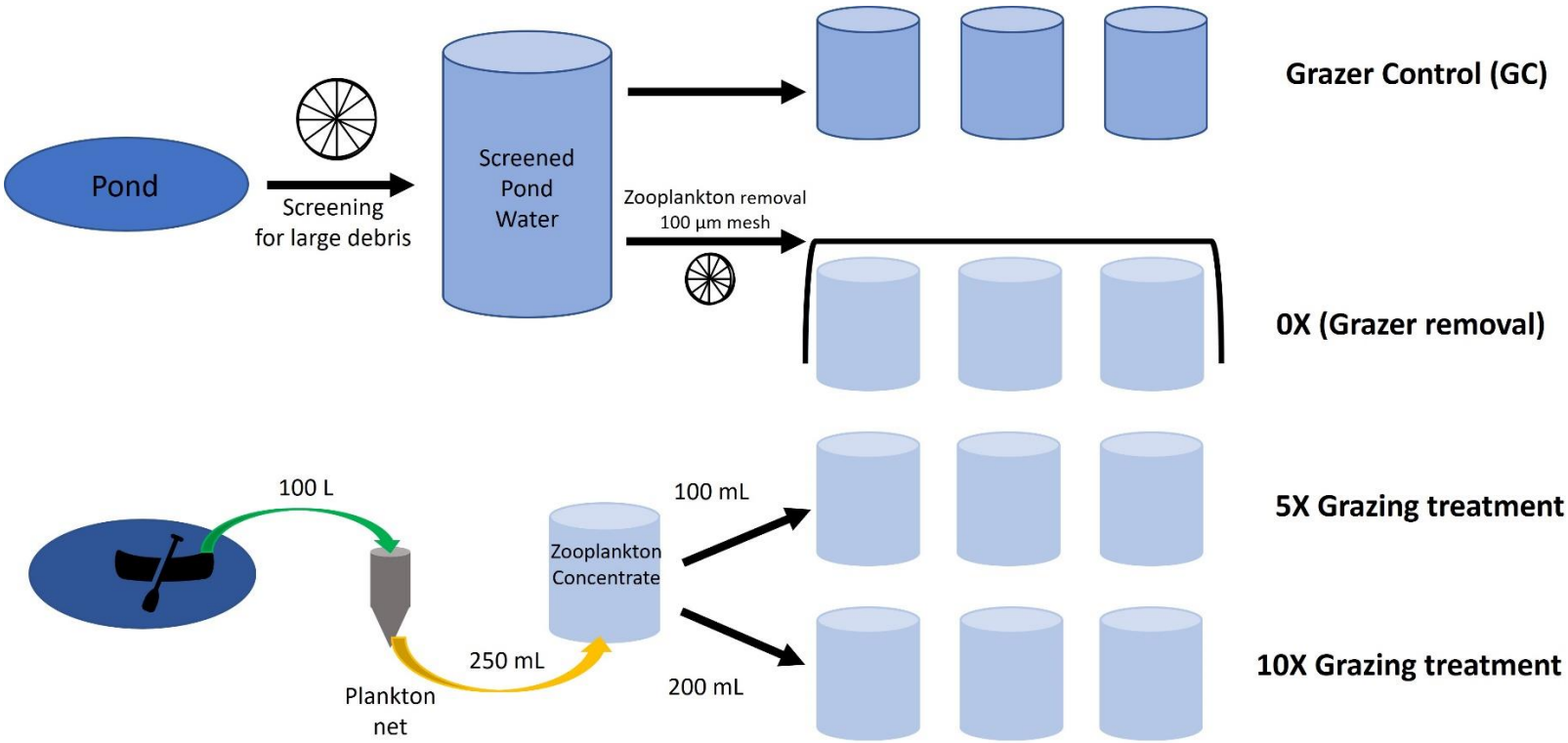

Figure 9. Schematic of experimental design used to assess grazing influence on cell mortality in Estabrook Park Pond. Water was collected from multiple locations in the pond and prepared for the experiment through a variety of filtration steps to establish 0X, 5X and 10X grazer concentrate experimental treatments. Screened () pond water was used to fill grazer control (GC) bottles. Water that was passed through 100 µm mesh was placed into remaining bottles treatment bottles to prepare for establishing the concentration gradient. All treatments were done in triplicate. Abbreviations: "GC" means grazer control, filled with screened pond water to mimic ambient zooplankton concentration in the pond; "0X" means zooplankton removed pond water; and "5X-10X" indicates treatments with an increased abundance of zooplankton compared to ambient concentrations.

RESULTS

Zooplankton abundance and community. The zooplankton community sampled in 2016 included cladocerans (*Daphnia, Bosmina*), copepods (predominantly calanoid), nauplii and rotifers. Copepods and nauplii were the most abundant zooplankton throughout the grazing studies in 2016 (Fig. 10A-B). In contrast, the 2019 zooplankton community was dominated by calanoid copepods and nauplii, with very few cladocerans. In September 2019, the zooplankton community was dominated by rotifers with some copepods and nauplii (Fig. 10C). The dominant zooplankton in October 2019 were copepods and nauplii with rotifers comprising a small proportion of the population (Fig. 10D). Overall, zooplankton abundance increased along a gradient though not in a linear fashion (Fig. 10A-D) with the maximum concentration of zooplankton being barely twice that of the grazing control (Table 6).

Phytoplankton biomass and flow cytometric observations. Changes (from beginning to end of the experiment) in phytoplankton biomass, measured as chl *a*, were negligible as zooplankton abundance increased (Fig. 11A-D). To determine this, chl *a* fluorescence was measured at both the beginning and end of the experiment to obtain algal biomass estimates. Initial biomass estimates were subtracted from final biomass estimates, then divided by the length of the experiment to determine the change in biomass per day of the experiment. Negative values indicated cells were being lost (i.e., death, sinking, grazing) faster than they could be replaced, while positive values indicated cells were growing faster than they were lost. Net changes in biomass near zero would suggest that cells were being lost and replaced within the bottle at equal rates. Pearson correlational analyses were then done to assess whether losses were significant in relation to the grazer gradient. In 2016, biomass did not decline significantly with

increasing zooplankton abundance, with grazing rates less than 1 µg chl *a* L^{-1} d^{-1}. Phytoplankton growth rates ranged between 3-7 µg chl *a* L^{-1} d^{-1}. In contrast, phytoplankton biomass minimally increased (growth rate <1 µg chl *a* L^{-1} d^{-1}) with increasing zooplankton abundance in 2019. Grazing rates were well below 1 µg chl *a* L^{-1} d^{-1} in 2019.

Flow cytometric group counts did not decrease with increasing zooplankton abundance in 2016 (Fig. 11E-F) with variations like those observed by changes in chl *a* biomass. In 2019 however, two of eleven flow cytometric groups had significant losses in abundance as zooplankton abundance increased (Fig. 11G-H), indicative of selective removal of particles. These two groups were chlorophytes (groups 1 and 5, mixed chlorophytes and mixed desmids – including *Ankistrodesmus* and *Scenedesmus*). The significance ($p < 0.05$) of the group 5 chlorophyte losses increased slightly from September ($r^2 = 0.88$) to October ($r^2 = 0.90$). However, the losses observed for group 1 chlorophytes decreased in significance ($p < 0.05$) from September ($r^2 = 0.92$) to October ($r^2 = 0.54$), although the total abundance of this group increased by more than an order of magnitude during the experiment. In most of the grazing studies, < 2% of cells stained as dead (Fig. 12A-C). October 2019 was an exception, with phytoplankton groups staining < 15% of cells as dead (Fig. 12D), but the cause of death was undetermined given that the group with the highest proportion of dead cells were green algae (Group 9, *Chlamydomonas*). Cells that did stain tended to be in rare or low abundance flow cytometric groups of phytoplankton (data not shown).

Nutrient effects. In 2019, total and dissolved phosphorus (TP and SRP, respectively) were measured at the onset and conclusion of the experiments (Fig. 13A-D). Initial time zero measurements indicated that grazer removal and grazer control treatments were very similar in

phosphorus concentrations, with the zooplankton concentrate significantly enhanced two (dissolved phosphorus, SRP) or three (total phosphorus) times relative to the control (Fig. 13A, 13C). At the conclusion of the experiment, there was no difference in total or dissolved phosphorus among the treatments, except for total phosphorus in October, where levels were slightly elevated in the enhanced treatments (Fig. 13B). Dissolved phosphorus levels were elevated slightly relative to initial measurements, although they did not vary much with an increase in grazer concentration, indicating that zooplankton were not providing phosphorus enrichment, or that dissolved phosphorus was not being taken up (Fig. 13D). A positive correlation ($r^2 = 0.71$, $p < 0.05$) was observed between total phosphorus and mean chlorophyll biomass. There was a negative relationship trend between dissolved phosphorus and mean chlorophyll, albeit insignificant. Total and dissolved phosphorus did not correlate with counts of individual flow cytometry groups or percentage of cells staining as dead.

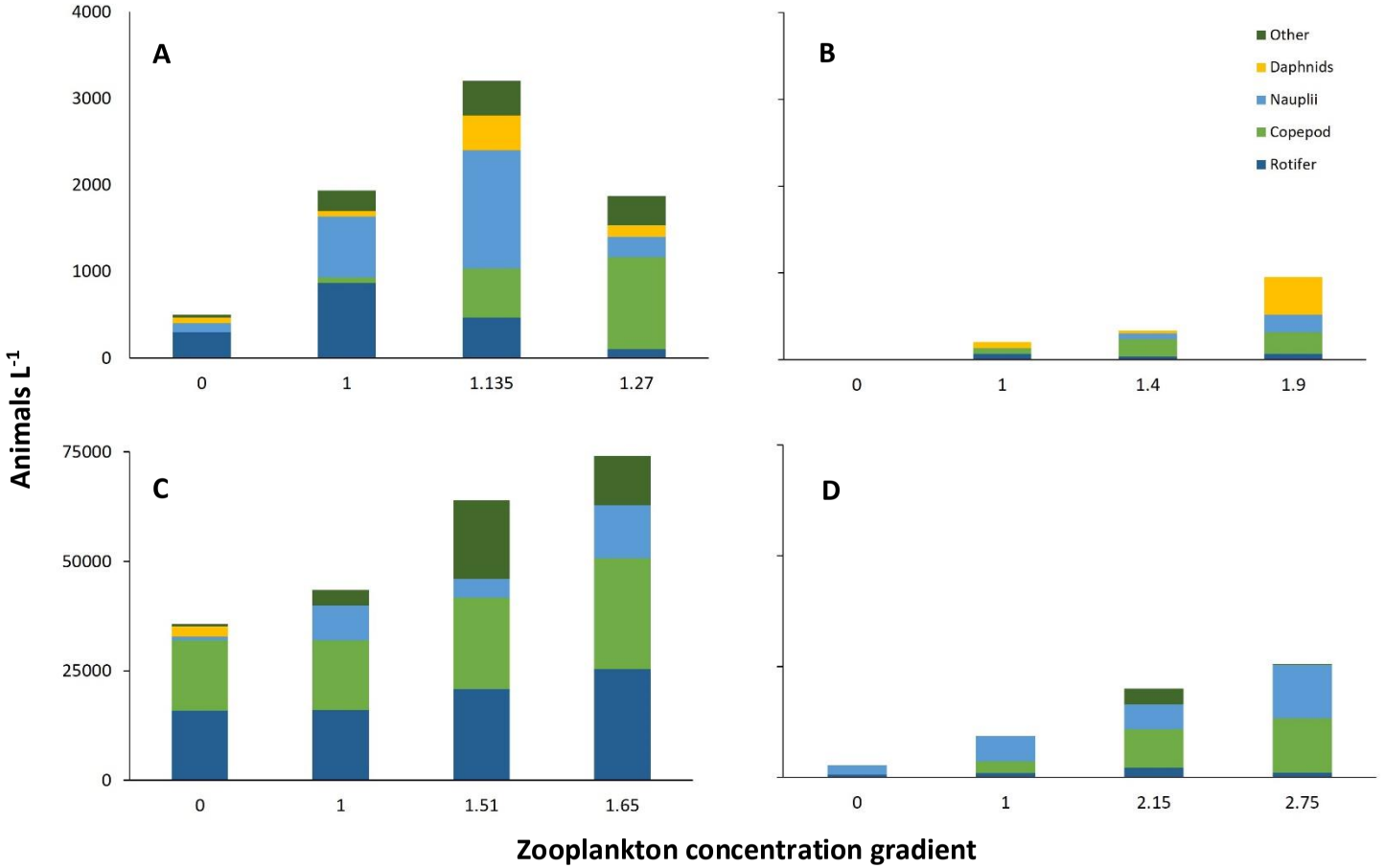

Figure 10. Zooplankton composition at the end of grazing experiments for experimental years. Data plotted represent the average number of animals observed in a treatment with microscopic enumeration. A. July 2016 zooplankton composition in experimental grazing treatments. B. November 2016 zooplankton composition in experimental grazing treatments. C. September 2019 zooplankton composition in grazing experimental treatments. D. October 2019 zooplankton composition in experimental grazing treatments. “0” denotes grazer removed treatment while “1” is indicative of the grazer control containing an ambient abundance of zooplankton. Note: “Copepods” includes both calanoid and cyclopoid copepods. “Daphnids” include *Daphnia* and *Bosmina*. “Other” includes ciliates and chironomids.

Table 6. Realized zooplankton concentrations relative to grazing control for experimental years 2016 and 2019. Concentrations were created through a series of screening and inoculations steps (Fig. 7) to artificially modify zooplankton concentrations. “Grazer Removal” is for bottles filled with pond water screened through 100-µm mesh to remove zooplankton. “Grazing Control” treatments had pond water that was only screened for large plant and detrital material and therefore contained the ambient zooplankton abundances. Other treatments indicative of artificial inflation of zooplankton concentration via experimental set-up. Concentrations calculated by dividing grazing treatment zooplankton abundance by abundance in respective control treatment to identify enhancement of zooplankton abundance.

	Realized zooplankton concentrations			
Desired concentration	*July, 2016*	*November, 2016*	*September, 2019*	*October, 2019*
Grazer Removal	0	0	0	0
Grazing Control	1	1	1	1
5X	1.14	1.4	1.2	1.7
10X	1.3	1.9	1.4	2.3

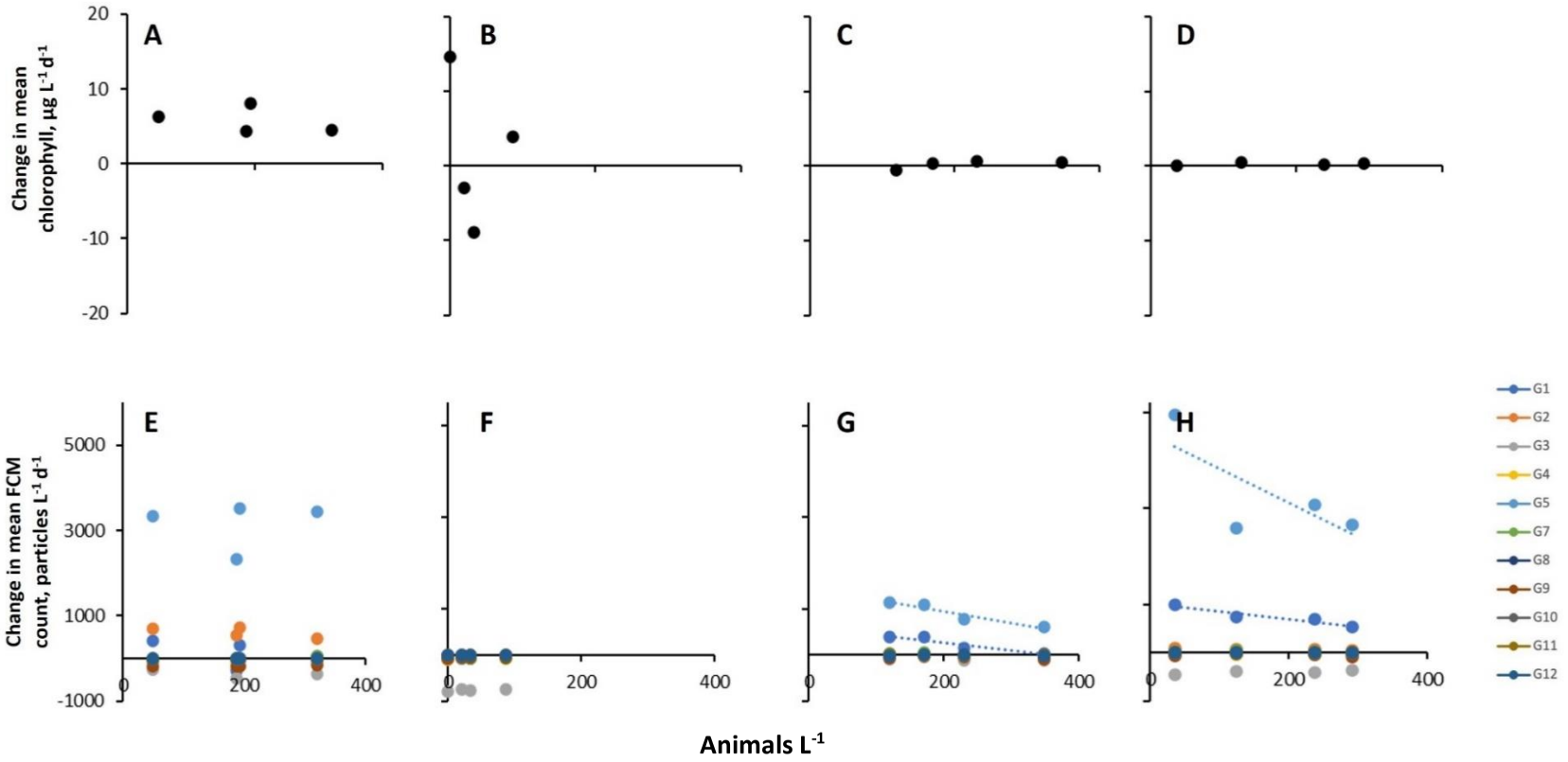
A
B
C
D
E
F
G
H
Change in mean chlorophyll, µg L-1 d-1
Change in mean FCM count, particles L-1 d-1
Animals L-1
G1
G2
G3
G4
G5
G7
G8
G9
G10
G11
G12

Figure 11. Comparison of change in mean chlorophyll *a* biomass and mean flow cytometric counts along a zooplankton gradient. Change is difference between the beginning and end of the experiment. A. Changes in chlorophyll *a* biomass along the grazer gradient in July 2016. B. Changes in chlorophyll *a* biomass along the grazer gradient in November 2016 over 2-day incubation. C. Changes in chlorophyll *a* biomass in September 2019 over 3-day incubation. D. Changes in chlorophyll *a* biomass in October 2019 over 3-day incubation. E. Changes in mean flow cytometric counts in July 2016 over 4-day incubation. F. Changes in mean flow cytometric counts in November 2016 over 2-day incubation. G. Changes in mean flow cytometric counts in September 2019 over 3-day incubation. H. Changes in mean flow cytometric counts in October 2019 over 3-day incubation. Regression lines shown only where significant relationships ($p<0.05$) were identified. See Table 1 in Chapter 2 for flow cytometric group identities.

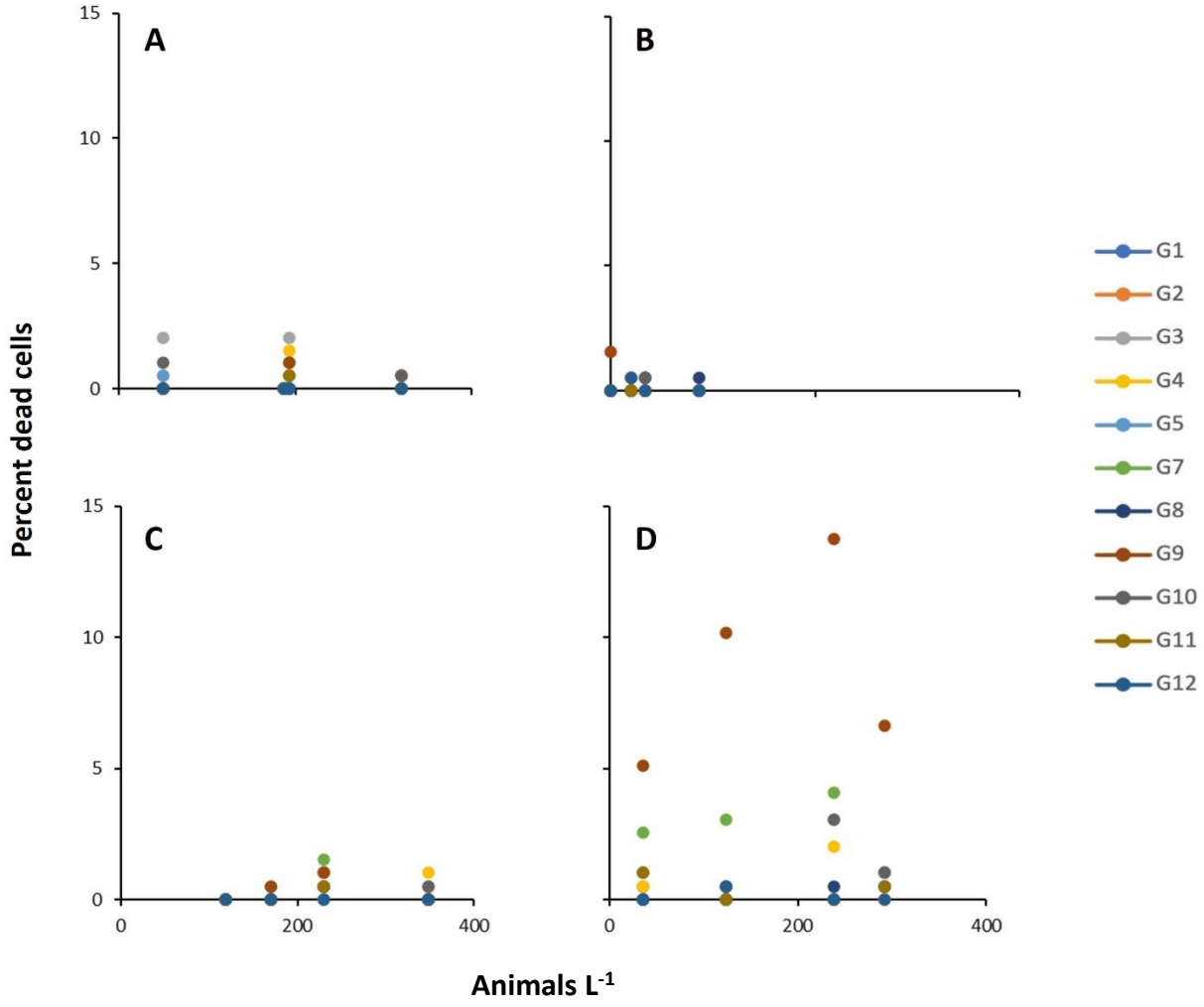

Figure 12. Relationship between mean zooplankton abundance (animals L^{-1}) and percent dead phytoplankton as determined by flow cytometry for grazing experiments in 2016 and 2019. Note that except for October 2019, less than 5% of phytoplankton in a group stained as dead. A. July 2016. B. November 2016. C. September 2019. D. October 2019. See Table 1 in Chapter 1 for flow cytometric group identities.

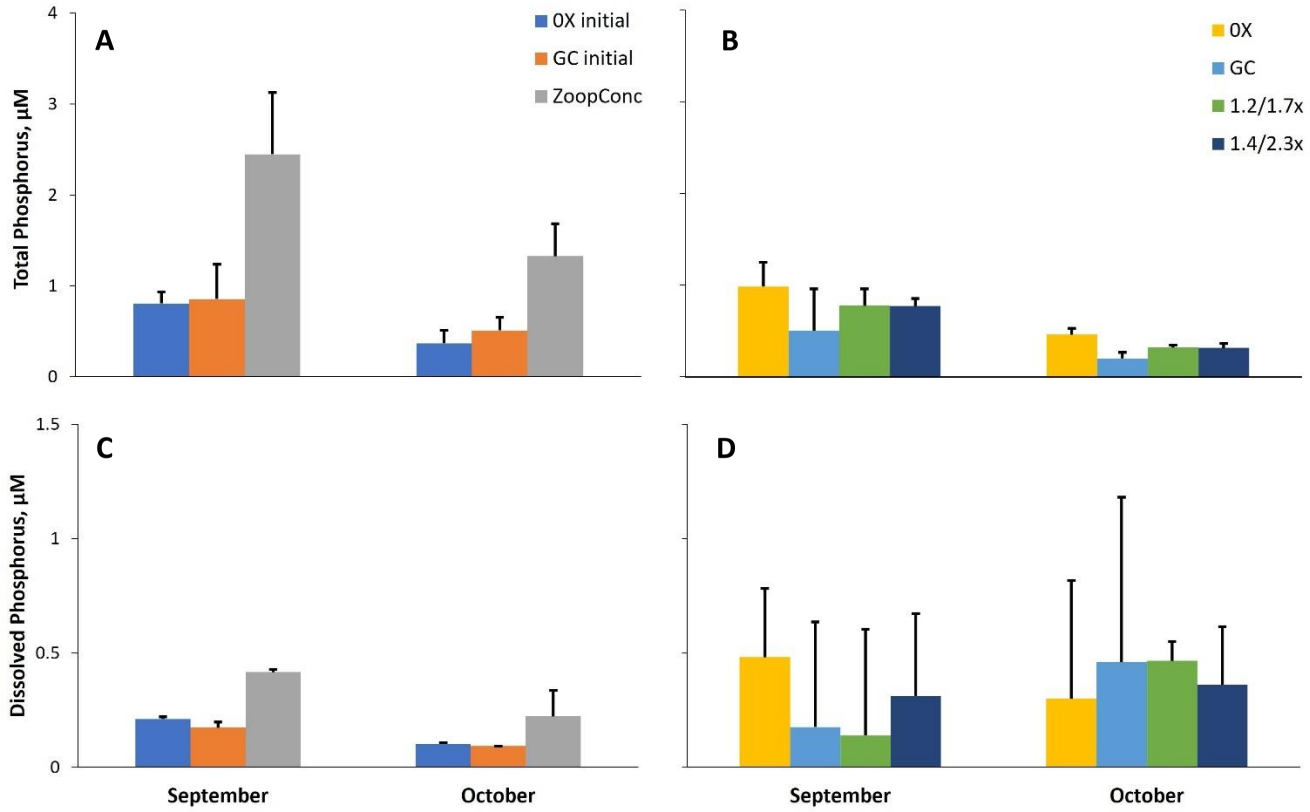

Figure 13. Mean phosphorus concentrations from 2019 grazing experiments. A. Mean total phosphorus concentration at beginning of experiment. B. Mean total phosphorus (SRP) concentration at end of experiment. C. Mean dissolved phosphorus (SRP) concentration at beginning of experiment. D. Mean dissolved phosphorus (SRP) concentration at end of experiment. Error bars indicate calculated standard deviations from mean (n=2). Abbreviations: 0X – grazer removal treatment; GC – grazer control/ambient concentration; ZoopConc – concentrated grazer sample used to inoculate experimental treatments.

DISCUSSION

This study was designed to investigate the role of grazing on phytoplankton cell mortality. Using laboratory experiments with enhanced zooplankton abundance and flow cytometry to monitor the phytoplankton community, it was found that grazing by zooplankton did not play a significant role in cell mortality in the phytoplankton community. Phytoplankton group abundances did not decline relative to increased zooplankton abundance. Further, the proportion of dead cells measured was low (< 5 %) and when dead cells were observed, the number of dead cells did not increase with zooplankton abundance, suggesting that grazing did not result in damaged cells or the release of compounds that could result in death.

Grazing methods and generation of dead cells. While grazing is often considered a factor in shaping phytoplankton community dynamics, low grazing rates were observed in our study with grazing rates of <1 µg chl *a* L^{-1} d^{-1}, and similarly low rates have been reported (Turner et al. 1999). Turner er al.'s (1999) study looking at grazing effects in the northern Adriatic Sea, grazing was found to minimally affect phytoplankton community composition, having had difficulty in enhancing zooplankton concentrations. Their attempts to concentrate ambient zooplankton failed as copepods and nauplii populations had large increases in treatment bottles. Our study did not have such explosive growth in the copepod and nauplii populations, but the zooplankton community was dominated by both throughout the experiments. The dominance of these smaller zooplankton can ultimately shift phytoplankton size classes, providing a refuge for large, difficult to handle prey items which are avoided by these smaller grazers, leading to changing dominance in the phytoplankton community (Vanni 1987). In the first experiments, we looked to concentrate phytoplankton larger than 100 µm but found that the zooplankton

size classes present warranted a smaller mesh (62 µm) for concentrating the plankton for future (2019) experiments. The smaller size classes could be due in part to grazing pressure from fish in the pond, which could lead to decreased zooplankton body size or the elimination of large-bodied zooplankton (O'Brien 1979), allowing for small-bodied zooplankton to exist with limited competition for food (Brooks and Dodson 1965). Smaller zooplankton tend to be less efficient at grazing however and are unable to "handle" large phytoplankton (Moore and Folt 1993), which could affect the phytoplankton community structure as well, functioning as a top-down control of the system.

In communities with copepods and nauplii present, as observed in Estabrook Park Pond, a variety of grazing responses have been observed. The marine copepod *Oithona davisae* has been found to be a voracious feeder, though the mouth opening of adults would indicate that some phytoplankton species are too big to be entirely consumed (Saiz et al. 2014). With nauplii being a dominant herbivore in our study system of Estabrook Park Pond, there is the possibility of raptorial feeding leading to only partial ingestion of cells, as has been observed in the nauplii of the marine copepod *Paracartia grani* (Helenius and Saiz 2017). Sloppy feeding habits as described above could result in dead cells remaining in the environment, such as what was observed in the October 2019 study when the highest amounts of dead cells were reached (Fig. 10D). In instances with higher amounts of dead cells observed (15 % dead) it was the *Chlamydomonas*-like cells with the highest proportion of dead cells, which would not be considered large species. An alternative consideration would be that some copepods cannot handle small prey items (Berggreen et al. 1988), which could lead to an increase in dead cells due to damage incurred from zooplankton handling. An alternative would be that cells remain

untouched, left to grazing pressure by other zooplankton or abiotic stress (e.g., changes in temperature or irradiance). Given the time of year that the highest dead cell proportions were observed, it may be more likely that in our study the *Chlamydomonas*-like cells were more sensitive to abiotic conditions that could lead to cell death. With seasonal variations of temperature and light identified in Chapter 2, an increase in dead cells could be associated with end-of-season cellular stress from abiotic conditions resulting in cell death.

Selective grazing of phytoplankton. In our study, grazing did not result in the appearance of dead cells, though selective grazing can still remove cells from the community with full ingestion of prey items. Minimal declines in chlorophyll *a* biomass were observed along with changes in phytoplankton group abundance in 2019 for two groups of green algae, including desmid species (Fig. 9G-H), which could suggest that selective grazing occurred. Previously, Coesel (1997) found that *Staurastrum* was easily ingested and digested by *Daphnia* species in comparative experiments looking at the edibility of *Staurastrum* and *Cosmarium*. *Cosmarium* was found to be consumed less due to the extracellular material covering the cell, though with some damage to the covering, the cells were ingested more readily. While the desmids preferentially consumed in our experiments tended to be *Ankistrodesmus* and *Scenedesmus*, the idea that they could be consumed readily is sound. *Ankistrodesmus* would be the more likely species to be consumed as it does not demonstrate the same variation in morphology as *Scenedesmus* does, with cells being able to be ingested with minimal effort. The spines and cellular organization of *Scenedesmus* colonies can hamper grazing efforts, as morphological differences function as a grazing defense (e.g., Mayeli et al. 2004) limiting which consumption of them to larger zooplankton (i.e., daphnids). Copepods and nauplii may very well graze upon

Ankistrodesmus in our study as there is evidence suggesting that both zooplankton are capable of consuming elongated cells, such as large (> 500 µm) diatom chains (Djeghri et al. 2018), though there may be fragmented cells remaining that could be quantified by mortal staining, if they do not sink to the sediment. Given these previous observations, the zooplankton community composition in this study and observed changes in the abundance of the desmid group, we could hypothesize that copepods and nauplii preferentially grazed upon *Ankistrodesmus* in the 2019 studies, though losses of cells could be related to seasonal declines in light and temperature (abiotic stressors).

Considering the classical view that phytoplankton that are susceptible to grazing are most abundant in spring with a shift in dominance to resistant taxa in the summer (Vanni and Temte 1990), the strength of phytoplankton-grazer relationships is not equal across all environments. This is due in part to seasonal variation in the zooplankton community, with systems such as Estabrook Park Pond dominated by copepods and nauplii during the late summer and autumn, while others may be dominated by daphnids or ciliates earlier in the year (spring/summer).

Limitations of the study. While this study provided a snapshot of minimal grazing effects on the phytoplankton community, we must use caution in generalizing the outcomes. The study only focused on mid-summer and autumn, which could lead to a misinterpretation of the influence of zooplankton, as zooplankton populations can be seasonal, influenced by abiotic factors just as we think phytoplankton dynamics can be (e.g., Talling 2002), which can shift grazing pressure to earlier in the year. To fully resolve the impact of grazing on cell mortality in the phytoplankton community, it is important to carry out an extended seasonal study, from ice-

out until ice-cover, to observe and test relationships among the phyto- and zooplankton of Estabrook Park Pond. By conducting such experiments, we can fully assess the zooplankton community structure and seasonal dynamics to identify if shifts in the community could be driving the phytoplankton responses observed. The dominance of smaller zooplankton, including copepods and rotifers, follows what is expected of seasonal zooplankton dynamics as has been observed in other studies (i.e., Castro and Gonçalves 2007, Ziadi et al. 2015). We could infer that the zooplankton community would then be dominated by cladocerans in the spring when phytoplankton biomass is typically higher, but in Estabrook Park Pond phytoplankton biomass typically peaks in the summer months. If this is the case, we cannot operate with assumption on the seasonal dynamics of the zooplankton community but need to conduct additional studies to better understand the dynamics within our system of study. Changes within the zooplankton community can also alter grazing rates, which may be significantly higher earlier in the year when grazer susceptible phytoplankton would be more abundant in the environment.

SUMMARY

Despite minimal grazing effects being observed in Estabrook Park Pond, this study was able to use a novel method (flow cytometry) to study the response of the phytoplankton community to grazing. Few studies have used this method to measure grazing in natural systems. Using a small system such as Estabrook Park Pond provided an opportunity to assess the system as a whole and to observe changes (i.e., nutrient availability, community composition) that in larger systems may be more difficult to identify. In the present study we found little evidence of significant grazing of phytoplankton in total or in any specific taxon, with no evidence that zooplankton grazing caused cell death. We tested this hypothesis only in two seasons, so it might be important to also try it in early or late spring to allow for considerations of seasonal variation in community composition and their effects on phytoplankton community structure and cell death.

REFERENCES

Berggreen, U., Hansen, B. & Kiørboe, T. 1988. Food size spectra, ingestion and growth of the copepod *Acartia tonsa* during development: Implications for determination of copepod production. *Mar Biol* 99, 341–352.

Berquist, A.M., Carpenter, S.R. and Latino, J.C. 1985. Shifts in phytoplankton size structure and community composition during grazing by contrasting zooplankton assemblages. *Limnol Oceanogr* 30: 1037-1045.

Brooks, J.L. and Dodson, S.I. 1965. Predation, body size, and composition of plankton. *Science* 150: 2835.

Carotenuto, Y., Wichard, T., Pohnert, G., and Lampert, W. 2005. Life-history responses of *Daphnia pulicaria* to diets containing freshwater diatoms: Effects of nutritional quality versus polyunsaturated aldehydes. *Limnol Oceanogr* 50: 449-454.

Castro, B.B. and Gonçalves, F. 2007. Seasonal dynamics of the crustacean zooplankton of a shallow eutrophic lake from the Mediterranean region. *Fundam Appl Limnol* 169: 189-202.

Coesel, P.F.M. 1997. The edibility of *Staurastrum chaetoceras* and *Cosmarium abbreviatum* (desmidiaceae) for *Daphnia galeate/hyaline* and the role of desmids in the aquatic food web. *Aquat Biol* 31: 73-78.

Cowles, T.J., Olson, R.J. and Chishold, S.W. 1988. Food selection by copepods: discrimination on the basis of food quality. *Mar Biol* 100: 41-49.

Cucci, T.L., Shumway, S.E., Brown, W.S. and Newell, C.R. 1989. Using phytoplankton and flow cytometry to analyze grazing by marine organisms. *Cytometry* 10: 659-669.

Dieghri, N., Atkinson, A., Fileman, E.S., Harmer, R.A., Widdicombe, C.E., McEvoy, A.J., Cornwell, J. and Mayor, D.J. 2018. High prey-predator size ratios and unselective feeding in copepods: a seasonal comparison of five species with contrasting feeding modes. *Prog Oceangr* 165: 63-74.

Elser, J.J., Elser, M.M., MacKay, N.A., and Carpenter, S.R. 1988. Zooplankton-mediated transitions between N- and P-limited algal growth. *Limnol Oceanogr* 33: 1-14.

Helenius, L.K. and Saiz, E.2017. Feeding behavior of the nauplii of the marine calanoid copepod *Paracartia grani* Sars: functional response, prey size spectrum, and effects of the presence of alternative prey. *PLoS ONE* 12:e0172902. doi:10.1371/journal.pone.0172902

Ianora, A., Miralto, A., Poulet, S.A., Carotenuto, Y., Buttino, I., Romano, G., Casotti, R., Pohnert, G., Wichard, T., Colucci-D'Amato, L., Terrazzano, G. and Smetacek, V. 2004. Aldehyde suppression of copepod recruitment in blooms of a ubiquitous planktonic diatom. *Nature* 429:403-407.

Jungbluth, M.J., Selph, K.E., Lenz, P.H. and Goetze, E. 2017. Species-specific grazing and significant trophic impacts by two species of copepod nauplii, *Parvocalanus crassirostris* and *Bestiolina similis*. *Mar Ecol Prog Ser* 572: 57-76.

Kamjunke, N. and Zehrer.R.F. 1999. Direct and indirect effects of strong grazing by *Daphnia galeata* on bacterial production in an enclosure experiment. *J Plank Res* 21:1175-1182.

Kubanek, J., Snell, T.W., and Pirkle, C. 2007. Chemical defense of the red tide dinoflagellate *Karenia brevis* against rotifer grazing. *Limnol Oceanogr* 52: 1026-1035.

Landry, M.R., Kirshtein, J. and Constantinou, J. 1995. A refined dilution technique for measuring the community grazing impact of microzooplankton, with experimental tests in the central equatorial Pacific. *Mar Ecol Prog Ser* 120: 53-63.

Lehman, J.T. and Sandgren, C.D. 1985. Species-specific rates of growth and grazing loss among freshwater algae. *Limnol Oceanogr* 30: 34-46.

Leitão, E., Panosso, R., Molica, R., Ger, K.A. 2020. Top-down regulation of filamentous cyanobacteria varies among a raptorial versus current feeding copepod across multiple prey generations. *Freshw Biol* 66: 142-156.

Lürling, M. 1998. Effect of grazing-associated infochemicals on growth and morphological, development in *Scenedesmus acutus* (Chlorophyceae). J. Phycol. 34: 578-586.

Maveli, S.M., Nandini, S. and Sarma, S.S.S. 2004. The efficacy of *Scenedesmus* morphology as a defense mechanism against grazing by selected species of rotifers and cladocerans. *Aquat Ecol* 38: 515-524.

McQueen, D.J. 1970. Grazing rates and food selection in *Diaptomus oregonensis* (Copepoda) from Marion Lake, British Columbia. *J Fish Res Board Can* 27: 13-20.

Moore, M. and Folt, C. 1993. Zooplankton body size and community structure: effects of thermal and toxicant stress. *TREE* 8: 178-183.

O'Brien, W.J. 1979. The predator-prey interaction of planktivorous fish and zooplankton: recent research with planktivorous fish and their zooplankton prey shows the evolutionary thrust and parry of the predator-prey relationship. *Am Sci* 67: 572-581.

Peters, R.H. and Downing, J.A. 1984. Empirical analysis of zooplankton filtering and feeding rates. *Limnol Oceanogr* 29: 763-784.

Pohnert, G. 2002. Phospholipase A2 activity triggers the wound-activated chemical defense in the diatom *Thalassiosira rotula*. *Plant Physiol* 129: 103-111.

Ribalet, F., Berges, J.A., Ianora, A., and Cassotti, R. 2007. Growth inhibition of cultured marine phytoplankton by toxic algal-derived polyunsaturated aldehydes. *Aquat Toxicol* 85: 219-227.

Saiz, E., Griffell, K., Calbet, A. and Isari, S. 2014. Feeding rates and prey: predator size ratios of the nauplii and adult females of the marine cyclopoid copepod *Oithona davisae*. *Limnol Oceangr* 59 :2077-2088.

Šimek, K., Nedoma, J., Znachor, P., Kasalický, V., Jezbera, J., Hornak, K. and Seďa, J. 2014. A finely tuned symphony of factors modulates the microbial food web of a freshwater reservoir in spring. *Limnol Oceangr* 59: 1477-1492.

Sterner, R.W. 1986. Herbivores' direct and indirect effects on algal populations. *Science* 231: 605-607.

Talling, J.F. 2002. Phytoplankton-zooplankton seasonal timing and the 'clear-water phase' in some English lakes. *Freshw Biol* 48: 39-52.

Titelman, J., Riemann, L., Holmfeldt, K. and Nilsen, T. 2008. Copepod feeding stimulates bacterioplankton activities in a low phosphorus system. *Aquat Biol* 2: 131-141.

Turner, J.T., Tester, P.A., Lincoln, J.A., Carlsson, P. and Granéli, E. 1999. Effects of N:P:Si ratios and zooplankton on phytoplankton communities in the northern Adriatic Sea. III. Zooplankton populations and grazing. *Aquat Micro Ecol* 18: 67-75.

Vanni, M.J. 1987. Effects of nutrients and zooplankton size on the structure of a phytoplankton community. *Ecology* 68: 624-635.

Vanni, M.J. and Temte, J. 1990. Seasonal patterns of grazing and nutrient limitation of phytoplankton in a eutrophic lake. *Limnol Oceangr* 35: 697-709.

Vanni, M.J. 2002. Nutrient cycling by animals in freshwater ecosystems. *Annu Rev Eco Syst* 33: 341–70

Venuleo, M., Raven, J.A., and Giordano, M. 2017. Intraspecific chemical communication in microalgae. *New Phytol* 215: 516-530.

Vrede, T. and Vrede, K.. 2005. Contrasting 'top-down' effects of crustacean zooplankton grazing

on bacteria and phytoflagellates. *Aquat Ecol* 39: 283-293.

Yoshida, T., Hairston Jr., N.G. and Ellner, S.P. 2004. Evolutionary trade-off between defence against grazing and competitive ability in a simple unicellular alga, *Chlorella vulgaris*. *Proc R Soc Lond* 271: 1947-1953.

Zhu, X., Wang, J., Chen, Q., Chen, G., Huang, Y. and Yang, Z. 2016. Costs and trade-offs of grazer-induced defenses in *Scenedesmus* under deficient resource. *Sci Rep* 6, 22594. https://doi.org/10.1038/srep22594

Ziadi, B., Dhib, A., Turki, S. and Aleya, L. 2015. Factors driving the seasonal distribution of zooplankton in a eutrophicated Mediterranean lagoon. *Mar Pollut Bull* 97: 224-233.

Chapter 4: Investigations of potential allelopathic interactions among phytoplankton

INTRODUCTION

While abiotic factors are commonly considered to be drivers of phytoplankton community dynamics (Hutchinson 1961) and subsequently cell death (Bidle and Falkowski 2004, Franklin et al. 2006), biotic interactions have the potential to be important drivers as well. Kozik et al. (2019) concluded in a limited study of phytoplankton dynamics in Estabrook Park Pond, that biotic rather than abiotic factors may be important in regulating community dynamics and cell death. Chapter 2 corroborated these findings, as the three-year study found few correlations of phytoplankton groups with abiotic factors; instead, correlations were observed among phytoplankton groups, suggesting inter-taxon relationships could be important in regulating phytoplankton dynamics. While some groups saw increases in total abundance in the presence of others (i.e., pennate diatoms and desmids), other groups showed to increases in dead cells in the presence of others (i.e., dinoflagellates and cyanobacteria), which could be indicative of cellular communication among phytoplankton groups where a stimulus (e.g., grazing, environmental conditions) generates a response that is then "detected" by another (e.g., Sukenik et al. 2002, Venuleo et al. 2017). The association of increased dead phytoplankton cells with other taxa could be indicative of allelopathic interactions, resulting in increased mortality of 'targeted' species (e.g., Vardi et al. 2002). To better understand these interactions, further investigation was warranted.

Allelopathy in phytoplankton. Allelopathy has been thought to play an important role in phytoplankton succession, influencing bloom formation and subsequent declines (Keating 1977,

Vardi et al. 2002). Allelochemicals and secondary metabolites released into the environment, can ward off predators (Pohnert 2002, Kubanek et al. 2007), limit competition for resources (LeFlaive & Ten-Hage 2007) or mediate symbiotic relationships among algae and bacteria (Labeeuw et al. 2017).

Production of allelopathic compounds may be influenced by environmental conditions (Falpeto and Vasconcelos 2016), especially abiotic stress and taxa competition for limiting resources. Under these conditions, allelochemical production increases, and the target species is more susceptible to the chemical (Reigosa et al. 1999, LeFlaive & Ten-Hage 2007) due to the combined stress of allelochemical exposure and resource limitation (Fistarol et al. 2005). Allelochemicals diffuse rapidly into the surrounding environment (Lewis 1986) so they can influence organisms within the immediate area (LeFlaive & Ten-Hage 2007). Chemicals released can affect organisms (animals, phytoplankton, bacteria) within the community, with various modes of action (formation of ROS, inhibition of photosynthesis, interference with protein or enzyme synthesis) resulting in growth inhibition or death (*reviewed by* LeFlaive & Ten-Hage 2007).

Studies have investigated how species respond to interactions with other phytoplankton (e.g., Proctor 1957, Maestrini & Bonin 1981, Barriero & Hairston 2013) while others have looked at the effects of compounds released by aquatic macrophytes on phytoplankton (Wium-Anderson et al. 1982, Søndergaard & Moss 1998, Mulderij et al. 2007). Early studies of allelopathy used co-culturing experiments to identify potential interactions among phytoplankton, though identification of allelochemicals was difficult. Proctor (1957) conducted co-culturing experiments using *Chlamydomonas reinhardtii* and *Haematococcus*, finding that *C.*

reinhardtii could produce a compound that eliminated *Haematococcus*. In the marine environment, Fistarol et al. (2004a) studied the effects of the dinoflagellate *Alexandrium*, that has both toxic and non-toxic strains, on natural phytoplankton assemblages. Exposing natural samples to cell-free filtrate from toxin-producing *Alexandrium tamarense*, the community response revealed that phytoplankton were not affected in the same way (positive, negative, neutral). Similarly, in freshwater, Barriero and Hairston (2013) found that the allelochemicals (fatty acids) produced by *C. reinhardtii* increased during periods of resource limitation had a variety of effects on target species.

Allelopathy may not always result in an inhibition response. While the production and release of allelochemicals can decrease resource competition with 'target' taxa (LeGrand et al. 2003, Gross 2003), there has been evidence that co-existing species can acclimate to allelochemicals (Reigosa et al. 1999), limiting effects on their cells. Exposure to allelochemicals may lead organisms to produce cysts (Fistarol et al. 2004b), giving them a protective advantage to prevent cellular damage from exposure. Cysts would then hatch as conditions improve to seed increases in the target population abundance. For other taxa, allelochemical production may be promoted under conditions where species are exposed to high densities of competitors (Vardi et al. 2002). When exposed to spent filtrate from *Perdinium gatunense*, *Microcystis aeruginosa* increased production of compounds affiliated with the allelochemical microcystin while cell viability decreased. This could be a communication strategy of *Microcystis*, as stressed *M. aeruginosa* cells underwent lysis, without a competitor present, releasing microcystin to the environment, informing the remaining population of the stress (Kaplan et al. 2012). Similar responses have also been observed with resource-limited *C. reinhardtii*, where

allelochemical production increased in the absence of competitors, suggesting communication with the remaining culture of the conditions and stress of the limited cells (Barriero and Hairston 2013).

Observations of cyanobacteria (e.g., *Microcystis*) responding to competing species as in Vardi et al.'s study (2002), communicating with conspecifics when stressed (Kaplan et al. 2012), or producing toxins that can be harmful to others within the environment (Huisman et al. 2005, Rastogi et al. 2015) highlight some of the interactions that cyanobacteria have within the community. These studies tend to focus on the growth of taxa and attempts to control cyanobacterial growth, with minimal consideration of loss processes (i.e., cell death, grazing, sedimentation) that could be involved in community succession. In the case of cyanobacteria, grazing and sedimentation may not be driving forces in community dynamics, as they can produce toxins to deter grazing, and cells float, limiting each as factors in their dynamics. Cell death, in response to abiotic and biotic (i.e., allelopathy) factors, could be influential to shaping the freshwater cyanobacterial community, but is seldomly considered (Franklin et al. 2006). Changes in abiotic conditions and/or interactions among phytoplankton may be more likely to elicit cell death.

Approaches to studying allelopathy. Given that allelopathic interactions can manifest in a variety of ways, studying allelopathy in aquatic systems can be difficult. Allelochemicals are water-soluble and known to diffuse quickly in water (Lewis 1986), limiting the ability to measure in situ and observe the effects of compounds on other species. Further, effects of the allelochemical are most apparent adjacent to the emitter (LeFlaive & Ten-Hage 2007) which can impede our ability to understand the overall effect of these chemicals on other species that

may be nearby. With the potential for abiotic and biotic stressors to influence toxin production, it is important to study these interactions more directly and understand how individual species respond to exudates. Small scale experiments provide options for high sampling frequencies and to make clear observations of factors affecting test species.

Frequently the use of exudates from spent cultures of test species are used to directly expose the 'target' to a high concentration of the chemical produced (e.g., Fistarol et al. 2004a, Sukenik et al. 2002, Wang et al. 2017, Xue et al. 2018). Exposure to high concentrations of exudates often elicits measurable responses in target species, though the artificial enhancement may make it difficult to fully interpret the role an exudate may play in the environment. Alternative methods can expose target species to cellular extracts from toxin-producing species at different concentrations of extracts (e.g., Periera et al. 2018) including dose-dependent studies using purified allelochemicals extracted from toxin-producing taxa (Hu et al. 2008). By using these methods, concentrations of exudates and/or allelochemicals can be controlled for, with lower concentrations being more like natural exposures. Additional studies can be done to observe the influence of varying nutrient conditions (e.g., Johansson and Granéli 1999, Granéli 2006) to better understand the role that nutrient availability plays in toxin production for the producer as well as the target species, helping to tease apart key drivers resulting in changes of growth rates and fluorescence of phytoplankton species.

Co-culturing methods described to study the species interactions (Proctor 1957, Hendzel and Nagy 1986) provide a way to separate test species while allowing for the passage of exudates between species. These methods use a semi-permeable divide between the species that allows for free movement of molecules smaller than the pore (or molecular) size. Species

can be placed in controlled, nutrient replete conditions with the only 'stressor' near another species. If allelochemicals/exudates are produced, species should respond if affected by the competing species.

Measuring effects of interactions: *Cell counts.* Effects of allelopathic interactions can be used to monitor target species for changes in fluorescence (F_v/F_m) and cell abundances, or other physiological parameters such as enzymatic activity (i.e., Chia and Bittencourt-Oliviera 2021). Target species cell abundance can be estimated using microscopy and flow cytometry (Kubanek et al. 2005, Suikannen et al. 2004). Observations via microscopy also provide evidence of cellular damage in response to allelochemical exposure (Hu et al. 2008, Śliwińska and Latala 2012). Flow cytometry can also be used to monitor cell morphological changes (Lelong et al. 2011) or cell viability through use of mortal stains. Pigment fluorescence measures provide insight to estimated biomass of target species (Suikannen et al. 2004, Kubanek et al. 2005, Wang et al. 2017), but also photosynthetic activity (e.g., Hu et al. 2008, Karlberg and Wulff 2013, Śliwińska-Wilczewska et al. 2016), as numerous studies have shown that allelochemicals tend to inhibit photosynthetic processes (e.g., Sukenik et al. 2002, Gross 2003). Sukenik et al. (2002) observed in their study of the effects of *Microcystis* on *Peridinium gatunense*, in addition to declines in growth in response to *Microcystis* exposure, *P. gatunense* exhibited declines in fluorescence, .

Fluorescence (F_v/F_m). Declines in fluorescence can be indicative of changes in cellular health and can be measured as quantum yield of photosystem II (ΦPSII, measured as F_v/F_m), where F_v is the difference between F_m and F_0. Measuring the chl *a* fluorescence of dark acclimated cells (F_0) followed by the emission of cells exposed (F_m) to the photosynthetic inhibitor, 3(3,4-

dichlorophenyl)-1,1-dimethlyurea (DCMU), which causes the PSII reaction centers to close, provides a measure of photosynthetic efficiency (Cullen and Renger 1979). Healthy, unstressed cells would have a high F_v/F_m, while low values indicate cells that are in decline (dead/dying) in response to exposure to a compound produced by its competitor.

ROS detection. Phytoplankton can exhibit an increase in reactive oxygen species (ROS) production, which can be indicative of a stress response to conditions. Increases in ROS levels have been observed in cells exposed to toxin-producing species (Franklin et al. 2004, Szivak et al. 2009, Chia et al. 2021). For example, *M. aeuruginosa* and *Pseudokirchneriella subcaptita* have been found to increase ROS production when exposed to allelochemicals produced by aquatic macrophytes, which can limit their photosynthetic abilities leading to oxidative damage and subsequently cell death (i.e., Wang et al. 2011). To measure ROS in cells, the stain carboxy-H_2DCFDA [5-(and 6)-carboxy-2',7'- dichlorodihydrofluorescein diacetate is used. The stain, which is low in fluorescence, can permeate cell membranes, but once inside is cleaved in the presence of ROS to release highly fluorescent and insoluble products that are retained in the cell and can be measured using flow cytometry (Franklin et al. 2004, Szivak et al. 2009), or microscopy (Franklin et al. 2004).

Objective and hypotheses. My objective in this chapter was to explore potential inter-taxon relationships of phytoplankton species found in Estabrook Park Pond to determine whether allelopathic interactions may contribute to changes in community dynamics and cell death. I approached this objective by conducting co-culturing experiments of cultured species found in Estabrook Park Pond that are commonly associated with allelochemical production (i.e., *Microcystis aeruginosa*) and other known species (i.e., *Chlamydomonas reinhardtii*, *Synedra*) to

better understand these relationships, as correlations among abundances and dead cells were observed in Chapter 2 studies with these groups (Table 5). I hypothesized that: 1) Taxa known to produce allelochemicals that reduce the growth of another will result in an increase in the proportion of dead cells in other taxa; 2) Taxa which are known to be toxic to humans will be more likely to produce allelopathic compounds, observed by declines of viable cells of competing taxa, with increases in dead cells; and 3) Taxa that produce their own allelochemical will be able to counteract the effects of toxin producing *Microcystis aeruginosa*, resulting in low quantities of cells detected as dead.

MATERIALS AND METHODS

Algal cultures. Based upon observations made in the three-year study of Estabrook Park Pond (*see* Chapter 2), algal species were selected using the inter-taxon relationships identified between cell abundances and dead cells (Table 5). These interactions could be due to allelopathic interactions given the groups which correlated with dead cell counts of groups, which included green algae (group 1), pennate diatoms (group 2) and cyanobacteria (group 12). *Microcystis aeruginosa* (CPCC 299, microcystin-producing up to 415 μg g^{-1} dry weight), obtained from the Canadian Phycological Culture Center (CPCC) and selected on the criteria that it was a known toxin-producing strain that was isolated from a freshwater environment. *Synedra* sp. and *Chlamydomonas reinhardtii* (c-9 wt) were used to test the potential allelopathic effects of the *M. aeruginosa* strain selected on the criterion that they are representative of taxa found in Estabrook Park Pond, as well as being representative of taxa that have been shown to have a response to *Microcystis* sp. in previous studies. All cultures were maintained using their native growth medium (liquid BG-11 for *M. aeruginosa*; DY-V for *Chlamydomonas* and *Synedra*), grown at 18°C under filtered fluorescent light (14:10 light/dark cycle) until needed for experiments. Prior to the beginning of experiments, *M. aeruginosa was* acclimated to DY-5 (modification of DY-III [Lehman 1976] by Sandgren [unpublished]) growth medium. In doing this, all species were exposed to the same nutrient-replete conditions at the time of the experiments, avoiding nutrient limitation.

Experimental design. Laboratory co-culturing experiments were conducted, growing taxa identified in the field (*Microcystis aeruginosa*, *Chlamydomonas reinhardtii*, *Synedra* sp.) under nutrient-replete conditions in custom-designed vessels that separated cells (membrane filters),

while allowing media to mix. The design of the apparatus was based on Hendzel and Nagy's (1986) dual-chamber chemostat used to study competition for resources among species of algae, though we used smaller volumes to promote exposure of potential allelochemicals released (Fig. 14). A similar vessel has also been used to study the effects of bacteria on diatom metabolism (Paul et al. 2012).

Experiments were conducted using replicate co-culturing apparatuses (Fig. 14), where 5 mL of culture was placed in each side containing 100 mL of growth medium, separated only by a membrane filter (pore size 0.2 µm). Species were paired as controls (i.e., Species A: Species A) as well as against one another (i.e., Species A: Species B). Apparatuses were gently bubbled and mixed with stir bars, which allowed for continuous mixing of samples throughout experiments, preventing cells from settling on the bottom of the apparatus. Experiments were done at 18 °C under 14:10 light/dark cycle for a minimum of 7 days. Subsamples (10 mL) were taken from each side of the apparatuses every 24 hours and analyzed for photosynthetic competence (F_v/F_m), cell abundance and cell viability (Sytox Green®) by flow cytometry. Volumes removed were replenished with DY-V media to ensure nutrient replete conditions were maintained.

Measurements. Cell abundance and mortality (Sytox Green® mortal staining), as well as photosynthetic efficiency (F_v/F_m) were measured every 24 h. Experimental controls, where each species was cultured with itself, were used to observe changes in F_v/F_m and cell mortality to determine whether there was an interaction occurring.

To evaluate photosynthetic competence, 5 mL samples of both species were collected from the co-culturing apparatus. To do this, a bench-top fluorometer (TD-700, Turner Designs,

Sunnyvale, CA) was used to measure fluorescence of the samples. Initial values (F_0) were measured using dark-acclimated cells (15 min.), while final fluorescence values (F_m) were measured following the addition of 10 µM (final concentration) of DCMU to the samples. To determine photosynthetic efficiency, F_v/F_m was calculated using the equation $(F_m-F_0)/F_m$ (Foyer et al. 1994).

Subsamples of the species were collected, and control samples (0.5 mL) counted using a BD Accuri C6 flow cytometer (BD Biosciences, Michigan), outfitted with blue (488 nm) and red (640 nm) excitation lasers and four emission detectors (FL-1 533/30 nm, 'green'; FL-2 585/40 nm, 'orange'; FL-3 > 670 nm, 'red'; FL-4 675/25 nm, 'far red'). 90% attenuation filters were used on FL-1, FL-2 and FL-3. Counts were set to trigger on red fluorescence (FL-3), with a threshold of 500 (relative units) on FL-3 so that only putative algal cells are counted. To assess cell viability, replicate samples were treated with Sytox Green®, a mortal stain that infiltrates compromised cells, indicating cells that were dead (Veldhuis et al. 2001), to estimate dead cells present in the sample.

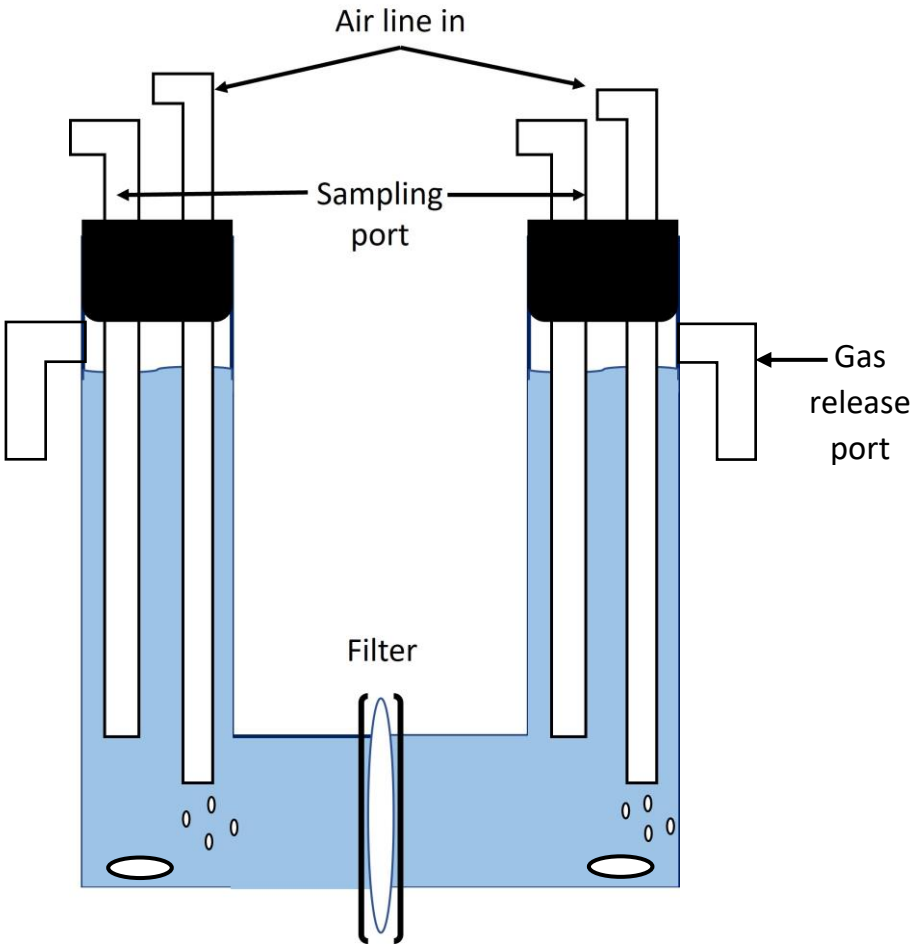

Figure 14. Schematic of co-culturing apparatus design used in allelopathic interaction experiments. Filter was in place to prevent movement of phytoplankton cells while allowing for movement of substances and/or exudates to either side of the experimental apparatus. Inflow air lines allowed for bubbling of cultures to limit sedimentation of non-motile cells.

RESULTS

***Microcystis* vs. *Chlamydomonas*: Cell abundance.** Cell abundances (Fig. 15A) for controls and experimental treatments of both species followed similar dynamics throughout the experiment. *Chlamydomonas* increased through day 8, declining after day 10. *Chlamydomonas* control appeared to stabilize around 5 x10^5 cells mL^{-1} for remainder of experiment (days 12-15), though the experimental treatment continued to decline. *Microcystis* continued to increase in abundance throughout the experiment.

Cell abundances for control and experimental treatments followed similar patterns of increase and decrease (Fig. 15D) in the second experiment. *Microcystis* was observed to be more abundant in the control treatment, reaching a maximum of over 6 x 10^5 cells mL^{-1}, compared to the *Chlamydomonas*-exposed treatment where maximum abundance on the final day of the experiment was about 2 x 10^4 cells mL^{-1}. *Chlamydomonas* exhibited increases and declines in abundance with similar abundances observed regardless of the treatment on most days (exception: Day 8 when abundance of the *Microcystis*-exposed cells was higher (> 3 x 10^5 cells mL^{-1}) compared to the control (< 15 x 10^4 cells mL^{-1}).

F_v/F_m. F_v/F_m measures (Fig. 15B) of both species, like cell abundances, displayed similar patterns regardless of being control or experimental treatments. In few instances (Days 2 and 7), co-cultured *Microcystis* exhibited an inverse relationship with *Chlamydomonas*, though measured fluorescence in the following sample mirrored the control.

Both *Chlamydomonas* and *Microcystis* exhibited similar trends in F_v/F_m for their respective treatments throughout the second experiment, though there were exceptions on

Day 2 for *Chlamydomonas* and Day 11 for *Microcystis* (Fig. 15E). In both cases, control cells exhibited higher Fv/Fm inverse of the experimental treatment. *Microcystis* exhibited a decline in F_v/F_m within the first couple of days of the experiment as was observed in experiment 1 (Fig. 15B).

Dead cell proportion. *Microcystis* was found to have a higher percentage of dead cells compared to *Chlamydomonas* (< 3 and < 1%, respectively; Fig. 15C). Dead cell proportions were similar between controls and experimental treatments for *Chlamydomonas* but not for *Microcystis*. *Chlamydomonas*-exposed *Microcystis* trended higher in dead cells through Day 8 of the experiment, though higher amounts of dead cells were observed in the control from day 10 through the end of the experiment.

Proportions of dead cells were similar in both controls and exposed cell treatments (Fig. 15F), with the percentage of dead cells relatively low for both species (< 5%). *Chlamydomonas* had the highest proportion of dead cells at the onset of the experiment, though after this, dead cells accounted for < 1% of cells counted for the species (Fig. 15F). Control treatment *Chlamydomonas* frequently had slightly (+ 0.5%) higher proportions of dead cells. *Microcystis* exhibited the highest proportion of dead cells on days 5 and 14, reaching 4% and 3% dead cells respectively. The percentage of dead cells of the *Chlamydomonas*-exposed *Microcystis* began increasing after day 9 through the end of the experiment, a trend that differs from the experimental results of the same pairing (Fig. 15C). The overall rise and fall of dead cells proportions on a cycle is like that observed in the first experiment (Figs. 15C, F).

General observations of *Microcystis* vs. *Chlamydomonas*. In the second experiment, membrane filters that had separated the cultures were inspected and it was observed that algal biomass had accumulated in controls and exposed-cell treatments (Fig. 16).

***Microcystis* vs. *Synedra*: Cell abundance.** Controls and exposed-cell treatments for both *Microcystis* and *Synedra* exhibited similar increases in cell abundance (Fig. 17A). Interestingly, from day 11 onward exposed-cell abundances for both species were almost identical, reaching cell abundances exceeding 6 x 10^5 cells mL^{-1}. Controls for both species increased in a similar way, thought *Microcystis* had higher abundances that *Synedra*.

In the second experiment (Fig. 17D), *Microcystis* had higher cell abundances compared to *Synedra* until the final day of the experiment when *Microcystis*-exposed *Synedra* reached an abundance greater than *Microcystis* in the same treatment (Fig. 17D). Overall trends in cell abundance for both species mirror observations from the first *Microcystis:Synedra* experiment (Fig. 17A), with controls and exposed-cell treatments increasing in similar ways.

F_v/F_m. Measures of F_v/F_m for both species in the first experiment (Fig. 17B) followed similar fluctuations in fluorescence values, reaching the highest photosynthetic activity on day 4 (F_v/F_m = 0.6). Fluorescence measures stabilized for both species around 0.3 for most of the experimental period, though *Synedra* did exhibit lower F_v/F_m values compared to *Microcystis* towards the end of the experiment (Day 11 onward).

In experiment 2, F_v/F_m in controls for both species was higher than that observed in exposed-cell treatments (Fig. 17E). *Microcystis* controls had higher fluorescence values than

Synedra, which could be due in part to differences in cell abundances (Fig. 17D). In exposed-cell treatments, *Microcystis* and *Synedra* had very similar F_v/F_m values, being stable around 0.10.

Dead cell proportion. Proportions of dead cells were variable for *Microcystis* throughout the experiment, while *Synedra* exhibited relatively stable percentages of dead cells (Fig. 17C). The proportion of dead *Microcystis* exhibited rises and falls throughout the experiment. Controls and exposed-cell treatments trended similarly throughout the experiment, though control treatments appeared to have higher percentages of dead cells compared to the exposed-cell treatments. *Microcystis* reached the highest number of dead cells in controls, with maximum percentage of almost 12 % on day 8 of the experiment. *Synedra*'s highest percentage was reached near the end of the experiment (6 %, day 15). Percentages of dead cells appeared to stabilize around 3 % for both *Microcystis* and *Synedra*.

Experiment 2 revealed similar dead cell cyclic patterns, with the percentage of dead cells measured rising and falling every other day (Fig. 17F). Proportions of dead cells were much higher than in the previous experiment, with *Synedra* reaching > 50% dead cells at the end of the experiment. *Synedra* had a higher proportion of dead cells, regardless of being of the control or exposed-cell treatments. *Microcystis* displayed < 10% dead cells throughout the experiment, with minimal differences between the control and exposed-cell treatments (Fig. 17F).

General observations of *Microcystis* vs. *Synedra*. In both experiments, *Synedra* had the tendency to adhere to the sides of the co-culturing apparatuses (Fig. 18A), in both control and exposed-cell treatment. In the second experiment, algal biomass accumulated on both sides of

the filter that separated the co-cultures of *Microcystis* and *Synedra* (Fig. 18B). Further, prior to removal of mixing (bubbling, stirring) the *Microcystis* side of the apparatus appeared a dense green color indicating a dense population of cells but without aggregates. Once the experiment concluded and mixing stopped, *Microcystis* appeared to form a cloud-like re-aggregate (Fig. 18C), potentially the reassociation of *Microcystis* colonies.

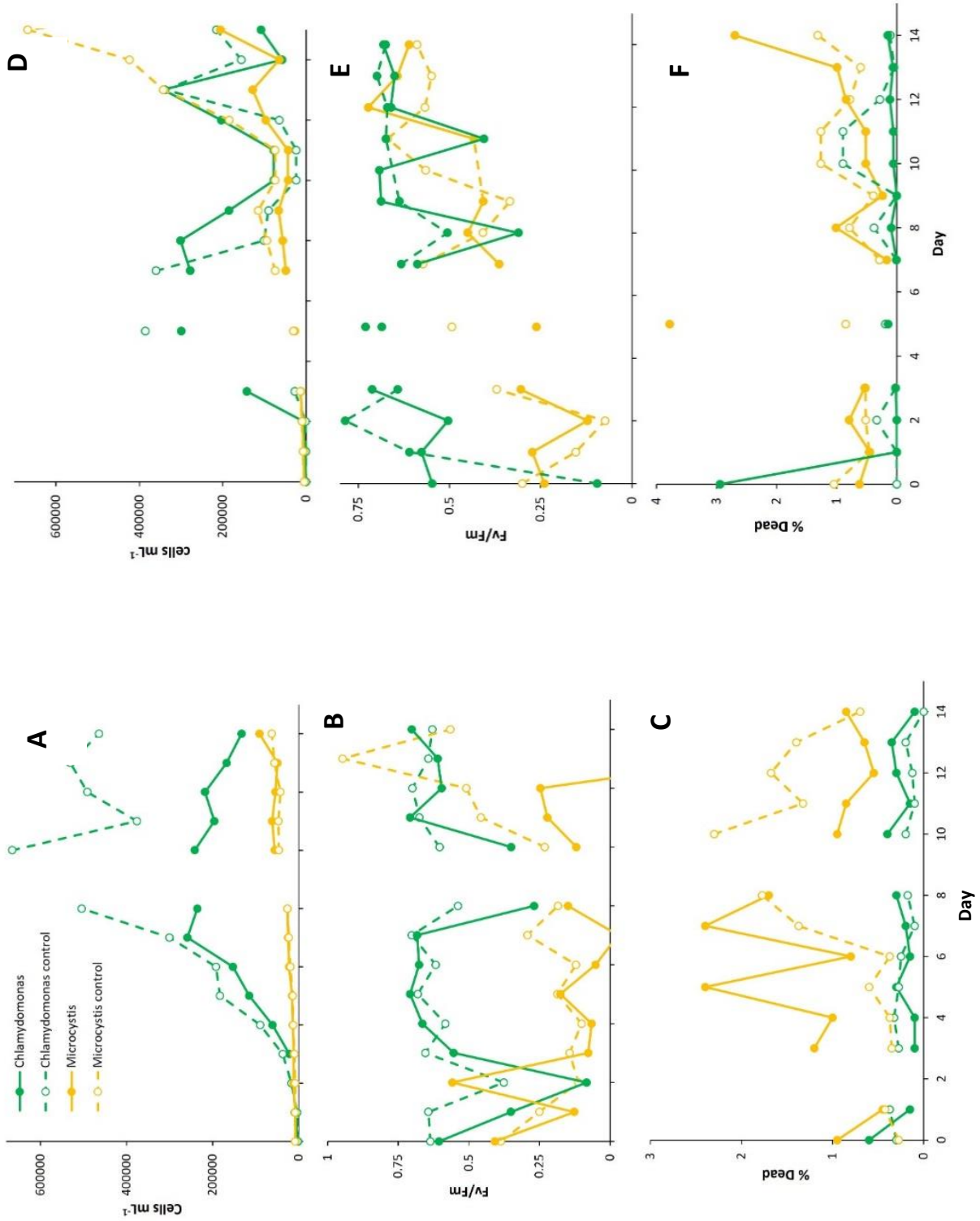
A
B
C
D
E
F
Chlamydomonas
Chlamydomonas control
Microcystis
Microcystis control
Cells mL-1
Fv/Fm
% Dead
Day

Figure 15. The effect of co-culturing on cell abundance, photosynthetic efficiency, and cell death for *M. aeruginosa* and *C. reinhardtii*. First experiment data shown in left column. Second experiment data shown in right column. A, D. Mean flow cytometric cell counts for taxa in first experiment. B, E. Photosynthetic competence (F_v/F_m) measures for taxa. C, F. Percentage of dead cells determined by use of Sytox Green® mortal stain for taxa. "Control" denotes treatment where species were paired with itself. Gaps in data indicate no data collected for that day in experiment.

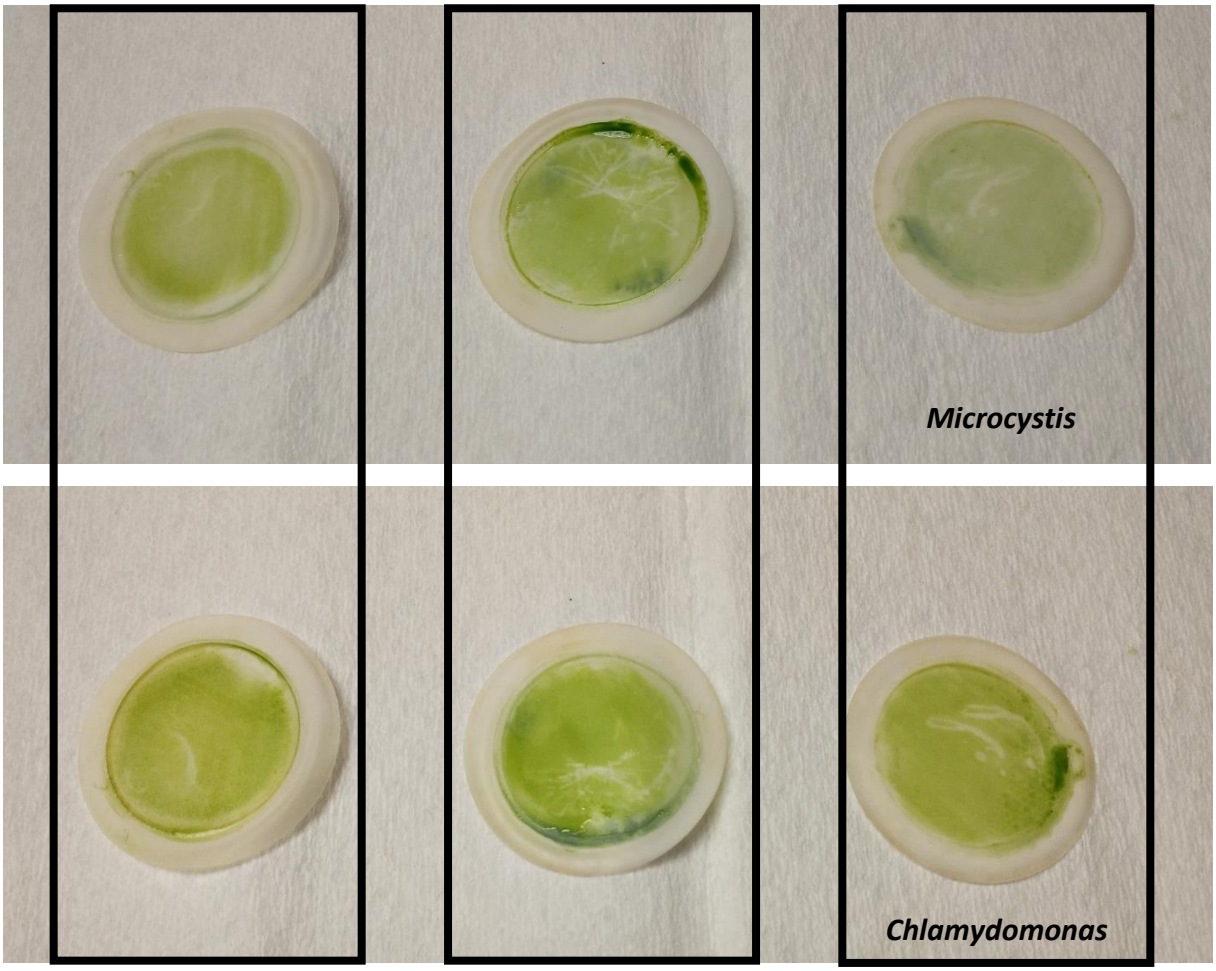

Microcystis control *Chlamydomonas* control Co-cultured pairing

Figure 16. *Microcystis* vs. *Chlamydomonas* co-culturing experiment filters at conclusion of the experiment. Filters were used to separate chambers to prevent cell passage but allow for movement of other materials. Left to right: *Microcystis* control; *Chlamydomonas* control; exposed cell/co-culture experiment.

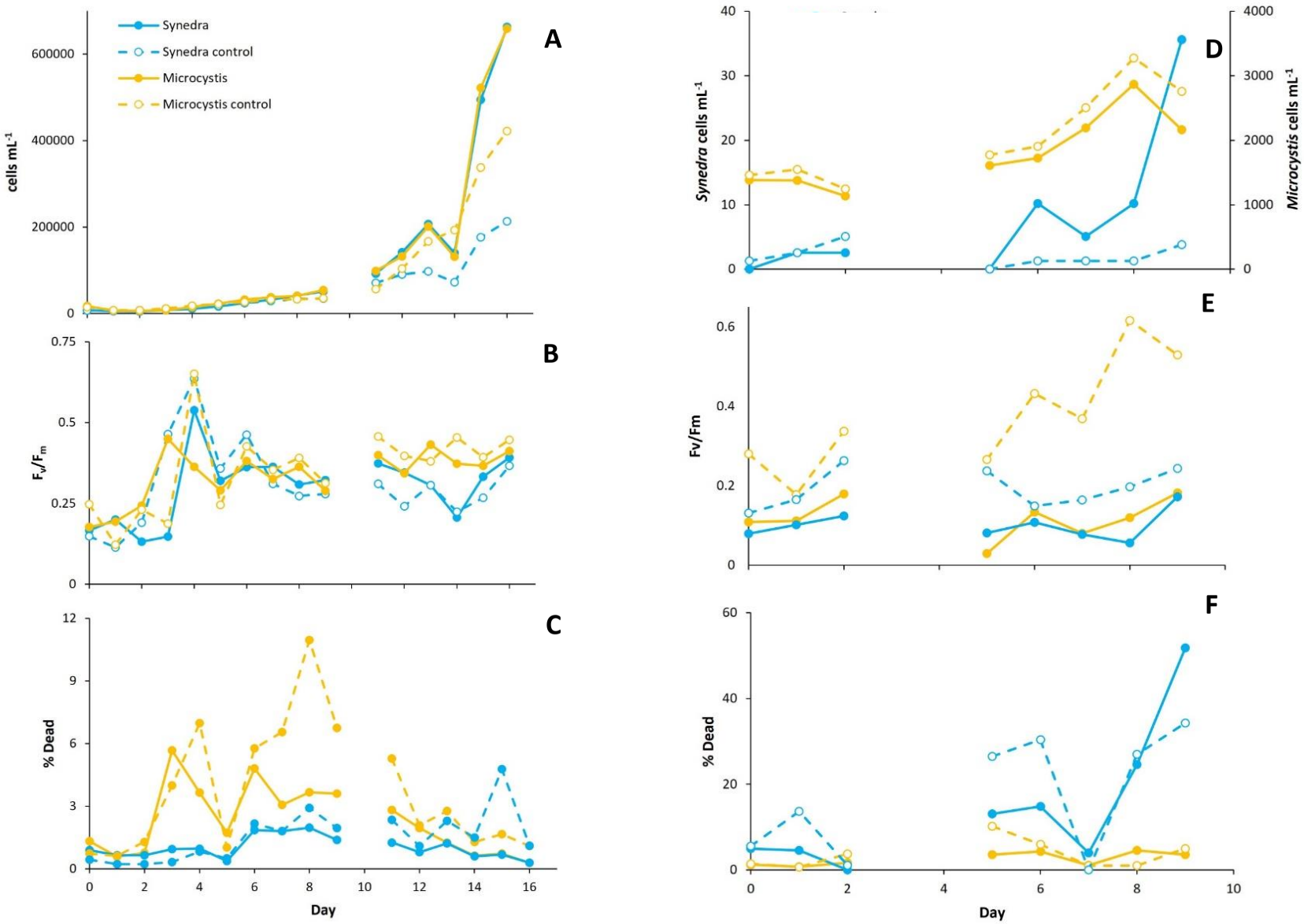
Synedra
Synedra control
Microcystis
Microcystis control
A
B
C
D
E
F
cells mL-1
Fv/Fm
% Dead
Synedra cells mL-1
Microcystis cells mL-1
Day

Figure 17. The effect of co-culturing on cell abundance, photosynthetic efficiency, and cell death for *M. aeruginosa* and *Synedra*. First experiment data shown in left column. Second experiment data shown in right column. A, D. Mean flow cytometric cell counts for taxa in first experiment. B, E. Photosynthetic competence (F_v/F_m) measures for taxa. C, F. Percentage of dead cells determined by use of Sytox Green® mortal stain for taxa. "Control" denotes treatment where species were paired with itself. Gaps in data indicate no data collected for that day in experiment.

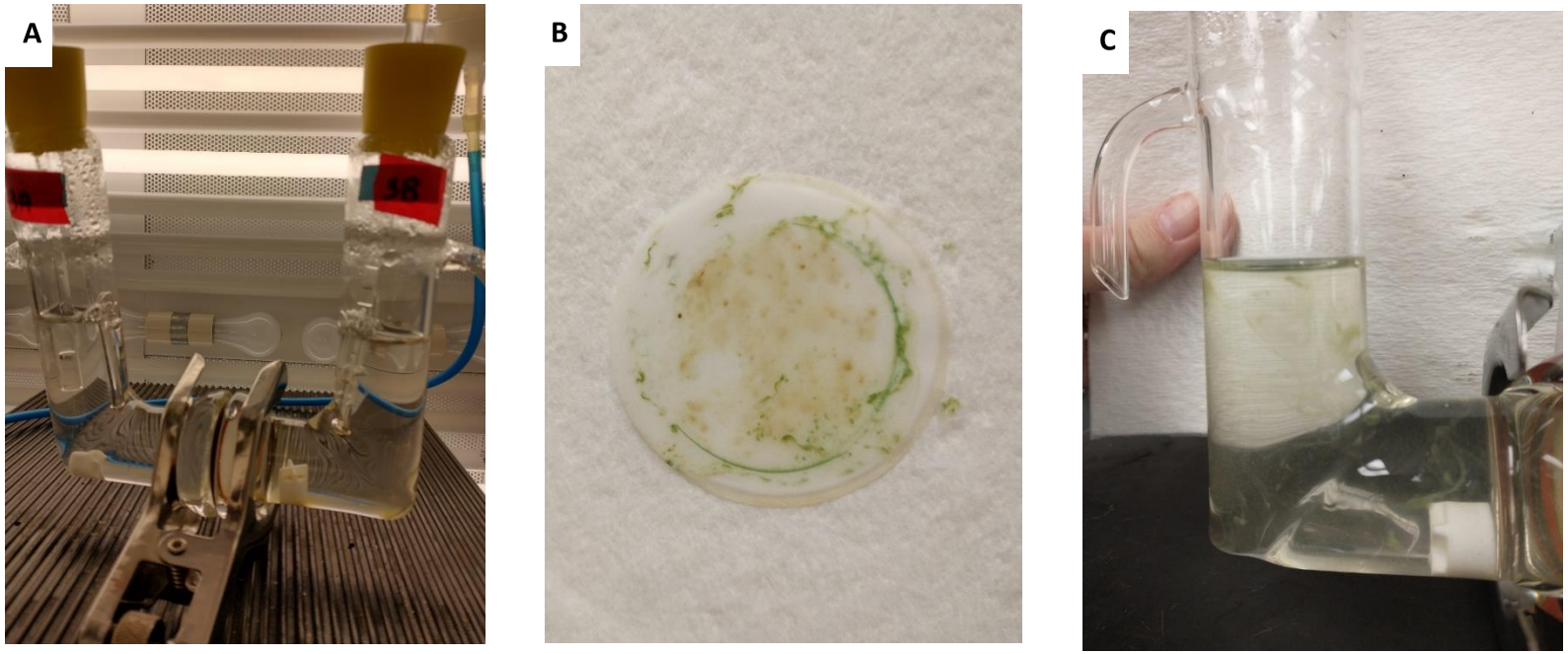

Figure 18. Qualitative observations of *Microcystis* vs. *Synedra* co-culturing experimetns. A. Example of *Synedra* cells adhering to co-culturing apparatus. By adhering to the glass, species responses to interactions with paired species may be difficult to interpret. B. Example of *Microcystis* biomass on the surface of membrane filter used to divide sides of co-culturing vessel. *Microcystis* filter side pictured. *Synedra* biomass can be viewed through the filter highlight density of growth. Cells did not adhere to filters in other treatments. C. "Bloom formation" of *Microcystis* at end of experiment once removed from gentle bubbling and stirring.

DISCUSSION

The studies included here were designed to help tease apart potential inter-taxon relationships among phytoplankton species found in Estabrook Park Pond. Test species were identified through Chapter 2 analyses that revealed that abundances of some phytoplankton groups (i.e., green algae, cyanobacteria) correlated with the appearance of dead cells of other groups and were used to conduct co-culturing experiments. Experiments were designed to observe changes in cell abundance, physiology and cell mortality as they related to interactions among organisms, comparing co-culture exposure to controls. While significant changes in measured parameters of 'target' species (i.e., *Chlamydomonas*, *Synedra*) did not occur, weak patterns of cell death and possible symbiotic relationships of *Chlamydomonas* and *Microcystis* were observed.

Interactions among *Microcystis* and *Chlamydomonas*. *Microcystis* and *Chlamydomonas* were selected as one of our pairings for understanding inter-taxon relationships as green algal abundance correlated with increased dead cells in the cyanobacteria as measured in our extensive study presented in Chapter 2. Both species were found in samples when evaluated by microscopy (Appendix B), in addition to each having been noted previously to produce compounds (i.e., fatty acids produced by *Chlamydomonas* [Barriero and Hairston 2013], microcystin by *Microcystis* [Vardi et al. 2002]) that could negatively impact others (i.e., cell death, decreased photosynthetic ability). Our findings suggest that if an interaction is occurring between these two species it is not of negative nature, as cell metrics of co-cultured cells were like that of controls (Figs. 15A-F).

This observation may be surprising as it has been thought that toxins produced by *Microcystis* can inhibit photosynthesis in nearby taxa (e.g., Gross 2003, *Aphanizomenon* in Hu et al. 2008) or limit cell growth (e.g., Hu et al. 2008). This would suggest that if *Chlamydomonas* was a targeted species of *Microcystis* as it produced (and released) microcystin, we would expect to see declines in the abundance of cells, photosynthetic ability (F_v/F_m) and potentially an increase in dead cells when exposed to the toxin. *Chlamydomonas* did not exhibit any of these changes, particularly with photosynthetic ability seldomly <0.5 (optimal F_v/F_m = 0.8, Masojídek et al. 2011). Perhaps *Chlamydomonas* and its ability to exude fatty acids that are harmful to other species (Proctor 1957) can affect *Microcystis* the way that other green algae (i.e., *Scenedesmus*) have been observed to inhibit growth of *Microcystis* (e.g., Bittencourt-Oliviera et al. 2014).

The relationship between *Microcystis* and *Chlamydomonas* was recently studied using similarly designed co-culturing experiments (Chia and Bittencourt-Oliveira 2021). They found that *Chlamydomonas* and *Microcystis* were capable of coexistence, as biovolume of the species increased regardless of exposure to the other, suggesting that each may stimulate the growth of the other. Declines in F_v/F_m were observed for *Microcystis* when paired with *Chlamydomonas* however, indicating a physiological response due to the interaction. Here we observed fluctuating measures of F_v/F_m, but nothing outside of the optimal range for cyanobacteria (0.5 – 0.7, Santabarbara et al. 2019). Cell abundances were variable, with *Microcystis* exhibiting lower cell counts compared to *Chlamydomonas*, though experiments were conducted at less-than-optimal temperatures for cyanobacteria, which could limit growth (Lürling et al. 2013). Cultures

had been acclimated to these temperatures prior to the experiment, so this is unlikely the cause of lower cell abundances observed for *Microcystis*.

Interactions among *Microcystis* and *Synedra*. The selection of *Synedra* as a test species for co-culturing investigations was made on the premise that like the green algae, diatom abundances were found to correlate with dead cells of various phytoplankton groups in Estabrook Park Pond (see Chapter 2). While this relationship was not observed with cyanobacteria, it was thought that given diatoms can produce their own exudates in the form of polyunsaturated aldehydes (PUAs) which can affect zooplankton reproduction (Ianora et al. 2004), function as a grazing deterrent (Pohnert 2002), as well as alter phytoplankton community structure (Pezzolesi et al. 2021), they would be a valuable species to pair against a known toxin-producing form of *Microcystis*. Impacts of PUAs on affected phytoplankton species can include changes in membrane integrity (indicative of death/dying) and growth (Pichierri et al. 2016), metrics which were measured in this study. Our findings suggest that *Microcystis* and *Synedra* were not inhibited by one another, as cell abundances remained comparable to controls when grown together and observed proportions of dead cells did not coincide with increases in toxin-producing species.

Both *Synedra* (optimal F_v/F_m = 0.5 for *Thalassiosira pseudonana* in culture; Gleich et al. 2020) and *Microcystis* exhibited lower F_v/F_m values ($F_v/F_m < 0.3$) compared to experiments done pairing *Chlamydomonas* and *Microcystis* (see above). A decrease in this measure is indicative of cellular stress which could be due to exposure to allelochemicals (e.g., Guo et al. 2022), nutrient limitation (Tan et al. 2019) or other abiotic stressors (i.e., temperature, irradiance). Given that we did not measure concentrations of exudates or allelochemicals, we cannot conclude that

lower fluorescence was due to species interaction, nor can we rule out other factors such as nutrient limitation which has also been found to inhibit photosynthetic activity (e.g., Tan et al. 2019). Observations of cells growing on the filter used to separate the species from each other while co-cultured, as well as the re-aggregation of *Microcystis*, may be indicate an interaction between *Microcystis* and *Synedra* in which cells were benefiting from compounds released from each other that were diffusing through the membrane or communicating with nearby cells, as has been described previously (e.g., Kaplan et al. 2012, Venuleo et al. 2017). One type of these compounds, exopolysaccharides (EPS), can be produced by *Microcystis* (Li et al. 2001, Rios et al. 2016) and diatoms (e.g., Aslam et al. 2018). EPS are known for their role as a key component of the mucilaginous covering of colonial cyanobacteria and in cellular adhesion, as demonstrated by *Synedra* in the experiments as they adhered to apparatuses. EPS coverings are also depositories of organic carbon which will get trapped in the EPS, making it unavailable to surrounding organisms (Aslam et al. 2018). When cells lyse with death, carbon sources become available to nearby species which can promote growth of nutrient-limited species (Orellana et al. 2013).

These insights regarding EPS and its role in the growth habits of *Microcystis* and *Synedra* can be applied to findings of our study of species interactions presented here. *Microcystis* was observed aggregation of the cells at the conclusion of the second experiment when paired with *Synedra*. Rios et al. (2016) found that species that had been in culture for extended periods of time (as our test species has been) lost their ability to produce EPS and thus their ability to aggregate. EPS was produced in response to microcystin exposure, indicating that allelopathic interactions could be facilitating the generation of EPS as a defensive response. If this is the

case, we could consider that perhaps *Synedra* was producing an exudate in the experiment, resulting in the aggregation of *Microcystis* following exposure as EPS may have been produced.

Considering the proportion of dead cells observed for *Synedra* (particularly in the second experiment) coupled with the observed growth on the filter by both species, it could be considered that in addition to the interaction described above, lysed *Synedra* cells may have released materials such as organic carbon to the benefit of other organisms, including *Microcystis*. In dying, cell contents will be released into the environment and taken up by nearby species facilitating continued growth and cellular health. In addition to this, bacteria found within EPS of *Synedra* can play an important role in nutrient cycling for the diatom, as has been seen with iron cycling in marine systems (Hassler et al. 2015). The bacterial/diatom relationship can help decrease nutrient limitation for associated species, providing additional nutrients to the environment upon death.

Limitations of the study. While interesting observations were made throughout the experiment on the responses of selected species, the drivers of observed responses cannot be attributed to the release of exudates/allelochemicals as we did not monitor for compounds produced by species. Instead, we operated under the assumption that species' responses would be in relation to production of an allelochemical given two things: 1. The cyanobacterium used in this study had been documented as a known toxin-producer, and 2. Experiments were conducted under controlled conditions, with the only manipulation/stressor would have been exposure to a competitor in the co-culturing apparatus. The latter was established to minimize abiotic stress which has been shown to induce allelochemical production (e.g., Barriero and Hairston 2013, Kaplan et al. 2012, Śliwińska-Wilczewska et al. 2016). To be sure that observed responses were

related to exposure to an allelochemical, sampling for allelopathic compounds – in this case, microcystin – should be completed at various times throughout the experiment. Further, observations of nutrient concentrations could also be done to verify nutrient-replete conditions, eliminating nutrient limitation as a possible driver of observed species changes.

SUMMARY

The studies conducted in this chapter involved direct observations of species-specific co-culturing that allowed for us to test for allelopathy. We did not observe inhibition of growth, changes in F_v/F_m or percentage of dead cells that would indicate allelopathic interactions. While these findings do not support our hypothesis, we successfully carried out co-culturing experiments over a couple of weeks in which we were able to monitor growth, F_v/F_m and cell death. Experiments were done under near ideal conditions (high light and nutrient concentrations) which could limit the potential for allelopathic interactions. Further investigation of these interactions with manipulation of abiotic conditions could help elucidate nutrient cycling and cell death in phytoplankton communities, as environmental stress may induce an allelopathic response in taxa.

REFERENCES

Aslam, S.N., Strauss, J., Thomas, D.N., Mock, T. and Underwood, G.J.C. 2018. Identifying metabolic pathways for production of extracellular polymeric substances by the diatom *Fragilariopsis cylindrus* inhabiting sea ice. *ISME* 12:1237-1251.

Barriero, A. and Hairston, Jr., N.G. 2013. The influence of resource limitation on the allelopathic effect of *Chlamydomonas reinhardtii* on other unicellular freshwater planktonic organisms. *J Plankton Res* 35: 1339-1344.

Bidle, K. and Falkowski, P. 2004. Cell death in planktonic, photosynthetic microorganisms. *Nat Rev Microbiol* 2: 643–655.

Bittencourt-Oliviera, M., Chia, M.A., Bezerra de Oliviera, H.S., Araujo, M.K.C., Molica, R.J.R. and Dias, C.T.S. 2014. Allelopathic interactions between microcystin-producing and non microcystin-producing cyanobacteria and green microalgae: implications for microcystins production. *J Appl Phycol* DOI 10.1007/s10811-014-0326-2

Chia, M.A. and Bittencourt-Oliviera, M.D.C. 2021. Allelopathic interactions between phytoplankton species alter toxin production, oxidative response, and nitrogen fixation. *Hydrobiologia* 848:4623-4635.

Cullen, J.J. and Regner, E.H. 1979. Continuous measurement of the DCMU-induced fluorescence response of natural phytoplankton populations. *Mar Biol* 53: 13-20.

Falpeto, A.B. and Vasconcelos, V.M. 2016. Allelopathic interactions in phytoplankton population ecology. *J Allel Inter* 2: 25-34.

Fistarol, G.O., Legrand, C., Selander, E., Hummert, C. Stolte, W., and Granéli, E. 2004a. Allelopathy in *Alexandrium* spp.: effect on a natural community and on algal monocultures. *Aquat Microb Ecol* 35: 45-56.

Fistarol, G.O., Legrand, C., Rengefors, K., and Granéli, E. 2004b. Temporary cyst formation in phytoplankton: a response to allelopathic competitors? *Environ Micro* 6: 791-798.

Fistarol, G.O., Legrand, C., and Granéli, E. 2005. Allelopathic effect on a nutrient-limited phytoplankton species. *Aquat Microb Ecol* 41: 153-161.

Foyer, C.H., Lelandais, M., and Kunert, K.J. 1994. Photooxidative stress in plants. *Physiol Plantarum* 92: 696-717.

Franklin, D.J., Hoegh-Guldberg, P., Jones, R.J., & Berges, J.A. 2004. Cell death and degeneration in the symbiotic dinoflagellates of the coral *Stylophora pistillata* during bleaching. *Mar Ecol Prog Ser* 272: 117-130.

Franklin, D.J., Brussaard, C.P.D. and Berges, J.A. 2006. What is the role and nature of programmed cell death in phytoplankton ecology? *Eur J Phycol* 41: 1-14.

Gleich, S.J., Plough, L.V. and Gilbert, P.M. 2020. Photosynthetic efficiency and nutrient physiology of the diatom *Thalassiosira pseudonana* at three growth temperatures. *Mar Biol* 167. https://doi.org/10.1007/s00227-020-03741-7

Granéli, E. 2006. Kill your enemies and eat them with the help of your toxins: an algal strategy. *African J Mar Sci* 28: 331-336.

Gross, E.M. 2003. Allelopathy of aquatic autotrophs. *Crit Rev Plant Sci* 22: 313:339.

Guo, X., Han, T., Tan, L., Zhao, T., Zhu, X., Huang, W., Lin, K., Zhang, N. and Wang, J. 2022. The allelopathy and underlying mechanism of *Skeletonema costatum* on *Karenia mikimotoi* integrating transcriptomics profiling. *Aquat Toxicol* https://doi.org/doi:.1016/j.aquatox.2021.106042

Hassler, C.S., Norman, L., Nichols, C.A.M., Clementson, L.A., Robinson, C., Schoemann, V. Watson, R.J. and Doblin, M.A. 2015. Iron associated with exopolymeric substances is highly bioavailable to ocean phytoplankton. *Mar Chem* 173: 136-147.

Hendzel, L. L. and Nagy, P. 1986. A Dual-chamber Chemostat for the Study of Algal Interactions. Canada: Central and Arctic Region, Department of Fisheries and Oceans

Hu, Z., Li, D., Xiao, B., Dauta, A. and Liu, Y. 2008. Microcystin-RR induces physiological stress and cell death in the cyanobacterium Aphanizomenon sp. DC01 isolated from Lake Dianchi, China. *Fundam Appl Limnol* 173: 111-120.

Huisman J. and Hulot F.D. 2005 Population Dynamics of Harmful Cyanobacteria. In: Huisman J., Matthijs H.C., Visser P.M. (eds) Harmful Cyanobacteria. Aquatic Ecology Series, vol 3. Springer, Dordrecht. https://doi.org/10.1007/1-4020-3022-3_7.

Hutchinson, G.E. 1961. The paradox of the plankton. *Am Nat* 95: 137-145.

Ianora, A., Miralto, A., Poulet, S.A., Carotenuto, Y., Buttino, I., Romano, G., Casotti, R., Pohnert, G., Wichard, T., Colucci-D'Amato, L., Terrazzano, G. and Smetacek, V. 2004. Aldehyde suppression of copepod recruitment in blooms of a ubiquitous planktonic diatom. *Nature* 429: 403-407.

Johansson, N. and Granéli, E. 1999. Influence of different nutrient conditions on cell density, chemical composition and toxicity of *Prymnesium parvum* (Haptophyta) in semi continuous cultures. *J Exp Mar Biol Ecol* 239: 243-258.

Kaplan, A., Harel, M., Kaplan-Levy, R.N., Hadas, O., Sukenik, A., and Dittmann, E. 2012. The languages spoken in the water body (or the biological role of cyanobacterial toxins). *Front Microbiol* doi: 10.3389/fmicb.2012.00138.

Karlberg, M. and Wulff, A. 2013. Impact of temperature and species interaction on filamentous cyanobacteria may be more important that salinity and increased pCO_2 levels. *Mar Biol* 160: 2062-2072.

Keating, K.I. 1977. Allelopathic influence on blue-green bloom sequence in a eutrophic lake. *Science* 196: 885-887.

Kozik, C.R., Young, E.B., Sandgren, C.D., and Berges, J.A. 2019. Cell death in individual freshwater phytoplankton species: relationshsips with population dynamics and environmental factors. *Eur J Phycol* 54: 369-379.

Kubanek, J., Hicks, M.K., Naar, J. and Villareal, T.A. 2005. Does the red tide dinoflagellate *Karenia brevis* use allelopathy to outcompete other phytoplankton? *Limnol Oceangr* 50: 883-895.

Kubanek, J., Snell, T.W., and Pirkle, C. 2007. Chemical defense of the red tide dinoflagellate *Karenia brevis* against rotifer grazing. *Limnol Oceanogr* 52: 1026-1035.

Labeeuw, L., Bramucci, A.R. and Case, R.J. 2017. Bioactive small molecules mediate microalgal-bacterial interactions. In M. Kumar and P. Ralph (Eds.), *Systems Biology of Marine Ecosystems* (pp. 279341). Cham, Switzerland: Springer.

Leflaive, J. and Ten-Hage, L. 2007. Algal and cyanobacterial secondary metabolites in freshwaters: a comparison of allelopathic compounds and toxins. *Freshwater Biol* 52: 199-214.

LeGrand, C., Rengefors, K., Fistarol, G.O. and Granéli, E. 2003. Allelopathy in phytoplankton – biochemical, ecological and evolutionary aspects. *Phycologia* 42:406-419.

Lehman, J.T. 1976. Ecological and nutritional studies of *Dinobryon* Ehrenb.: Seasonal periodicity and the phosphate toxicity problem. *Limnol Oceanogr* 21: 646-658.

Lelong, A., Haberkorn, H., Le Goic, N., Hegaret, H. and Soudant, P. 2011. A new insight into allelopathic effects of *Alexandrium minutum* on photosynthesis and respiration of the diatom *Chaetoceros neogracile* revealed by photosynthetic-performance analysis and flow cytometry. *Microb Ecol 62*, 919-930.

Lewis, W.M. 1986. Evolutionary interpretations of allelochemical interactions in phytoplankton algae. *Am Nat* 127: 184-194

Li, P., Harding, S.E. and Liu, Z. 2001. Cyanobacterial Exopolysaccharides: Their Nature and Potential Biotechnological Applications. *Biotechnol Genet Eng Rev* 18:375-404.

Lürling, M., Eshetu, F., Faassen, E.J., Kosten, S. and Huszar, V.L.M. 2013. *Freshw Biol* 58: 552-559.

Maestrini, S.Y. and Bonin, D.J. 1981. Allelopathic relationships between phytoplankton species. *Can Bull Fish Aquat Sci* 210: 323-338.

Masojíde, J., Vonshak, A. and Torzillo, G. 2011. Chlorophyll fluorescence applications in microalgal mass cultures *in Chlorophyll* a *Fluorescence in Aquatic Sciences: Methods and Applications*, Developments in Applied Phycology 4, D.J. Suggett et al. (eds), Springer Science Business Media B.V.

Mulderij, G., Van Nes, E.H., and Van Donk, E. 2007. Macrophyte-phytoplankton interactions: the relative importance of allelopathy versus other factors. *Ecol Model* 204: 85-92.

Orellana, M.V., Pang, W.L., Durand, P.M., Whitehead, K. and Baliga, N.S. 2013. A role for programmed cell death in the microbial loop. PLoS ONE 8(5): e62595. doi:10.1371/journal.pone.0062595.

Paul, C., Mausz, M.A. and Pohnert, G. 2012 A co-culturing/metabolomics approach to Investigate chemically mediated interactions of planktonic organisms reveals influence of bacteria on diatom metabolism. *Metabolomics* 9: 349-359.

Pereira, A.L., Santos, C., Azevedo, J., Martins, T.P., Castelo-Branco, R., Ramos, V., Vasconcelos, V. and Campos, A. 2018. Effects of two toxic cyanobacterial crude extracts containing microcystin-LR and cylindrospermopsin on the growth and photosynthetic capacity of the microalga *Parachlorella kessleri*.*Algal Res* 34: 198-208.

Pezzolesi, A.S., Rindi, F., Samorì, C., Totti, C., and Pistocchi, R. 2021. Survey of the allelopathic potential of Mediterranean macroalgae: production of long-chain polyunsaturated aldehydes (PUAs). *Phytochemistry* 189. https://doi.org/10.1016/j.phytochem.2021.112826

Pichierri, S., Pezzolesi, L., Vanucci, S., Totti, C. and Pistocchi, R. 2016. Inhibitory effect of polyunsaturatedaldehydes (PUAs) on the growth of the toxic benthic dinoflagellate *Ostreopsis cf. ovata*. *Aquat Toxicol* 179: 125-33.

Pohnert, G. 2002. Phospholipase A2 activity triggers the wound-activated chemical defense in the diatom Thalassiosira rotula. *Plant Physiol* 129: 103-111.

Proctor, V.W. 1957. Studies of algal antibiosis using *Haematococcus* and *Chlamydomonas*. *Limnol Oceanogr* 2: 125-139.

Rastogi, R.P., Madamwar, D. and Incharoensakdi, A. 2015. Bloom Dynamics of Cyanobacteria and Their Toxins: Environmental Health Impacts and Mitigation Strategies. *Front Microbiol. 6:1254*, doi: 10.3389/fmicb.2015.01254.

Reigosa, M.J., Sánchez-Moreiras, A. and González, L. 1999. Ecophysiological approach in allelopathy. *Crit Rev Plant Sci* 18: 577-608.

Rios, J.F., Leal, C.R., Leite, S.A.C., Janaina, R. and Retz, C.L. 2016. Phenotypic plasticity and negative allelopathy in Microcystis strains. *Ann Microbiol* 66: 1265-1276.

Santabarbara, S., Villafiorita, M.F., Remelli, W., Rizzo, F., Menin, B. and Casazza A.P. 2019. Comparative excitation-emission dependence of the F_V /F_M ratio in model green algae and cyanobacterial strains. *Physiol Plant* 166: 351-364.

Śliwińska, S. and Latala, A. 2012. Allelopathic effects of cyanobacterial filtrates on Baltic diatom. *Contemporary Trends in Geoscience* 1: 103-107.

Śliwińska-Wilczewska, S., Pniewski, F. and Latala, A. 2016. Allelopathic activity of the picocyanobacterium *Synechococcus* sp. under varied light, temperature, and salinity conditions. *Int Rev Hydrobiol* 101: 69-77.

Søndergaard, M. and Moss, B. 1998. Impact of submerged macrophytes on phytoplankton in shallow freshwater lakes. In: Jeppesen E., Søndergaard M., Søndergaard M., Christoffersen K. (eds) The Structuring Role of Submerged Macrophytes in Lakes. Ecological Studies (Analysis and Synthesis), vol 131. Springer, New York, NY.

Suikannen, S., Fistarol, G.O. and Granéli, E. 2004. Allelopathic effects of the Baltic cyanobacteria *Nodularia spumigena*, *Aphanizomenon flos-aquae* and *Anabaena lemmermannii* on algal monocultures. *J Exp Mar Biol Ecol* 308: 85-101.

Sukenik, A., Eshkol, R., Livne, A. and Hadas, O. 2002. Inhibition of growth and photosynthesis of the dinoflagellate *Peridinium gatunense* by *Microcystis* sp. (cyanobacteria): a novel allelopathic mechanism. *Limnol Oceangr* 47: 1656-1663.

Szivak, I., Behra, R., and Sigg, L. 2009. Metal-induced reactive oxygen species production in *Chlamydomonas reinhardtii* (Chlorophyceae). *J Phycol* 45: 427-435.

Tan, L., Xu, W., He, X. and Wang, J. 2019. The feasibility of Fv/Fm on judging nutrient limitation of marine algae through indoor simulation and *in situ* experiment. *Estuar Coast Shelf S* 229 https://doi.org/10.1016/j.ecss.2019.106411.

Vardi, A., Schatz, D., Beeri, K., Motro, U., Sukenik, A., Levine, A. and Kaplan, A. 2002. Dinoflagellate-cyanobacterium communication may determine the composition of phytoplankton assemblage in a mesotrophic lake. *Curr Biol* 12: 1767-1772.

Venuleo, M., Raven, J.A., and Giordano, M. 2017. Intraspecific chemical communication in microalgae. *New Phytol* 215: 516-530.

Wang, J., Zhu, J., Liu, S., Liu, B., Gao, Y. and Wu, Z. 2011. Generation of reactive oxygen species in cyanobacteria and green algae induced by allelochemicals of submerged macrophytes. *Chemosphere* 85: 977-982.

Wang, L., Zi, J., Xu, R., Hilt, S., Hou, X. and Chang, X. 2017. Allelopathic effects of Microcystis aeruginosa on green algae and a diatom: Evidence from exudates addition and co-culturing. *Harmful Algae* 61: 56-62.

Wium-Anderson, S., Anthoni, U., Christophersen, C., and Houen, G. 1982. Allelopathic effects on phytoplankton by substances isolated from aquatic macrophytes (Charales). *Oikos* 39: 187-190.

Xue, Q., Wang, R., Xu, W., Wang, J. and Tan, L. 2018. The stresses of allelochemicals isolated from culture solution of diatom *Phaeodactylum tricornutum* Bohlin on growth and physiology of two marine algae. *Aquat Toxicol* 205: 51-57.

Chapter 5: General Conclusions

Our study looked to determine whether biotic interactions within the planktonic community rather than abiotic conditions were main drivers of phytoplankton community dynamics and cell death. The influence of abiotic conditions on the phytoplankton community were found to have few effects on changes within the community, particularly when looking at the influences of temperature and light on cell death, with higher proportions of dead cells during periods of low temperatures and light. Additional observations were made of potential interactions among phytoplankton groups that could indicate species responding to similar abiotic conditions or interacting with each other, inducing a change in abundances and cell death of competing species. Further investigations of these potential biotic interactions among representative phytoplankton – *Microcystis*, *Chlamydomonas* and *Synedra* – did not reveal identifiable interactions when tested via co-culturing methods. Additionally, investigations of the effects of grazing on natural phytoplankton assemblages revealed minimal grazing in Estabrook Park Pond. Collectively, these findings lead to our central hypothesis not being supported, as biotic interactions did not seem to be drivers of change within the phytoplankton community.

Conclusions from our studies on the effects of abiotic and biotic factors on phytoplankton community dynamics and cell death are presented as answers to questions based on the study aims presented in Chapter 1.

1. Are declines in specific taxa or the appearance of dead cells associated with changes in abiotic parameters in Estabrook Park Pond? In the time-series study of the phytoplankton community, dead cells were observed with minimal declines in few

phytoplankton groups. Temperature and irradiance weakly correlated with dead cells observed throughout the time-series, but these relationships do not suggest that they are drivers of phytoplankton declines in Estabrook Park Pond.

2. Does grazing by macrozooplankton lead to declines of specific phytoplankton taxa, resulting in the appearance of dead cells? Using natural phytoplankton assemblages from Estabrook Park Pond, we observed minimal evidence of grazing and the appearance of few dead cells with increasing zooplankton abundance. Some evidence of selective grazing was observed in two of eleven observed phytoplankton groups, but dead cells did not increase with grazing pressure. This is indicative that grazing is not generating dead cells.
3. Are correlations among taxonomic groups of phytoplankton, specifically living cells of one species and dead cells of another, due to allelopathic interactions? While there is indirect evidence of interactions among phytoplankton observed in the time-series presented in Chapter 2, attempts to characterize these relationships experimentally were unsuccessful. Using a novel co-culturing technique, we observed that species tested exhibited no inhibition in growth, but rather remained relatively unchanged in the interactions.

While these findings were not supportive of our initial hypothesis, the methods used to complete this work are novel and infrequently used as we have done. Flow cytometry is still a newer method of monitoring phytoplankton in freshwater systems (e.g., Agustí et al. 2006, Read et al. 2014, Yang et al. 2019), and methods to identify and quantify phytoplankton groups can vary greatly. Studies using the method in marine systems often use fluorescence and size

characteristics to group phytoplankton, whereas in our study it was necessary to develop a gating strategy (Appendix A) for monitoring our populations, as size characteristics were not good indicators of difference within the community. Further, we were able to detect and monitor cell death within natural phytoplankton assemblages using mortal staining practices with these gating strategies. These methods were also used to monitor biotic interactions, both among zooplankton and phytoplankton groups, as well species-species interactions of phytoplankton. In our grazing studies (Chapter 3), the effects of zooplankton on the phytoplankton community were investigated using flow cytometric methods to measure changes in phytoplankton groups (abundance, cell death) rather than changes in chlorophyll *a* biomass, which has been done by few previously (e.g., Cucci et al. 1989, Tijdens et al. 2008, Jungbluth et al. 2017). In our allelopathy studies (Chapter 4), we used a novel co-culturing system (e.g., Hendzel and Nagy 1986, Paul et al. 2012) to make observations of interactions between pairs of phytoplankton to identify direct interactions were occurring between them. The ability to rapidly count and assess phytoplankton in each of these studies allowed for comprehensive data and observations to be collected to further our understanding of how abiotic and biotic factors affect phytoplankton community dynamics and cell death.

The methods developed and used in the studies throughout this dissertation will be useful to others looking to conduct long-term research with frequent monitoring of freshwater systems. The methods provide unique ways to look at interactions that may otherwise be difficult to understand *in situ*. Having a comprehensive time-series also provides additional background information for the basis of future studies looking to identify key factors to

manipulate and monitor as a combination of abiotic and biotic factors are most likely to be driving changes in the phytoplankton community of Estabrook Park Pond.

REFERENCES

Agusti, S., Alou, E., Hoyer, M.V., Frazer, T.K., and Canfield, D.E. 2006. Cell death in lake phytoplankton communities. *Freshw Biol* 51: 1496-1506.

Cucci, T.L., Shumway, S.E., Brown, W.S. and Newell, C.R. 1989. Using phytoplankton and flow cytometry to analyze grazing by marine organisms. *Cytometry* 10: 659-669.

Hendzel, L. L. and Nagy, P. 1986. A Dual-chamber Chemostat for the Study of Algal Interactions. Canada: Central and Arctic Region, Department of Fisheries and Oceans

Jungbluth, M.J., Selph, K.E., Lenz, P.H. and Goetze, E. 2017. Species-specific grazing and significant trophic impacts by two species of copepod nauplii, *Parvocalanus crassirostris* and *Bestiolina similis*. *Mar Ecol Prog Ser* 572: 57-76.

Paul, C., Mausz, M.A. and Pohnert, G. A co-culturing/metabolomics approach to investigate chemically mediated interactions of planktonic organisms reveals influence of bacteria on diatom metabolism. Metabolomics 2012, 9, 349-359, doi:10.1007/s11306-012-0453 1.

Read, D.S., Bowes, M.J., Newbold, L.K. and Whiteley, A.S. 2014. Weekly flow cytometric analysis of riverine phytoplankton to determine seasonal bloom dynamics. *Environ Sci: Processes Impacts* 16: 594-603.

Tijdens, M., Van de Waal, D.B., Slovackova, H., Hoogveld, H.L. and Gons, H.J. 2008. Estimates of bacterial and phytoplankton mortality caused by viral lysis and microzooplankton grazing in a shallow eutrophic lake. *Freshw Biol* 53: 1126-1141.

Yang, Y., Gu, X., Te, S. H., Goh, S. G., Mani, K., He, Y., and Gin, K. Y. H. 2019. Occurrence and distribution of viruses and picoplankton in tropical freshwater bodies determined by flow cytometry. *Water Research*, *149*, 342-350.

APPENDIX A

Flow cytometric gating and determination of dead cells

INTRODUCTION

Flow cytometry allows for a rapid assessment of phytoplankton samples by using naturally occurring red fluorescence to count cells. Methods often used to study marine phytoplankton utilize red fluorescence detected from the excitation of chlorophyll *a* in the cell with size estimators, such as forward scatter (e.g., Veldhuis and Kraay 2000, Thompson and van den Engh 2016, Vaharanta et al. 2020). These methods help identify groups of phytoplankton but work best when there is range of size classes present in the field. In Estabrook Park Pond, many of our species were similar in size limiting the functionality of such methods, leading to the use of red and orange fluorescence to determine phytoplankton groups via flow cytometry.

As groups were identified and gated as described below, cell abundances for representative groups were obtained. When the mortal stain Sytox Green® was used added to samples to detect dead cells to obtain mortality estimates, the signal from the stain (emitted as green fluorescence, FL-1) bled significantly into the signal for orange fluorescence (FL-2) and to a lesser extent, red fluorescence (FL-3). Spillover from green fluorescence can obscure representative counts of dead cells within the community due to overlapping fluorescence gates, leading to a loss of cells in a gate and the inability to follow/recognize them in the flow cytometry output. Standard methods of applying compensation, a correction for fluorochrome spillover into another channel on the flow cytometer (FlowJo, n.d.), cannot correct this problem with field samples where community fluorescence is different every time it is observed.

METHODS

Seasonal flow cytometric data (2014-2016) were consolidated into a single database for analysis using FlowJo (V10) flow cytometry software. To obtain count estimates for representative groups, geometric gates were drawn on plots using FL-3/FL-2 (red and orange fluorescence, respectively) parameters to identify groups based upon cell counts and densities as they appeared on the plot (ex. Fig. 19A). Gates were applied to all sampling dates (n=105) and made to be of best fit across all data, establishing eleven groups of interest. Gated groups were then extracted and plotted separately (Fig. 19B—C) to aid in the determination of the proportion of dead cells within a particular group. Using far-red fluorescence and forward scatter (FL-4 and FSC, respectively), each group was plotted individually and had an additional FL4/FSC gate applied to it (Fig. 19C). These gated populations were then plotted on an FL-1 (green fluorescence) histogram to determine the control (unstained) threshold of FL-1, done by establishing a positive/negative gate (Fig. 19D). The positive/negative gates provided the ability to estimate the number of dead (positively stained) cells within a particular group.

RESULTS AND CONCLUSION

Red and orange fluorescence (FL-3 and FL-2) were used to establish eleven gates denoting relatively distinct phytoplankton populations (Fig. 19A). Gates were created manually and applied to the entire dataset to find the best fit. Each group was then extracted and had additional gating applied (as described above) to establish negative/positive stained (live/dead) gates to obtain estimates of mortality on a group basis. This was done to accommodate variation in how compromised (dead) cells stain, as phytoplankton do not stain to the same

extent (Veldhuis et al. 1997, Peperzak and Brussard 2011, Franklin et al. 2012) due to inherent physiological differences.

In using this approach to estimate phytoplankton mortality, a more robust approach to estimating mortality can be applied to mixed assemblages of phytoplankton. Teasing apart differences in fluorescence and subsequently size provide a more directed approach and work to minimize spillover concerns or uneven staining of dead cells (Znachor et al. 2015). This method also grants the opportunity to generate group-specific estimates of mortality rather than community estimates as Elovaara et al. (2020) have done previously. Group-specific estimates provide an opportunity to quantify phytoplankton mortality which can be applied in management decisions and provide improvements in monitoring bloom dynamics in diverse systems.

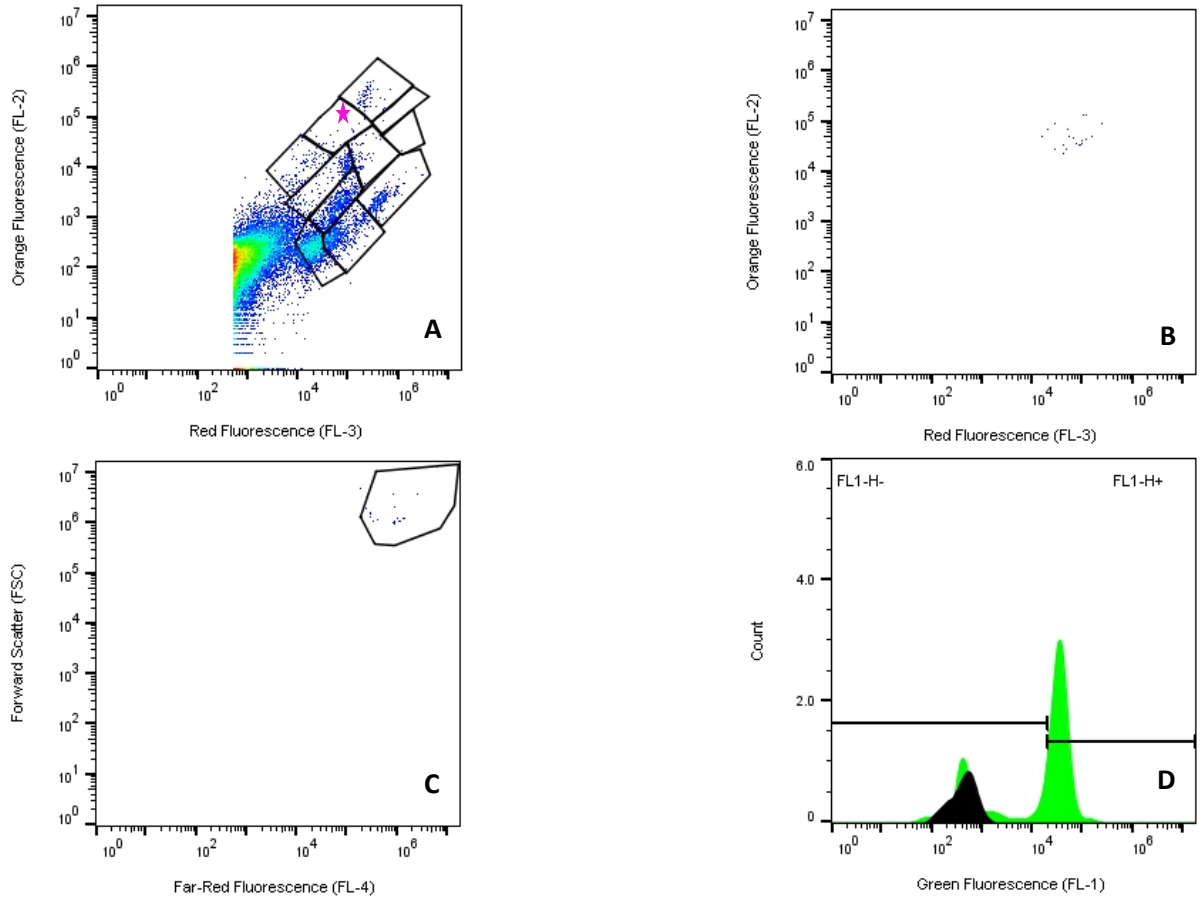

Figure 19. Gated flow cytometry gating method example from July 20, 2016. A. Eleven gated populations as determined by manual assessment of all sampling dates. Each box was drawn manually utilizing FlowJo software, with each indicating a group of phytoplankton based upon their detected red and orange fluorescence. B. Individual group isolated from plot featured in panel A (starred group). C. Isolated group from panel B shown and gated with far red fluorescence (FL-4) and forward scatter axes. D. Histogram of gated group from panel C plotted to determine positive (FL1-H+) or negative (FL1-H-) green fluorescence, where positive staining indicates dead cells when treated with Sytox Green®. Black area represents unstained control. Green area is of stained sample.

REFERENCES

Elovaara, S., Degerlund, M., Franklin, D.J., Kaartokallio, H. and Tamelander, T. 2020. Seasonal variation in estuarine phytoplankton viability and its relationship with carbon dynamics in the Baltic Sea. *Hydrobiologia* 847: 2485-2501.

Franklin, D.J., Airs, R.L., Fernandes, M., Bell, T.G., Bongaerts, R.J., Berges, J.A. and Malin, G. 2012. Identification of senescence and death in *Emiliania huxleyi* and *Thalassiosira pseudonana*: cell staining, chlorophyll alterations, and dimethylsulfoniopropionate (DMSP) metabolism. *Limnol Oceanogr* 57: 305-317.

FlowJo. n.d. Biologist's guide to spectral compensation. https://docs.flowjo.com/flowjo/experiment-based-platforms/plat-comp-overview/plat-comp-users/. Accessed April 5, 2022.

Peperzak, L. and Brussard. C.P.D. 2011. Flow cytometric applicability of fluorescent vitality probes on phytoplankton. *J Phycol* 47: 692-702.

Rychtecký, P., Znachor, P. and Nedoma, J. 2014. Spatio-temporal study of phytoplankton cell viability in a eutrophic reservoir using SYTOX Green nucleic acid stain. *Hydrobiologia* 740: 177-189.

Thompson, A.W. and van den Engh, G. 2016. A multi-laser flow cytometry method to measure s Single cell and population-level relative fluorescence action spectra for the targeted Study and isolation of phytoplankton in complex assemblages. *Limnol Oceanogr-Meth* 14: 39-49.

Vanharanta, M., Elovaara, S., Franklin, D.J., Spilling, K. and Tamelander, T. 2020. *Aquat Ecol* 54: 119-135.

Veldhuis, M.J.W., Cucci, T.L. and Sieracki, M.E. 1997. Cellular DNA content of marine phytoplankton using two new fluorochromes: taxonomic and ecological implications. *J Phycol* 33: 527-541.

Veldhuis, M.J.W. and Kraay, G.W. 2000. Application of flow cytometry in marine phytoplankton research: current applications and future perspectives. *Sci Mar* 64: 121-134.

Znachor, P., Rychtecký, P., Nedoma, J. and Visocká, V. 2015. Factors affecting growth and viability of natural diatom populations in the meso-eutrophic Římov Reservoir (Czech Republic). *Hydrobiologia* 762: 253-265.

APPENDIX B

Phytoplankton species of each flow cytometric group

SUMMARY

The species list provided on the following page (Table 7) provides phytoplankton species that were identified through microscope counts of Lugol's preserved pond samples. Identified species were representative of the groups created by gating cells of similar fluorescence characteristics (Appendix A). Table on next page.

Table 7. Species list representative of taxa identified through microscopic observations of preserved field samples from Estabrook Park Pond.

FCM Group	Taxonomic classification	Species
1	Chlorophyceae	*Carteria* *Coelastrum* *Crucigenia* *Tetraedon*
2	Bacillariophyceae	*Navicula* *Pinnularia biceps* *Rhizosolenia* *Synedra*
3	Cryptophyceae Chrysophyceae	*Cryptomonas* sp. *Dinobryon* sp.
4	Euglenophyceae	*Euglena* sp. *Euglena acus* *Phacus* *Phacus spiralis* *Trachelomonas*
5	Chlorophyceae	*Ankistrodesmus* sp. *Ankistrodesmus spiralis* *Scenedesmus*
7	Dinophyceae	*Gymnodinium* sp. *Peridinium* sp.
8	Chlorophyceae	*Cosmarium* sp.
9	Chlorophyceae	*Chlamydomonas* *Dictyosphaerium* *Eudorina*
10	Chlorophyceae	*Closterium* *Euastrum* *Staurastrum*
11	Bacillariophyceae Chrysophyceae Synurophyceae	*Fragilaria* *Tabellaria* *Dinobryon* sp. *Mallomonas*
12	Cyanophyceae	*Anabaena* *Merismopedia* *Microcystis* *Oscillatoria*

APPENDIX C

Modeling phytoplankton dynamics of Estabrook Park Pond

INTRODUCTION

A combination of abiotic and biotic stressors can influence changes within the phytoplankton community but given the inter-specific diversity in a community and inter-individual diversity in a population may not affect all taxa (i.e., Lehman and Sandgren 1985, Thackeray et al. 2008, Marzetz et al 2020), or even all individuals within a single taxon, in the same way. Understanding how these stressors can influence community structure, and how individuals respond will improve our interpretation of community ecology within aquatic environments. Modeling methods can be used to test how populations may respond under various conditions, helping to develop a clearer understanding of complex community interactions.

Conventional phytoplankton models have tended to focus on whole community responses rather than an individual or specific phytoplankton group responses (Grover et al. 2012, DeAngelis and Grimm 2014). Conventional equations such as the Monod (1949) and Droop (1973) models, allow for a general understanding of how nutrients can affect phytoplankton growth and reproduction in one population of phytoplankton. The Monod model provides a way to assess growth responses of a phytoplankton population to external nutrient concentrations but fails to consider additional factors (i.e., irradiance, temperature, cell condition) that could influence nutrient uptake, thus altering the life of an alga (Goldman and Carpenter 1974). Droop's cell quota model (1973), considers average internal nutrient stores of an alga, allowing for a better understanding of how intracellular nutrient

concentrations affect growth rates of the phytoplankton in question. Such models can allow for a general understanding of how phytoplankton species respond to a set of factors.

In contrast, there is now considerable emphasis being placed on approaches that consider the characteristics (i.e., morphology, nutrient use, temperature, and light thresholds) of specific taxa ("trait-based") when developing models. Trait-based techniques consider how taxonomic groups vary in acquisition and uptake of resources, allowing for the incorporation of taxon-specific parameters in the modeling approach (Litchman et al. 2007), and can also accommodate how cells may respond to variable abiotic factors (Daines et al. 2014). Important parameters such as cell size and shape, which can vary within taxonomic groups, are linked to a cell's ability to take in and assimilate nutrients (Meunier et al. 2017) or receive communication from conspecifics (Venuelo et al. 2013). By incorporating a parameter such as cell size into existing models, considerations for differences of distribution of uptake sites, molecular diffusion rates and nutrient storage of cells can be considered. Fiksen et al. (2013) looked to improve modeling of nutrient uptake, which has traditionally used a modified Michaelis-Menten enzyme kinetics model (Monod 1949). The modified version incorporates nutrient concentrations, but not cell size, which Fiksen et al. looked to further parameterize. Compared to models not considering cell size, Fiksen found that the extension and parameterization for cell size improved estimates of organismal traits in the system. Cell size can also affect the grazing rates of zooplankton on phytoplankton, which are often incorporated into models of predator/prey dynamics. Grazing rates can be impacted by the production of anti-grazing compounds by prey items, which can function as a feedback loop with phytoplankton growth rates. Harvey et al. (2015) found that species-specific interactions occur among predator and

prey, with variability resulting from cell size. Cell size and grazing rates into existing models, trait-based taxonomic estimates can provide further insight into species dynamics.

In the natural environment diverse groups of phytoplankton are present, which require the use of multiple differential equations to model phytoplankton community dynamics. Differential equations look to determine how the entire community responds to conditions by applying average cellular properties to populations (Hellweger and Kianirad, 2007). This can be useful if knowing which taxa are responding to a set of conditions is unnecessary, but the equations have limitations when developing a better understanding of how different populations respond to conditions. By applying average properties, natural variation of individuals within groups of phytoplankton taxa is dismissed, which does not give an accurate depiction of how different phytoplankton groups within the community respond. However, it is more difficult to use such equations to address differences among individual groups of phytoplankton because they apply the same coefficients to all organisms within a group. This can be problematic, as there is natural variability in cellular health/condition among individuals, which may affect processes like cell death (Hellweger et al. 2008, Kozik et al. 2019). In a conventional model, where all individuals within a group respond the same way, if one cell dies, then they all die, but this is not what is observed in nature (Kozik et al. 2019).

To account for variation among individuals within groups of phytoplankton, incorporating specific parameters can improve our models. Grover et al. (2012) tested a model to assess community dynamics of *Prymnesium parvum* and an allelopathic cyanobacterium. In parameterizing the model, they found that by incorporating more specific parameters (toxin production and degradation, allelopathic effects on grazing by zooplankton), the model was

better able to model/predict the historical data for the relationship between *P. parvum* and the cyanobacterium. When these parameters were removed, model performance declined. Further, in Litchman and Klausmeier's review of trait-based approaches to modeling (2008), it was suggested that a more generalized grazing component, that considers the size of both phytoplankton and grazers, should be included in models rather than more specific terms (ex. nutritional quality, catch efficiency, etc.). These specific terms can make interpretations of the community interactions difficult, as many of these are specific to phytoplankton/grazer relationships. Being able to apply a variety of parameters that are representative of the taxa present would serve to improve our modeling capabilities.

Using agent-based (individual-based) modeling provides an alternative method for modeling complex interactions. The method provides a way to understand responses of individuals/agents (Hellweger et al. 2008, DeAngelis and Grimm 2014) within the environment, accounting for the dynamic nature of individuals and intra-population variation. Individuals are randomly assigned a unique set of cellular properties (ex. size, nutrient quotas), that will mimic variation among individuals. Agent-based models provide a way to more directly assess how individuals respond to changing conditions, such as nutrient availability or irradiance (Grimm et al. 2006) understanding of what is occurring at the population level because of the accumulating individual responses. By developing agent-based models further, our ability to understand and interpret phytoplankton interactions and responses improves.

Using a previously developed agent-based model with only one type of phytoplankton, I am providing an outline of modeling the phytoplankton found in Estabrook Park Pond. A preliminary simulation was done to test use and attempted to refine the model using

observations from the pond. Ultimately, work provided here will help to further the model's development, with application to include multiple types of phytoplankton, improve the model's performance and have output more representative of what would be expected in a mixed environment. The goal was simply to compare different approaches to incorporating cell death into the model and determine the feasibility and implications.

METHODS

General modeling approach. Using free, open-source NETLOGO software (version 6.0.3), the model was used to follow individual cells (agents) of a single phytoplankton group to identify how individuals responded to the parameters (varying nutrient levels, temperature, irradiance) used. Tracking individual cells allowed for direct observations to be made regarding an individual's cellular properties and limitations, as all cells of the same type do not typically respond in the same way. The program simulated varied environmental conditions (irradiance, temperature, nutrients) individuals were exposed to over time while simultaneously recording responses of individuals. The model used allowed for mortality responses of one type of alga to be modeled, developed from a model of *Anabaena*'s life cycle (Hellweger et al. 2008), as it incorporated aspects of cell conditions and mortality in response to changing environmental conditions.

Computational limits can be reached when modeling individuals of a population of phytoplankton if the number of individuals grows too large. This is inevitable for microbial population, however. To work around this and reduce the number of individuals in the model, similar individuals were grouped into representative "super individuals" that represented fixed numbers of the total of individuals in a population:

$$S_R = \frac{N}{n} \qquad \text{(Equation 1)}$$

where N is the total number of individuals in a population, and n is a function of the distribution characteristics of the individual population of phytoplankton. In each time step the super individual representation is adjusted as numbers increase or decrease. This method does limit the model because it is inefficient in simulating rapid change among individuals, but parallel simulation run with much larger number of individuals using super-computers show that general dynamics are well represented by this simplification (Hellweger et al. 2007). The total number of individuals in a population should change over time as cells die and divide, therefore, if the number of individuals in a group (n) is allowed to vary, but not the "super individual" number, we should be able to account for changes among the individuals. At this point of the model, the model super individual value is equal to one, with each super individual representing one individual. This is modified as the abundance of individuals in a group increases over 1000, to aid in computational abilities of the computer.

Growth components. The model first considered how temperature affected algal growth, resulting in the maximum growth rate for the alga. The algal response to nutrients and irradiance was then evaluated to determine which is most limiting, ultimately influencing reproduction. This was done using a series of simple equations to understand the dynamics of the individuals. Initial settings for the model included setting the pond volume to one liter with a minimum temperature of 5°C. The initial population was set to 400 individuals, with those cells being set to be no smaller than 45 pmol C and able to uptake at most 0.025 pmol P d^{-1}. Cells were then "passed through" varying environmental conditions, with only some cells ultimately surviving and moving on to the next time step.

First, cells were allowed to take up available nutrients. The average uptake rate was determined using the equation:

$$v = v_{max} \times \frac{S}{Km+S} \qquad \text{(Equation 2)}$$

Then, a maximum growth rate for the individual was determined based upon temperature (Goldman and Carpenter 1974).

$$\mu_{\max(T)} = 1.8 \times 10^{-10} e^{\frac{-6842}{T}} \quad \text{(Equation 3),}$$

Where T is temperature. Then to determine the achievable growth rate for an individual, dependent upon irradiance, the current (measured) irradiance and μ_{max} from Equation 1 are used in the following equation (Jassby and Platt 1976):

$$\mu_{\max(I)} = \mu_{\max(T)} \tanh\left(\frac{\alpha I}{\mu max}\right) \text{ (Equation 4)}$$

where $\mu_{max(T)}$ is the maximum growth rate for a group given the temperature, α is light saturation, and *I* is measured irradiance. Then using the observed nutrient concentration and $\mu_{max(T)}$, the achievable growth rate given nutrient availability ($\mu_{max(A)}$) was calculated (Currie and Kalff 1984, Pederson and Borum 1996):

$$\mu_{\max}(A) = \mu_{\max}(T) \times \frac{1-q^0}{q} \qquad \text{(Equation 5)}$$

where q is the cell nutrient quota and q_0 is the subsistence cell quota.

From here, cells will divide, and individuals were then randomly assessed for their mortality, which occurred stochastically based on whether environmental conditions exceed assigned thresholds. Mortality was calculated at each step and surviving individuals were then exposed to varied variable environmental conditions. Nutrient uptake and growth rates were

modified by the model as changes in population size can increase/decrease competition among individuals in the environment, thus affecting the average rates of both.

Table 8. Algae and model parameters used in the Estabrook Park model.

Symbol	Units	Parameter Description
μ_{max}	d^{-1}	Maximum growth rate
S	mol L^{-1}	Concentration of limiting nutrient in pond
q_o	mol P $cell^{-1}$	Cell nutrient content
v	mol $cell^{-1}$ d^{-1}	Uptake of nutrient
K_m	mol L^{-1}	Constant for nutrient uptake
T	°K	Temperature
I	mol m^2 sec^{-1}	Irradiance
α	mol m^2 sec^{-1}	Light saturation
v_{max}	mol P $cell^{-1}$ d^{-1}	Maximum nutrient uptake rate
m	mol C $cell^{-1}$	Cell size
FL-1		Green fluorescence property
FL-2		Orange fluorescence property
FL-3		Red fluorescence property

Mortality components. We initially tried two approaches: 1) cells die randomly at a fixed rate, or 2) cells die randomly in proportion to the degree of stress (i.e., how much the thresholds are exceeded). This death module is based upon whether critical thresholds for irradiance, nutrients and temperature have been met or exceeded. If the thresholds are not exceeded,

probability for mortality is zero. For example, when the temperature threshold is not exceeded, the random probability of death for an individual cell in a single time-step is 0.2, but, in the second cases if the critical threshold is exceeded, probability of mortality in response to temperature is equal to zero, as we assume that death occurs as temperature decreases from the threshold 0.6. A similar sequence is done for irradiance and nutrient availability. Once each of these mortalities are calculated, the overall probability of mortality is calculated as the average of the three and applied stochastically to each cell in that time-step. Once individuals have gone through this analysis once, survivors will move on to the next time step. Parameters are updated with respect to the number of individuals, which will influence average nutrient uptake and subsequent growth rates, as individuals will respond to having more/less competitors. Environmental parameters, such as temperature and irradiance, could be varied.

Modeling phytoplankton dynamics. Using the model and seasonal data collected for Aim #1 (Chapter 2), the model was tested to see if the seasonal patterns observed could be replicated with the model as it was for individuals of a single phytoplankton group. To do this, the model was used to evaluate the responses of the selected group of phytoplankton to the measured phosphate concentrations in the environment. Nutrient uptake rates and cell quotas were obtained from the literature for phytoplankton species counted with flow cytometry and identified (Table 9). Data (external phosphate, irradiance, temperature) from the seasonal dataset were into the model and allowed to run until their end points. Model data were compared to what was observed to determine the applicability of the current model. If the model did not perform well in response to phosphate levels in the pond, nitrogen sources (NH_4, NO_3) would then be tested, with the model equations adjusted accordingly.

Table 9. Example of individual algal parameters from the literature for an example alga (*Scenedesmus*) typical of one found (group 5) in Estabrook Park Pond.

Symbol	Units	Parameter Description	Value	Reference, comments
μ_{max}	d^{-1}	Maximum growth rate	1.33	Rhee, 1973
q_o	mol P $cell^{-1}$	Cell nutrient content		
v	mol $cell^{-1}$ d^{-1}	Uptake of nutrient		
K_m	mol L^{-1}	Constant for nutrient uptake	6×10^{-7}	Rhee, 1973
α	mol m^2 sec^{-1}	Light saturation	8.1×10^{-5}	Difusa et al. 2015
v_{max}	mol P $cell^{-1}$ d^{-1}	Maximum nutrient uptake rate	1.23×10^{-5}	Rhee, 1974 *Under nitrogen limitation*
m	mol C $cell^{-1}$	Cell size		
FL-1		Green fluorescence property	Arbitrary	--
FL-2		Orange fluorescence property	Arbitrary	--
FL-3		Red fluorescence property	Arbitrary	--

Plotting and running model simulations. As the model ran simulations (updated every 0.005 days), plots for cell abundance, nutrient availability, cell size and fluorescence parameters were generated (see Fig. 20 example). The cell abundance plot provides an estimate of the quantity of living and dead cells throughout the simulation, allowing for a visual determination of when there was a change in cell mortality. Nutrient availability is plotted over time and can be used to compare the cell mortality response to changes in nutrient availability. Cell size plots provide estimated abundances of cells of a given size (as C $cell^{-1}$). Plotting of fluorescence parameters, such as FL-1, FL-2, and FL-3 provided a way to verify the fluorescence of individuals. An FL-3/FL-2 plot can be used to compare the modeled individuals to the observed fluorescence from FCM-

processed environmental samples, while an FL-3/FL-1 plot can be used to see changes in cell mortality (ex. an increase on FL-1 fluorescence is indicative of mortality).

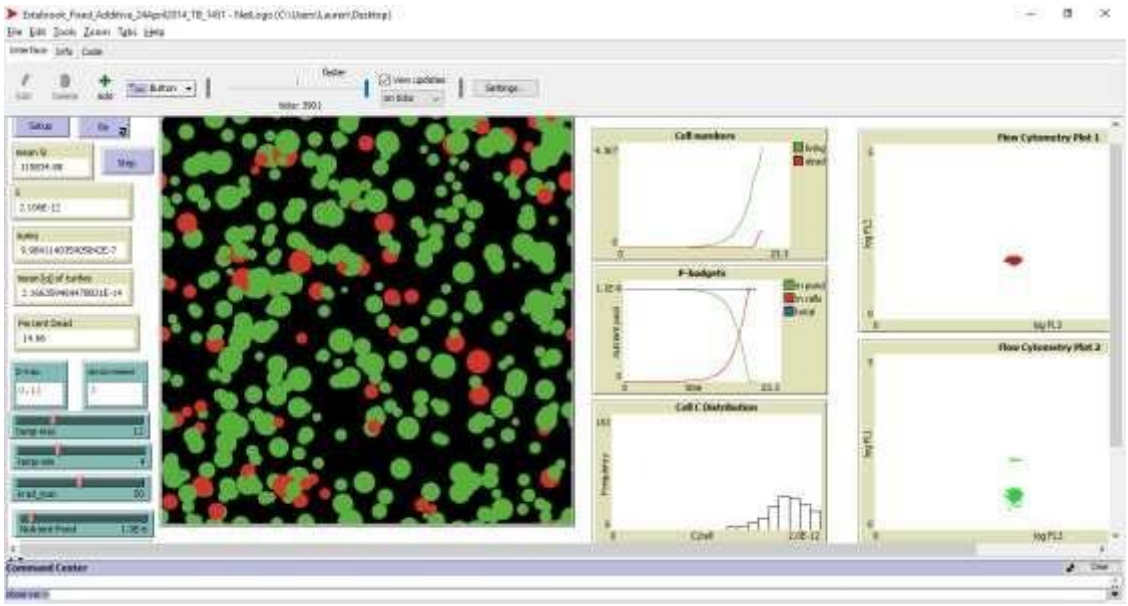

Figure 20. Sample view of NetLogo plots and output data. When running simulations, green and red dots in large panel change over time, indicative of living (green) and dead (red) individuals, changing in size as well. Additional plots of overall cell abundance, nutrient availability and fluorescence characteristics are also included as output.

RESULTS AND DISCUSSION

To test the model as it is currently programmed, ten simulations were run. The simulation results were combined to obtain an average response for individuals of one type of phytoplankton, which was then compared to observed data (Fig. 21). Temperatures were set to range between 19-22° C, with phosphorus levels being set to mimic availability in the pond at the beginning of the 30 days being modeled. A group of phytoplankton was selected from Summer, 2015 flow cytometry data to establish an initial cell abundance (1000) for the model. Simulations were run to model the changes in the population over 30 days.

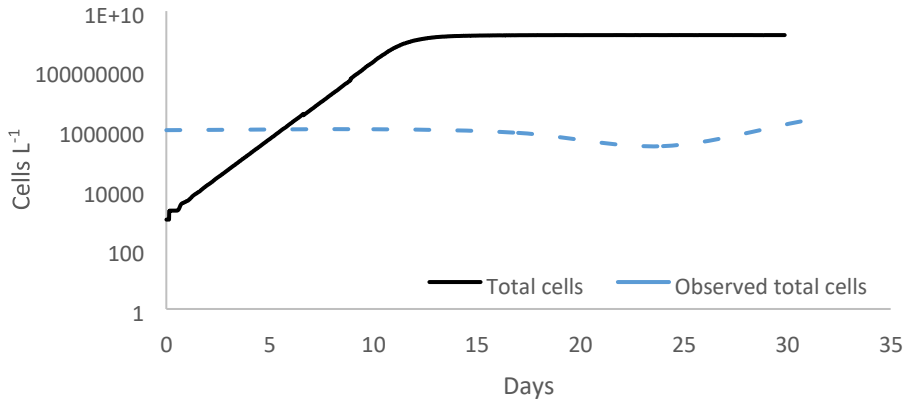

Figure 21. Comparison of modeled ('total cells') and observed total cells for a selected phytoplankton group over 30 days.

At the conclusion of 10 simulations, output data for living and dead cell abundances were plotted. The average output for the population being modeled estimated that approximately 95% of the population was dead at 30 days. While this could be a potential outcome for some phytoplankton populations as was observed with some cyanobacteria in Estabrook Park Pond (Chapter 2), the observed flow cytometry for the taxonomic group selected (cryptomonads) did not suggest such a high level of mortality. Mortality was variable throughout field studies (detected by Sytox Green fluorescence; data not shown; described in Chapter 2), with many groups having mortality levels of less than five percent on a given sampling date. The modeled abundance of mortal cells exceeded the living cells at 15 days (Fig. 22), in contrast to those field observations

Given the findings of Chapters 2-4, incorporating taxonomic specific parameters such as growth rates by estimated cell shape or size could work to refine the model on the basis that individual cells would vary in size and shape over time given abiotic and biotic factors imposing stress on the population. This could prove problematic as low mortality observed in the field has been difficult to replicate in simulations. This could warrant the use of stochastic mortality

coefficients, with the same value applied to all individuals within the population Further, losses due to grazing measured as dead cells should be investigated further, as grazing rates provide estimates of biomass lost and not dead cells observed. Estimates of dead cells as an effect of grazing were minimal in our studies (Chapter 3) which did not help to further parameterization of this model. While grazing observations could be an anomaly, they do warrant the use of published grazing rates for representative taxonomic groups (Table 9) until additional studies can be completed. Further, incorporation of a parameter for dead cells because of grazing may severely underestimate the amount of loss/death that occurs within taxonomic groups as zooplankton grazing tends to leave minimal cell debris behind. Minimal cell debris limits the ability to measure proportions of living/dead cells, as staining methods used in the grazing experiment require DNA from compromised cells for the Sytox Green to bind to.

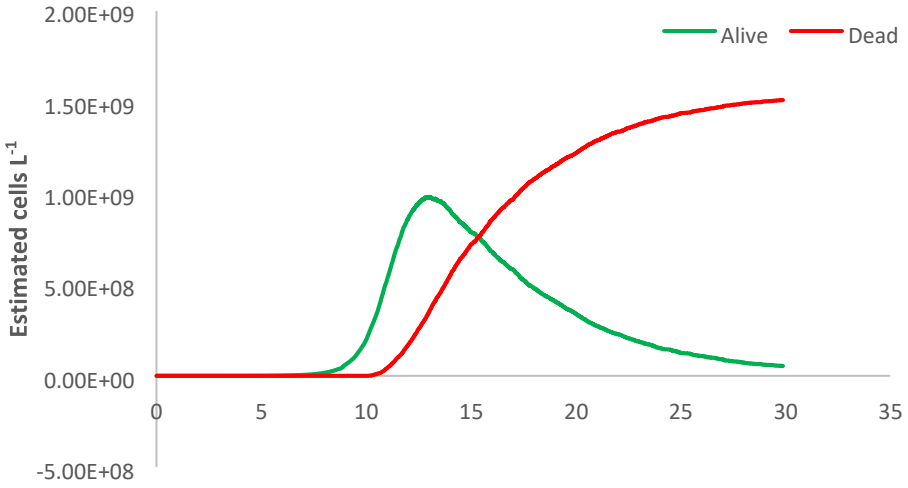

Figure 22. Average response (10 simulations) of one type of phytoplankton using the current Estabrook Park Pond model.

Despite the inability to model observed mortality and cell abundances from the field, we were able to demonstrate that the model does indeed work, though modifications of input

parameters are certainly necessary. Identifying key abiotic stressors (as a start) are critical to refining how individuals are treated in the model example provided here. Using flow cytometry to further tease apart observations of cell sizes and fluorescence of known taxa will help to provide critical cell characteristics to manipulate. These observations can be then compared to individuals from field samples to develop the best estimate of each parameter which will ultimately affect individuals' nutrient uptake and mortality rates in the field, furthering our ability to predict the incidence of changing phytoplankton community composition.

REFERENCES

Currie, D.J. and Kalff, J. 1984. A comparison of the abilities of freshwater algae and bacteria to acquire and retain phosphorus. *Limnol Oceanogr* 29: 298-310.

Daines, S.J., Clark, J.R., and Lenton, T.M. 2014. Multiple environmental controls on phytoplankton growth strategies determine adaptive responses of the N:P ratio. *Ecol Lett* 17: 414-425.

DeAngelis D.L. and Grimm, V. 2014. Individual-based models in ecology after four decades. *F1000prime reports* 6 doi:10.12703/P6-39.

Difusa, A., Talukdar, J., Kalita, M.C., Mohanty, K. and Goud, V.V. 2015 Effect of light intensity and pH condition on the growth, biomass and lipid content of microalgae *Scenedesmus* species. *Biofuels* 6: 37-44, DOI: 10.1080/17597269.2015.1045274

Droop, M.R. 1973. Some thoughts on nutrient limitation in algae. *J Phycol* 9: 264-272.

Fiksen, O., Follows, M.J., and Aksnes, D.L. 2013. Trait-based models of nutrient uptake in microbes extend the Michaelis-Menten framework. *Limnology and Oceanography* 58(1): 193-202.

Goldman, J.C. 1977. Temperature effects on phytoplankton growth in continuous culture. *Limnol Oceanogr* 22: 932-936.

Goldman, J.C. and Carpenter, E.J. 1974. A kinetic approach to the effect of temperature on algal growth. *Limnol Oceanogr* 19: 756-766.

Grimm, V, Berger, U., Bastiansen, F. and Eliassen, S. 2006. A standard protocol for describing individual-based and agent based models. *Ecol Model* 198:115-126.

Grover, J.P, Roelke, D.L. and Brooks, B.W. 2012. Modeling of plankton community dynamics characterized by algal toxicity and allelopathy: A focus on historical *Prymnesium parvum* blooms in a Texas reservoir. *Ecol Model* 227: 147-161.

Harvey, E.L., Bidle, K.D., and Johnson, M.D. 2015. Consequences of strain variability and calcification in Emiliania huxleyi on microzooplankton grazing. *J Plank Res* 37(6): 1137 1148.

Hellweger, F.L. and Kianirad, E. 2007. Individual-based modeling of phytoplankton: evaluating approaches for applying the cell quota model. *J Theor Biol* 249: 554-565.

Hellweger, F.L., Kravchuk, E.S., Novotny, V. and Gladyhshev, M.I. 2008. Agent-based modeling of the complex life cycle of a cyanobacteria (*Anabaena*) in a shallow reservoir. *Limnol Oceanogr* 53: 1227-1241.

Jassby, A.D. and Platt, T. 1976. Mathematical formulation of the relationship between photosynthesis and light for phytoplankton. *Limnol Oceanogr* 21: 540-547.

Kozik, C.R., Young, E.B., Sandgren, C.D., and Berges, J.A. 2019. Cell death in individual freshwater phytoplankton species: relationshsips with population dynamics and environmental factors. *Eur J Phycol* https://doi.org/10.1080/09670262.2018.1563216.

Lehman, J.T. and Sandgren, C.D. 1985. Species-specific rates of growth and grazing loss among freshwater algae. *Limnol Oceanogr* 30: 34-46.

Litchman, E., Klausmeier, C.A., Schofield, O.M., and Falkowski, P.G. 2007. The role of functional traits and trade-offs in structuring phytoplankton communities: scaling from cellular to ecosystem level. *Ecol Lett* 10(12): 1170-1181.

Litchman, E. and Klausmeier, C.A. 2008. Trait-based community ecology of phytoplankton. *Annu Rev Ecol Evol Syst* 39: 615-639.

Marzetz, V., Spijkerman, E., Striebel, M. and Wacker, A. 2020. Phytoplankton community responses to interactions between light intensity, light variations, and phosphorus supply. *Front Envrion Sci* https://doi.org/10.3389/fenvs.2020.539733.

Meunier, C.L., Boersma, M., El-Sabaawi, R., Halvorson, H.M., Herstoff, E.M., Van de Waal, D.B., Vogt, R.J., and Litchman, E. 2017. From Elements to Function: Toward Unifying Ecological Stoichiometry and Trait-Based Ecology. *Front Environ Sci* 5:18 doi: 10.3389/fenvs.3017.00018.

Monod, J. 1949. The growth of bacterial cultures. *Annu Rev Microbiol* 3: 371-394.

Pederson, M.F. and Borum, J. 1996. Nutrient control of algal growth in estuarine waters: nutrient limitation and the importance of nitrogen requirements and nitrogen storage among phytoplankton and species of macroalgae. *Mar Ecol Prog Ser* 142: 261-272.

Rhee, G. 1973. A continuous culture study of phosphate uptake and growth rate and polyphosphate in *Scenedesmus* sp. *J Phycol* 9: 495-506.

Rhee, G. 1974. Phosphate uptake under nitrate limitation by *Scenedesmus* sp. and its ecological implications. *J Phycol* 10: 470-475.

Thackeray, S.J., Jones, I.D. and Maberly, S.C. 2008. Long-term change in the phenology of spring phytoplankton: species-specific responses to nutrient enrichment and climactic change.

J Ecol 96: 523-535.

Venuleo, M., Raven, J.A., and Giordano, M. 2017. Intraspecific chemical communication in microalgae. *New Phytol* 215: 516-530.

CURRICULUM VITAE

LAUREN SIMMONS

EDUCATION

PhD in Biological Sciences ***M*ay 2022**
University of Wisconsin – Milwaukee, Milwaukee, WI
Dissertation: Phytoplankton mortality in an urban pond: Understanding the roles of abiotic factors, grazing pressure and allelopathy
Advisor: John A. Berges

MS in Biological Sciences **December 2012**
University of Wisconsin – Milwaukee, Milwaukee, WI
Thesis: Freshwater phytoplankton populations detected using high-pressure liquid chromatography (HPLC) of taxon-specific pigments
Advisors: John A. Berges and Craig D. Sandgren

BA in Conservation & Environmental Science **May 2006**
University of Wisconsin – Milwaukee, Milwaukee, WI

PROFESSIONAL TEACHING APPOINTMENTS

Interim Full-time Instructor of Natural Science **2019 – Present**
Adjunct Assistant Professor of Natural Science **2011 – 2019**
Natural Sciences, Milwaukee Institute of Art & Design

- Patterns in Nature
- Defenders of the Environment
- Environmental Literacy
- Sustainable Future

GRADUATE TEACHING APPOINTMENTS

Graduate Teaching Assistant **2018 – Present**
Biological Sciences, University of Wisconsin – Milwaukee **2006 –2013**

- Anatomy & Physiology I & II
- Introduction to Biological Sciences
- Limnology
- Marine Seaweeds
- Biology of Algae

RESEARCH EXPERIENCE

Doctoral/Graduate Research Assistant ***2013 – 2022***
University of Wisconsin – Milwaukee ***2007 – 2012***

- Phytoplankton Ecology Laboratory: Drs. Craig Sandgren & John Berges

PUBLICATIONS

Fleck, M.S., M. Dinan, **L.J. Simmons**, et al. 2021. Investigating the Relationship between Sociodemographic Factors and Bird Identification by Landowners Across a Rural-to-Urban Gradient. Environ Manage 68, 65–72 DOI: 10.1007/s00267-021-01475-w

Simmons, L.J., C.D. Sandgren, and J.A. Berges. 2016. Problems and pitfalls in using HPLC pigment analysis to distinguish Lake Michigan phytoplankton taxa. J Great Lakes Res. 42, 397-404. DOI: 10.1016/j.jglr.2015.12.006.

PUBLICATIONS IN PREP

Simmons, L.J., Fobbe, D.J., Berges. J.A. and Young, E.B. Environmental influences on phytoplankton community structure and cell mortality in an urban pond. *in prep*.

PRESENTATIONS

Berges, J.A., **Simmons, L.J.** and Young, E.B. 2022. Estabrook Park Pond: A model for aquatic ecosystem processes. Joint Aquatic Sciences Meeting, Grand Rapids, MI (May 19, podium presentation)

Simmons, L.J. and Berges, J.A. 2021. Going with the flow: phytoplankton mortality and community dynamics. Phycological Society of America Meeting, (Held virtually, July 15, Recorded presentation)

Simmons, L.J., D.J. Fobbe, and J.A. Berges. 2016. Where do all the phytoplankton go? Challenges in keeping track of viable cells in phytoplankton communities using flow cytometry and cell staining. Ocean Sciences Meeting, New Orleans, LA (February 23, Poster)

Fobbe, D.J., **L.J. Simmons**, and J.A. Berges. 2016. All microorganisms must die, but how many getted lysed by viruses? Approaches to assessing the significance of nano-sized agents of mortality among communities of phytoplankton. Ocean Sciences Meeting, New Orleans, LA (February 23, Poster)

Simmons, L.J. and J.A. Berges. 2015. Factors affecting freshwater phytoplankton mortality: grazing and allelopathy. University of Wisconsin – Milwaukee. Milwaukee, WI. (May 1, Podium presentation).

Fobbe, D.J., **L.J. Simmons**, and J.A. Berges. 2014. Phytoplankton life and death in an urban freshwater pond. Joint Aquatic Sciences Meeting. Portland, OR. (May 22, Poster)

Simmons, L.J. and J.A. Berges. 2013. Estimation of Lake Michigan phytoplankton taxonomic composition using pigment-based methods. Biological Sciences Research Symposium. University of Wisconsin – Milwaukee. Milwaukee, WI. (April 18, Podium presentation)

Simmons, L.J., C.D. Sandgren, and J.A. Berges. 2013. Estimating phytoplankton taxonomic

composition using pigment-based methods: illustrating limitations using Lake Michigan datasets. Association for the Societies of Limnology and Oceanography Aquatic Sciences Meeting. New Orleans, LA. (February 19, Podium presentation)

Simmons, L.J., C.D. Sandgren, J.A. Berges, and P.M. Engevold. 2011. Interpreting phytoplankton seasonal dynamics in the Great Lakes: application of high-performance liquid chromatography (HPLC). International Association of Great Lakes Research Annual Conference. Duluth, MN. (May 31, Poster)

Simmons, L.J., C.D. Sandgren, J.A. Berges, and P.M. Engevold. 2010. Application of high-performance liquid chromatography (HPLC) for interpretation of nutrient phytoplankton-zooplankton interactions in the Great Lakes. International Association of Great Lakes Research Annual Conference. Toronto, Ontario, Canada. (May 18, Podium presentation)

Simmons, L.J., C.D. Sandgren, J.A. Berges, and P.M. Engevold . 2010. Using high – performance liquid chromatography (HPLC) to interpret plankton community interactions in Lake Michigan. Biological Sciences Research Symposium. University of Wisconsin-Milwaukee. Milwaukee, WI. (April 27, Podium presentation)

Simmons, L.J., C.D. Sandgren, J.A. Berges, and P.M. Engevold. 2009. Winners and losers: herbivore transformation of lake phytoplankton communities through size selective mortality and growth rate enhancement. Ecological Society of America Annual Conference. Albuquerque, NM. (August 4, Poster)

Simmons, L.J. and C. Sandgren. 2009. Understanding seasonal changes in Lake Michigan phytoplankton communities using high-performance liquid chromatography (HPLC). Biological Sciences Research Symposium. University of Wisconsin - Milwaukee. Milwaukee, WI. (April, Podium presentation)

Simmons, L.J. and C. Sandgren. 2008. Limiting nutrients in Lake Michigan. Biological Sciences Research Symposium. University of Wisconsin – Milwaukee. Milwaukee, WI. (April, Poster)

Krueger, L.J. and C. Lepczyk. 2006. Relationships between social and demographic factors and bird identification. Biological Sciences Research Symposium. University of Wisconsin Milwaukee. Milwaukee, WI. (April, Poster)

AWARDS AND HONORS

2017	Louise Neitge Mather Scholarship: University of Wisconsin Milwaukee, Department of Biological Sciences
2016-2017	Distinguished Graduate Student Fellowship: University of Wisconsin – Milwaukee Graduate School
2015	Hannah T. Croasdale Fellowship: Phycological Society of America

2008, 2010	Ruth Walker Grant-in-Aid: University of Wisconsin – Milwaukee, Department of Biological Sciences
2013-2018	Chancellor's Award: University of Wisconsin – Milwaukee, Graduate School
2009-2011, 2013-2016	Ruth Walker Research Travel Award: University of Wisconsin Milwaukee Department of Biological Sciences
2009, 2013-2014	Clifford H. Mortimer Award: University of Wisconsin – Milwaukee Department of Biological Sciences
2010, 2016	Graduate School Travel Award: University of Wisconsin – Milwaukee, Graduate School

UNIVERSITY SERVICE

Thesis Mentor **2021-Present**
Milwaukee Institute of Art and Design

Independent Study Supervisor **2020**
Milwaukee Institute of Art & Design

SOCIETY MEMBERSHIPS

American Society of Limnology and Oceanography
International Association for Great Lakes Research
Phycological Society of America